Prepared for

Santee Cooper
One Riverwood Drive
Moncks Corner, SC 29461

2021 PERIODIC SAFETY FACTOR ASSESSMENT
ASH POND B

WINYAH GENERATING STATION
Georgetown, South Carolina

Prepared by

Geosyntec Consultants, Inc.
1300 South Mint Street, Suite 300
Charlotte, North Carolina 28203

Project No. GC8100

October 2021

TABLE OF CONTENTS

LIST OF FIGURES

LIST OF ATTACHMENTS

CERTIFICATION STATEMENT

This periodic safety factor assessment meets the requirements of §257.73(e) of the Code of Federal Regulations Title 40, Part 257, Subpart D, and was prepared in accordance with current practices and the standard of care exercised by scientists and engineers performing similar tasks in the field of civil engineering, and no other warranty is provided in connection therewith. The contents of this report are based solely on the observations of the conditions observed by Geosyntec personnel and information provided to Geosyntec by Santee Cooper. Consistent with applicable professional standards of care, our opinions and recommendations were based in part on data furnished by others. Although we were not able to independently verify such data, we found that it was consistent with other information that we developed in the course of our performance of the scope of services. The information contained in this report is intended for use solely by Santee Cooper.

SOUTH CAROLINA
LICENSED PROFESSIONAL ENGINEER
No. 36052
WOO-KUEN SHIN

Woo-Kuen Shin, Ph.D, P.E.
South Carolina License No. 36052

10/14/2021

Date

1. INTRODUCTION

1.1 Project Background

The Winyah Generating Station (WGS or Site) is an electric generating facility owned and operated by Santee Cooper. WGS is located between Pennyroyal and Turkey Creeks, tributaries to Sampit River, and is situated approximately four miles southwest of Georgetown, South Carolina (SC) (see Figures 1a and 1b for Site Location and Site Vicinity Maps).

On 17 April 2015, the United States Environmental Protection Agency (USEPA) published rules in 40 CFR Part 257 that regulate the design and management of existing and new CCR units (CCR Rule). The CCR Rule became effective on 17 October 2015. Within the CCR Rule, §257.73(e) specifies the safety factor criteria for existing CCR surface impoundments.

Ash Pond B is situated southeast of the power block and west of the Site's Cooling Pond. (Figure 2). Ash Pond B contains CCR in the form of fly ash, boiler slag, and bottom ash as well as stormwater. It is considered as an existing surface impoundment under the CCR Rule. In accordance with §257.102(g), a Notice of Intent for Ash Pond B was posted to the Operating Record on 9 April 2021 to initiate pond closure, and CCR and wastewater inflow to Ash Pond B ceased in April 2021. Santee Cooper indicated the surface impoundment is planned to be closed by CCR removal within five years.

This *2021 Periodic Safety Factor Assessment: Ash Pond B* (Safety Factor Assessment Report) was prepared by Geosyntec Consultants, Inc. (Geosyntec) on behalf of Santee Cooper to demonstrate that Ash Pond B satisfies criteria for the periodic safety factor assessments in accordance with §257.73(e) of the CCR Rule.

1.2 Project Site and Construction History

Ash Pond B spans approximately 65 acres. This unlined surface impoundment was commissioned in 1975 and was designated for the disposal of fly ash, bottom ash, boiler slag, decanted sluice water, low volume wastewater, and stormwater from Ash Pond A. Ash Pond B is bounded by the divider dike and Ash Pond A to the north, the Discharge Canal to the west, and the Cooling Pond to the south and east. Ash Ponds A and B were constructed simultaneously and are separated by a recompacted, earthen divider dike spanning west to east from the Discharge Canal to the Cooling Pond. Ash Pond B was assigned "Low Hazard Potential" classification (Geosyntec, 2021a).

Ash Pond B was constructed by recompacting excavated soils from the impoundment interior to form the perimeter dikes and a divider dike. The Ash Pond B perimeter dikes are approximately 12 ft to 15 ft in height adjacent to the Discharge Canal and approximately 20 ft to 24.5 ft in height along the east and south sides adjacent to the Cooling Pond (Thomas and Hutton, 2012). The upstream and downstream slopes of the perimeter dikes range from 2 Horizontal to 1 Vertical (2H:1V) to 3H:1V. The Ash Pond B dike crest was originally constructed in the early 1970s with a 12- to 15-ft width and an elevation of 34.5 ft National Geodetic Vertical Datum of 1929 (NGVD29), which was approximately 7 ft lower than the Ash Pond A perimeter and divider dikes. The Ash Pond B dike crest was raised to a design elevation of 41.0 ft NGVD29 in 1997 using downstream construction methods. The crest of Ash Pond B is currently at an elevation between 39.7 ft and 41.4 ft NGVD29 (Thomas and Hutton, 2012; Thomas and Hutton, 2016).

1.3 Report Organization

This Safety Factor Assessment Report presents the subsequent periodic safety factor assessments for Ash Pond B at WGS based on the results of the initial periodic safety factor assessments (2016 Safety Factor Assessment) (Geosyntec, 2016), recent survey dated September 2021 (McKim & Creed, 2021), subsequent hydrologic and hydraulic (H&H) analyses and geotechnical engineering analyses, and reviews of available Site information. The remainder of this Safety Factor Assessment Report is organized as follows:

- Summary of changes in site conditions since the 2016 Safety Factor Assessments is presented in Section 2.
- H&H evaluation of Ash Pond B is presented in Section 3;
- Seismic hazard evaluations for WGS and the site response analysis of the Ash Pond B perimeter dikes are presented in Section 4;
- Liquefaction potential evaluation is presented in Section 5;
- Slope stability analyses performed for the safety factor assessment are discussed in Section 6; and
- The summary and general conclusions are presented in Section 7.

2. CHANGES IN SITE CONDITIONS

Santee Cooper personnel indicated that no changes were made for the Ash Pond B perimeter dikes and adjacent areas outside the dikes since preparation of the 2016 Safety Factor Assessment Report. Also, no additional geotechnical subsurface investigations were conducted since 2016; therefore, the subsurface stratigraphy developed in the 2016 Safety Factor Assessment remains valid. A review of the topographic survey dated September 2021 (McKim & Creed, 2021) and the topographic survey used in the 2016 Safety Factor Assessment indicated that CCR have been moved to the west side of the surface impoundment (i.e., adjacent to the Discharge Canal) and that insignificant changes in the CCR surface were observed on the east side of the surface impoundment (top of CCR surface in the east side of Ash Pond B is similar to the surface used for the 2016 Safety Factor Assessment). The volume of CCR impounded within the surface impoundment is very similar to that observed during the last assessment.

Santee Cooper provided available water level measurements from wells in the area of Ash Pond B. The recorded water levels in these wells have generally been steady over the last five years. Based on the review of the topographic survey (McKim & Creed, 2021) and available water level measurements adjacent to the selected profile, the water levels within the perimeter dike and beyond the downstream toe of the perimeter dike are expected to be similar to those used for the 2016 Safety Factor Assessment.

As discussed above, CCR and wastewater inflow to Ash Pond B ceased in April 2021. After the 2016 Safety Factor Assessment, an emergency spillway was constructed between Ash Ponds A and B to provide sufficient storage capacity in the two surface impoundments for 100-year storm event.

3. HYDROLOGIC AND HYDRAULIC EVALUATION

3.1 <u>Hydrologic and Hydraulic Analysis</u>

The following subsections discuss the regulatory framework, the methodology and assumptions, and the results of the hydrologic and hydraulic (H&H) analysis for Ash Pond B and its appurtenances.

3.1.1 Regulatory Framework

The CCR Rule (§257.73(d)(1)) requires that a periodic stability assessment:

"...at a minimum, document whether the CCR unit has been designed, constructed, and maintained with:

...

(v) a single spillway or a combination of spillways configured as specified in paragraph (d)(1)(v)(A) of this section. The combined capacity of all spillways must be designed, constructed, operated, and maintained to adequately manage flow during and following the peak discharge event specified in paragraph (d)(1)(v)(B) of this section."

The CCR Rule (§257.73(d)(1)(v)(B)(3)) also states that the spillways must manage the peak discharge from the *"100-year flood for a low hazard potential CCR surface impoundment."* Additionally, §257.73(d)(1)(v)(A) indicates that "*All spillways must be either:*

(1) Of non-erodible construction and designed to carry sustained flows; or

(2) Earth- or grass-lined and designed to carry short-term, infrequent flows at non-erosive velocities where sustained flows are not expected."

Meanwhile, §257.73(e)(1) of the CCR Rule indicates:

"(ii) The calculated static factor of safety under the maximum surcharge pool loading condition must equal or exceed 1.40."

Because Ash Pond B was classified as a "Low Hazard Potential" surface impoundment, the 100-year storm event with a rainfall duration of 72 hours was selected as the inflow design flood (IDF). H&H analyses were performed to demonstrate that the Ash Pond B spillway is able to adequately manage flow during and following the 100-year design rainfall (i.e., peak discharge event) without overtopping of perimeter dikes, meeting the criteria in §257.73(d)(1)(v). This Safety Factor Assessment Report established the "maximum surcharge pool" elevation in the slope stability analysis to demonstrate that the requirements of §257.73(e)(1)(ii) are met, based on the maximum surface water elevation within Ash Pond B computed from the H&H analyses.

3.1.2 Methodology and Assumptions

HydroCAD® Version 10.0 software (HydroCAD, 2019) was utilized to compute the stormwater volume using the Soil Conservation Service (SCS) Technical Release 20 (TR-20) method (SCS, 1982) and to model the performance of the hydraulic structures of Ash Pond B during the IDF. The 100-yr rainfall event with a 72-hour (hr) duration precipitation event resulted in a rainfall depth of 12.8 in. (NOAA, 2021) and was modeled within HydroCAD® using a SCS Type III rainfall distribution.

Ash Pond B historically decanted ash sluice water, low volume wastewater, and the former Unit 2 Slurry Pond stormwater from Ash Pond A. Ash Pond B now only receives stormwater inflows from the pond area, and process water inflow to the pond has been halted. Ash Pond A does not have an outfall structure but routes water southward through rim ditches and culverts to Ash Pond B. Ash Ponds A and B are hydraulically connected through a 30-inch diameter corrugated metal pipe (CMP), a 48-inch diameter smooth steel pipe, and a 42-inch diameter smooth steel pipe (Thomas and Hutton, 2012; and Thomas and Hutton, 2016). As indicated in Section 2, an emergency spillway was constructed between Ash Ponds A and B to provide capacity in the two surface impoundments for the 100-year storm event. The operating level in Ash Pond B is maintained by a concrete riser structure with a top stop log elevation of 34.9 ft NGVD 29 (Thomas and Hutton, 2016). A 24-inch diameter smooth interior, corrugated exterior high density polyethylene pipe culvert with a downstream invert elevation of 17.99 ft NGVD 29 conveys water from the riser structure to the Discharge Canal of the Cooling Pond (Santee Cooper, 2012; and Thomas and Hutton, 2016). The average operating elevation provided by Santee Cooper from February 2011 through September 2021 is 34.1 ft NGVD 29. The operating elevation is decreasing as dewatering occurs to facilitate closure of Ash Pond B.

Details of the H&H analysis are provided in a document titled *"Inflow Design Flood Control System Plan: Ash Pond B"* (Geosyntec, 2021b). Note that the vertical datum conversion between

NGVD 29 and North American Vertical Datum of 1988 (NAVD 88) is -1.0 ft (i.e., NGVD 29 – 1.0 ft = NAVD 88) (FEMA, 2015).

3.1.3 Analysis Results

Under the conditions and assumptions described in Section 3.1.2, the maximum surface water level during and following the IDF event (100-year rainfall with a 72-hour duration) was computed as 36.1 ft NGVD29. The H&H analysis results (i.e., HydroCAD® results) are included as Attachment 2 to this Safety Factor Assessment Report.

4. SEISMIC HAZARD EVALUATION AND SITE RESPONSE ANALYSIS

This section presents the results of seismic hazard evaluation and site response analysis of the Ash Pond B perimeter dikes. Seismic hazard evaluation includes the selection of an appropriate hazard level and associated hazard parameters (e.g., peak ground acceleration, or PGA). Site response analysis was performed to evaluate the local site effects on selected time history records propagated from the hypothetical, firm ground outcrop to the ground surface at the Site. Details and results for these analyses are presented in Attachment 3 of this Safety Factor Assessment Report and summarized herein.

4.1 <u>Seismic Hazard Evaluation</u>

A seismic hazard evaluation typically consists of the selection of appropriate hazard level and associated seismic parameters, which include the target acceleration response spectra, PGA, and the controlling earthquake magnitude. The seismic hazard analysis also involves the selection of ground motions that envelop the target response spectrum.

4.1.1 Seismic Hazard Level

The appropriate hazard level is often expressed in probabilistic terms as a specific hazard level that has a certain probability of exceedance in a given time period. The CCR Rule states in §257.63(a) that:

"New CCR landfills, existing and new CCR surface impoundments, and all lateral expansions of CCR units must not be located in seismic impact zones, unless the owner or operator demonstrates by the dates specified in paragraph (c) of this section that all structural components including liners, leachate collection and removal systems, and surface water control systems, are designed to resist the maximum horizontal acceleration in lithified earth material for the site."

§257.53 defines the maximum horizontal acceleration in lithified earth material as:

"... the maximum expected horizontal acceleration at the ground surface as depicted on a seismic hazard map, with a 98 percent or greater probability that the acceleration will not be exceeded in

50 years, or the maximum expected horizontal acceleration based on a site-specific seismic risk assessment."

A 98 percent or greater probability of not being exceeded in 50 years (or two percent probability of exceedance in 50 years) corresponds to a return period of approximately 2,500 years. The Preamble of the CCR Rule indicates that USEPA selected this return period by considering a typical operating life for CCR surface impoundments (i.e., 50 years) and its common use in seismic design criteria throughout engineering (e.g., American Society of Civil Engineers [ASCE] 7-16 [2016]). For the CCR surface impoundments at WGS, closure was initiated in 2021 and is expected to be complete in less than 15 years. Therefore, an earthquake return period of approximately 750 years was conservatively selected for the 2021 Safety Factor Assessment of Ash Pond B (i.e., two percent probability of exceedance in 15 years) following the basis for selecting the return period of approximately 2,500 years for typical CCR surface impoundments.

4.1.2 Peak Ground Acceleration (PGA)

PGA values corresponding to different hazard levels and different site conditions, including firm ground outcrops, are published as seismic hazard maps or curves. The 2016 Safety Factor Assessment Report (Geosyntec, 2016) referenced seismic hazard maps presented in the South Carolina Department of Transportation (SCDOT) Geotechnical Design Manual (GDM) (SCDOT, 2010) for selection of a PGA to incorporate local site effects for the Charleston Seismic Zone researched by Chapman and Talwani (2006). The GDM was updated in 2019 (SCDOT, 2019) and does not present the seismic hazard maps referenced in the 2016 Safety Factor Assessment Report. Moreover, SCDOT is updating seismic hazard maps at the time of this seismic hazard evaluation.

As an alternative, United States Geological Survey (USGS) hazard curves for two percent probability of exceedance in 15 years (i.e., approximately 750-year return period event) at the BC boundary (i.e., boundary between National Earthquake Hazard Reduction Program [NEHRP] site classes B and C with a mean shear wave velocity of 2,500 ft/s) were used to estimate the PGA and spectral accelerations for a hypothetical firm ground outcrop, similar to "geologically realistic" site conditions, at the Site. The data available at the USGS website (Petersen et al., 2019) use pre-calculated hazard values at nearby grid locations and interpolate the hazard value for a given site location. As discussed in Attachment 3, the interpolated PGA from USGS Hazard Curves is 0.15g for the Site.

4.1.3 Earthquake Magnitude

In a probabilistic seismic hazard analysis, the PGA cannot be associated with a single earthquake event due to the hazard contribution from multiple possible events. An earthquake moment magnitude (M_W) value is required to conduct liquefaction potential analyses and to select earthquake time histories. A process called deaggregation can be performed for sites that have multiple hazard sources using the most up-to-date USGS (2014) deaggregation tool. As discussed in Attachment 3, a 7.3 moment magnitude was selected for liquefaction potential analyses and time history selection for the Site by applying this deaggregation tool.

4.1.4 Target Acceleration Response Spectra and Time History Selection

A target acceleration response spectrum was established using the USGS seismic hazard curves at different spectral periods (or frequencies). Time histories of ground motions are selected such that their response spectra match or envelope the target acceleration response spectrum. Six acceleration time histories used for the 2016 Safety Factor Assessment were still considered adequate as input for site response analyses since the scaled time histories provide a conservative, reasonable match with the target acceleration response spectrum. The response spectra of scaled time histories selected for the site responses analyses are presented on Figure 4 of Attachment 3.

4.2 Site Response Analysis

Site response analyses computed the cyclic shear stresses within the select representative soil profile located along the perimeter dike centerline. Computed cyclic shear stresses were applied for the liquefaction potential analysis, and were also utilized to evaluate the seismic safety factor as part of this Safety Factor Assessment.

4.2.1 Analysis Model Setup

Site response analyses presented herein were conducted using DEEPSOIL® (Hashash et al., 2020), a one-dimensional, nonlinear site response analysis program. The program assumes that all the soil layers are perfectly horizontal (i.e., "layer cake") and that ground response is mainly caused by vertically-propagating, horizontally polarized shear waves. This assumption is valid for many geotechnical cases including the response analyses of the Site. Under these assumptions, the subsurface stratigraphy is modeled as a one-dimensional column of soil layers for the analyses. One critical profile was selected for the site response analyses of the Ash Pond B perimeter dikes based on the 2016 Safety Factor Assessment results and is shown on Figure 6 of Attachment 3.

DEEPSOIL® employs a viscoelastic material model, described by its shear modulus (G), mass density (ρ) or unit weight (γ), and damping (D). Preliminary equivalent-linear site response analyses yielded calculated maximum cyclic shear strains greater than five percent in some layers, which is greater than the cyclic shear strains for which equivalent-linear analyses are considered applicable (i.e., one to two percent). Therefore, nonlinear site response analyses were performed. Additional discussion of input parameters, such as the V_s profile, soil plasticity, and shear modulus reduction/damping curves applied in the DEEPSOIL® program, are discussed in Attachment 3.

As discussed in Section 2, the water level within the perimeter dike is expected to be similar to the water level used in the 2016 Safety Factor Assessment. Therefore, the site response analyses for the 2021 Safety Factor Assessment were performed with the water table used in the 2016 Safety Factor Assessment Report, as discussed in Attachment 3.

4.2.2 Site Response Analysis Results

Maximum shear stresses within the representative soil profiles were computed and presented on Figures 9 and 10 of Attachment 3. Additional site responses analysis results are presented in Attachment 3. The maximum cyclic shear stresses at depths were calculated and these values were used to calculate a measure of shear stress developed during the design earthquake (cyclic stress ratios, or CSR) in the evaluation of liquefaction potential, presented in Section 5 of this Safety Factor Assessment Report. The site response analysis results were also used to calculate the horizontal seismic coefficient (k_h) as presented in Section 6 of this Safety Factor Assessment Report.

5. EVALUATION OF LIQUEFACTION POTENTIAL

This section presents the liquefaction potential evaluation for the critical section of the Ash Pond B perimeter dikes. The evaluation applies the cyclic shear stress computed as part of the site response analysis (Section 4). Further details of the liquefaction potential evaluation are presented in Attachment 4 of this Safety Factor Assessment Report.

5.1 Regulatory Framework

A periodic safety factor assessment is required by the CCR Rule to evaluate whether the existing CCR surface impoundments meet minimum safety factors (also referred to as "factors of safety") for slope stability provided in §257.73(e)(1). Specifically, §257.73(e)(1)(iv) requires that:

"embankments constructed of soils that have susceptibility to liquefaction, the calculated liquefaction factor of safety must equal or exceed 1.20."

The purpose of this section is to discuss the methodology, analysis, and results of the liquefaction potential analysis to evaluate if the Ash Pond B dike fill and foundation soils are susceptible to liquefaction triggering under the design earthquake. If soils are not found to be susceptible to liquefaction within the dike fill and foundation soils, then the liquefaction factor of safety is not required and is not evaluated as part of this Safety Factor Assessment.

5.2 Methodology

Liquefaction potential analysis was performed based on the Simplified Procedure recommended by Seed and Idriss (1971) and an update by Boulanger and Idriss (2014). This approach is based on comparing in-situ test results with case histories of occurrences and non-occurrences of liquefaction due to past earthquakes. The analyses presented herein were conducted for soil borings and CPT soundings along the critical section of Ash Pond B. The factor of safety against liquefaction (FS_{liq}) was computed as the ratio of a measure of a soil's resistance to triggering of liquefaction (cyclic resistance ratio, or CRR) to CSR.

5.2.1 Dike Phreatic Surface Conditions

As described in Section 2, the water level within the perimeter dike is anticipated to be similar to the water level used in the 2016 Safety Factor Assessment. The phreatic surface at the time of the boring/CPT sounding was used to estimate CRR profiles. CSR profiles were estimated for the time at which the design earthquake event occurs using the phreatic surface used for the 2016 Safety Factor Assessment.

5.2.2 Age Correction Factor

Correlations associated with liquefaction potential analysis were developed based on case histories of relatively young soil deposits (i.e., Holocene age). As described in SCDOT (2019), liquefaction resistance, as represented by the CRR, may be adjusted to account for aging effects in older soils based on time from deposition (i.e., geologic age) and time from last occurrence of liquefaction (i.e., geotechnical age). As described in Attachment 4, an age correction factor (K_{dr}) of 1.2 was applied for the Pleistocene-aged soils at the WGS site (typically foundation soils below the base of the dike), and an age correction factor of 1.0 was applied to the dike fill soils.

5.3 Evaluation Results

The FS_{liq} was computed at every depth interval where data were collected for soil test borings (2-ft or 5-ft intervals) and CPT sounding (0.16-ft intervals) advanced in the vicinity of the Ash Pond B perimeter dikes. Analysis results for each soil boring and CPT sounding analyzed are provided on Figures 3 through 7 of Attachment 4 to this Safety Factor Assessment Report. FS_{liq} values computed for dike fill and foundation soils were found to exceed 1.0 for the conditions described within this Safety Factor Assessment Report (i.e., no zones expected to undergo triggering of liquefaction under the design earthquake were identified for borings and CPT soundings advanced through the critical section of the Ash Pond B perimeter dikes).

6. SAFETY FACTOR ASSESSMENT

This section presents the periodic safety factor assessments for the Ash Pond B perimeter dikes. This evaluation is presented in detail in Attachment 5 of this Safety Factor Assessment Report and summarized herein.

6.1 Regulatory Framework

Slope stability analyses were conducted to assess whether the Ash Pond B perimeter dikes satisfy the safety factor (also referred to as "factor of safety") criteria of §257.73(e)(1) of the CCR Rule. Specifically, §257.73(e)(1) requires that:

"(i) *The calculated static factor of safety under the long-term, maximum storage pool loading condition must equal or exceed 1.50.*

(ii) The calculated static factor of safety under the maximum surcharge pool loading condition must equal or exceed 1.40.

(iii) The calculated seismic factor of safety must equal or exceed 1.00.

(iv) For embankments constructed of soils that have susceptibility to liquefaction, the calculated liquefaction factor of safety must equal or exceed 1.20."

Because the dike fills and foundation soils beneath the dike fill along the critical section of Ash Pond B are not found to be susceptible to liquefaction, as described above, the liquefaction factor of safety (i.e., §257.73(e)(1)(iv)) is not required and is not evaluated as part of this Safety Factor Assessment. The remainder of Section 6 describes the geometric model, methodology, and analysis results for each case.

6.2 Analysis Models

The models used for the 2016 Safety Factor Assessment were updated with a topographic surface within the pond (Section 2). Consistent with observations regarding the water level described in Section 2, the water levels (within the perimeter dike and beyond the downstream toe of the perimeter dike) selected for the analyses are those used for the 2016 Safety Factor Assessment. One representative cross section was selected for the assessment based on factors of safety calculated in the 2016 Safety Factor Assessment.

6.3 Methodology

6.3.1 Static Slope Stability

Global slope stability analyses were performed using Spencer's method (Spencer, 1973), as implemented in the computer program SLIDE®, version 6.039 (Rocscience, 2016). Spencer's method, which satisfies vertical and horizontal force equilibrium as well as moment equilibrium, is considered to be more rigorous than other methods, such as the simplified Janbu method (Janbu, 1973) and the simplified Bishop method (Bishop, 1955).

Both the rotational mode (e.g., non-circular slip surfaces) and the non-rotational mode (i.e., block slip surfaces) were considered during the factor of safety assessment analyses, and the slip mode resulting in the lowest calculated FS was reported. SLIDE® generates potential slip surfaces, calculates the FS for each of these surfaces, and identifies the most critical slip surface with the lowest calculated FS.

6.3.2 Seismic Slope Stability

Pseudo-static slope stability analyses were performed utilizing Spencer's method to evaluate the seismic performance of the perimeter dike structures using a procedure consistent with a guidance document prepared for the USEPA (USEPA, 1995) and recommendations made by Hynes-Griffin and Franklin (1984). The seismic factor of safety was evaluated by applying a seismic horizontal force coefficient (k_h) to compute an additional horizontal force ($F = k_h \times W$) for each slice, based on slice weight (W), during the design seismic event. The k_h for each evaluated cross section was developed from the Maximum Horizontal Equivalent Acceleration (MHEA) computed during the site response analysis (Section 4) at the depth of the anticipated critical slip surface for each cross section. The k_h value is dependent on the allowable displacement (u) for a dike structure. For the purpose of this Safety Factor Assessment Report, the allowable displacement of Ash Pond B perimeter dike structures was selected as 12 inches. Based on this allowable displacement and the upper bound relation, the Hynes-Griffin and Franklin (1984) procedure was used to adjust the MHEA at the target depth to compute the k_h applied in SLIDE®, resulting in $k_h = 0.032g$.

6.4 Static Safety Factor – Maximum Normal Storage Pool

§257.73(e)(1)(i) requires that the static factor of safety meets or exceeds 1.50 for the maximum normal storage pool conditions within the surface impoundment. The static safety factor was evaluated for the critical cross section of Ash Pond B as shown on Figure 2 of Attachment 5.

6.5 Static Safety Factor – Maximum Surcharge Pool

§257.73(e)(1)(ii) requires that the static factor of safety meets or exceeds 1.40 for the maximum surcharge pool conditions within the surface impoundment. The static safety factors were evaluated with a more conservative water level (37.2 ft NGVD29) within Ash Pond B than the maximum surface water level (36.1 ft NGVD 29) from the H&H analyses (Section 3). The static safety factor was evaluated for the critical cross section of Ash Pond B as shown on Figure 3 of Attachment 5.

6.6 Seismic Safety Factor – Maximum Normal Storage Pool

§257.73(e)(1)(iii) requires that the seismic factor of safety meets or exceeds 1.00 for the maximum normal storage pool conditions within the surface impoundment. The seismic safety factor was evaluated for the critical cross section with the computed seismic horizontal force coefficient (i.e., 0.032g) applied to each slice within SLIDE®. During the evaluation of the seismic safety factor, soil shear strengths for cohesive soils were conservatively reduced by 20% to account for the influence of cyclic degradation (Hynes-Griffin and Franklin, 1984).

6.7 Summary of Results

As presented in Table 3 of Attachment 5, the calculated factors of safety for the static case with the maximum normal storage pool, the static case with the maximum surcharge pool, and seismic case with the maximum normal storage pool are 1.54, 1.51, and 1.06, respectively. These analysis results indicate that the perimeter dikes of Ash Pond B at WGS satisfy the periodic safety factor assessment criteria given in §257.73(e)(1) of the CCR Rule. Further details of the safety factor assessment for Ash Pond B can be found in Attachment 5.

7. SUMMARY AND GENERAL CONDITIONS

The following provides a summary and general conclusion of the safety factor assessments presented in this Safety Factor Assessment Report:

- The maximum surcharge pool within Ash Pond B for the safety factor assessment was established based on the H&H performance of Ash Pond B during the IDF.

- The seismic hazard evaluation resulted in the selection of the design PGA as 0.15g at the Site. This PGA corresponds to a seismic event with a two percent probability of exceedance in 15 years, established conservatively with consideration of the remaining operating life of Ash Pond B in a consistent manner with the return period specified in the CCR Rule. Also, this PGA represents a peak ground motion corresponding to "geologically realistic" conditions. The site response analyses were performed to compute the maximum cyclic shear stresses and MHEAs, which were applied to evaluate the liquefaction potential analyses and seismic safety factors of the Ash Pond B perimeter dikes, respectively.

- Liquefaction potential analysis was performed based on the Simplified Procedure recommended by Seed and Idriss (1971) and an update by Boulanger and Idriss (2014). The FS_{liq} was computed as the ratio of CRR to CSR and indicated that dike fill and foundation soils are not found to be susceptible to liquefaction under the design earthquake event. Therefore, the liquefaction factor of safety is not required and is not evaluated as part of this Safety Factor Assessment.

Based on the safety factor assessment of the critical cross section of the Ash Pond B perimeter dikes, Ash Pond B satisfies the required safety factors presented in §257.73(e)(1) as shown below.

Safety Factor Case	Target FS	Calculated FS
Static - Maximum Normal Storage Pool	1.50	1.54
Static FS- Maximum Surcharge Pool	1.40	1.51
Seismic - Maximum Normal Storage Pool	1.00	1.06
Liquefaction Slope Stability	1.20	Not Applicable

8. REFERENCES

Bishop, A. (1955), "The Use of the Slip Circle in the Stability Analysis of Slopes," Géotechnique, Vol. 5, No. 1, Jan 1955, pp. 7-17.

Boulanger, R. W. and Idriss, I. M. (2014), "CPT and SPT Based Liquefaction Triggering Procedures," Report No. UCD/CGM-14/01, Center for Geotechnical Monitoring, University of California, Davis, CA

Chapman, M.C. and Talwani, P. (2006), "Seismic Hazard Mapping for Bridge and Highway Design in South Carolina," South Carolina Department of Transportation, FHWA-SC-06-09.

Federal Emergency Management Agency (FEMA) (2015), "Flood Insurance Study: Georgetown County, South Carolina and Incorporated Areas," Preliminary, 13 November 2015.

Geosyntec Consultants, Inc. (2016), "2016 Surface Impoundment Periodic Safety Factor Assessment Report: Ash Pond B," Project No. GSC5242.

Geosyntec Consultants, Inc. (2021a), "Periodic Hazard Potential Classification Assessment: Ash Pond B," Project No. GC8100.

Geosyntec Consultants, Inc. (2021b), "Inflow Design Flood Control System Plan: Ash Pond B," Project No. GC8100.

Hashash, Y.M.A., Musgrove, M.I., Harmon, J.A., Ilhan, O., Xing, G., Numanoglu, O., Groholski, D.R., Phillips, C.A., and Park, D. (2020), "DEEPSOIL 7.0, User Manual", Board of Trustees of University of Illinois at Urbana-Champaign, Urbana, Illinois.

HydroCAD (2019), "HydroCAD Stormwater Modeling," HydroCAD Software Solutions, LLC.

Hynes-Griffin, M. and Franklin, A. (1984), "Rationalizing the Seismic Coefficient Method", Department of the Army, Waterways Experiment Station, Corps of Engineers, Vicksburg, Mississippi, Miscellaneous Paper GL-84-14, July.

Janbu, N., (1973), "Slope Stability Computations in Embankment-Dam Engineering", R.C. Hirschfeld and S.J. Poulos, Eds. New York: Wiley, pp. 47-86.

Lockwood Greene (1978), "South Carolina Public Service Authority – Georgetown Generating Station."

McKim & Creed (2021), "Topographic Survey for Winyah Generating Station."

National Oceanic and Atmospheric Administration (NOAA) (2021), "Precipitation-Frequency Atlas of the United States," Atlas 14, Volume 2, Version 3.

Petersen, M.D., Shumway, A.M., Powers, P.M., Mueller, C.S., Moschetti, M.P., Frankel, A.D., Rezaeian, S., McNamara, D.E., Luco, N., Boyd, O.S., Rukstales, K.S., Jaiswal, K.S., Thompson, E.M., Hoover, S.M., Clayton, B.S., Field, E.H., and Zeng, Y. (2019), "The 2018 update of the US national seismic hazard model: Overview of model and implications", Earthquake Spectra, Vol. 36, No. 1, 2019, pp. 5-41.

Rocscience (2016), "SLIDE® – 2-D Limit Equilibrium Slope Stability for Soil and Rock Slopes," User's Guide, Rocscience Software, Inc., Toronto, Ontario, Canada.

Santee Cooper. (2012), "Inter-Office Communication - WGS Ash Pond B – Abandon Existing Drawdown Structure."

Seed, H.B, and Idriss, I.M. (1971), "Simplified Procedure for Evaluation Soil Liquefaction Potential", Journal of the Soil Mechanics and Foundations Division, ASCE, Vol. 107, NO. SM9.

Soil Conservation Service (SCS) (1982), "Technical Release Number 20 (TR-20)," National Technical Information Service.

South Carolina Dept. of Transportation (SCDOT) (2010), Geotechnical Design Manual, available: http://www.scdot.org/doing/structural_Geotechnical.aspx

South Carolina Dept. of Transportation (SCDOT) (2019), Geotechnical Design Manual Version 2.0, available: https://www.scdot.org/business/pdf/geotech/SCDOT-Geotechnical-Design-Manual.pdf

Spencer, E. (1973), "The Thrust Line Criterion in Embankment Stability Analysis," Géotechnique, Vol. 23, No. 1, pp. 85-100, March.

Thomas and Hutton (2012). "Topographic Survey of A Portion of Santee Cooper Winyah Generating Station", prepared for Santee Cooper, 14 January 2014.

Thomas and Hutton. (2015). "Topographic Survey of the Cooling Pond at Santee Cooper Winyah Generating Station."

U.S. Geological Survey (USGS), (2014), "Dynamic: Conterminous U.S. 2014 (v4.2.0) Interactive Deaggregations", 2014. https://earthquake.usgs.gov/hazards/interactive/

FIGURES

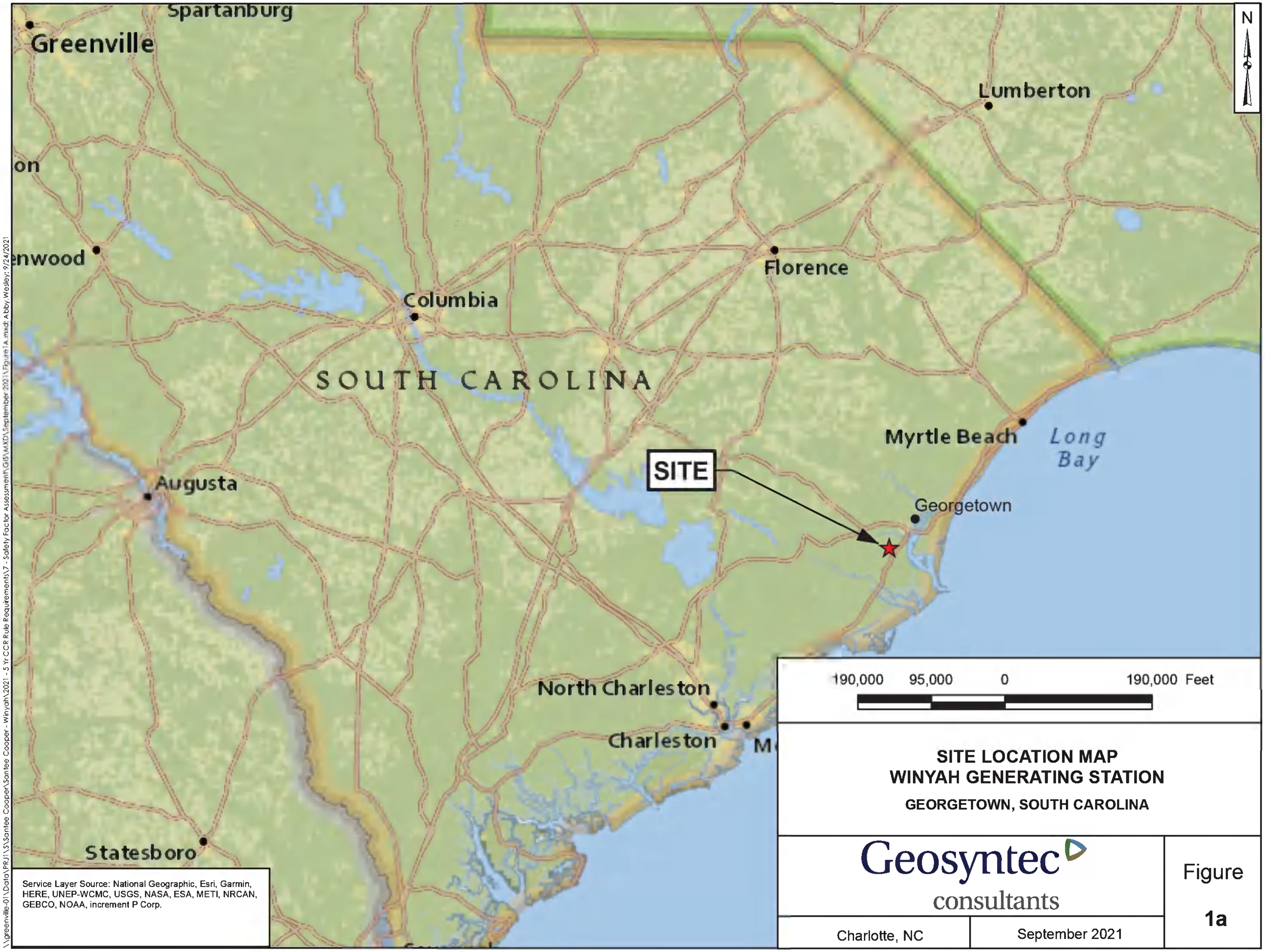

SITE LOCATION MAP
WINYAH GENERATING STATION
GEORGETOWN, SOUTH CAROLINA

Geosyntec consultants

Charlotte, NC | September 2021

Figure **1a**

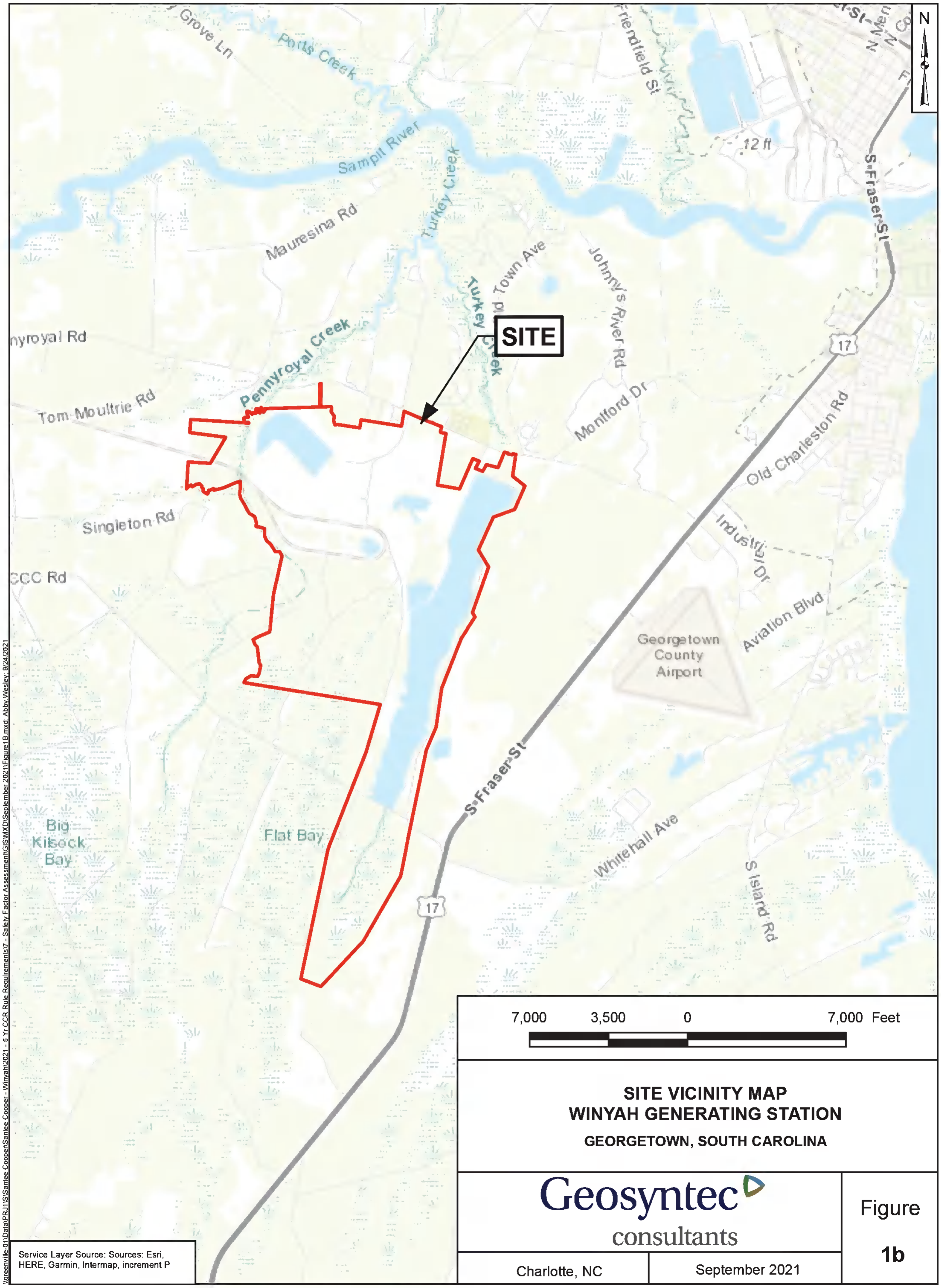

7,000 3,500 0 7,000 Feet

SITE VICINITY MAP
WINYAH GENERATING STATION
GEORGETOWN, SOUTH CAROLINA

Geosyntec consultants

Charlotte, NC | September 2021

Figure **1b**

Service Layer Source: Sources: Esri, HERE, Garmin, Intermap, increment P

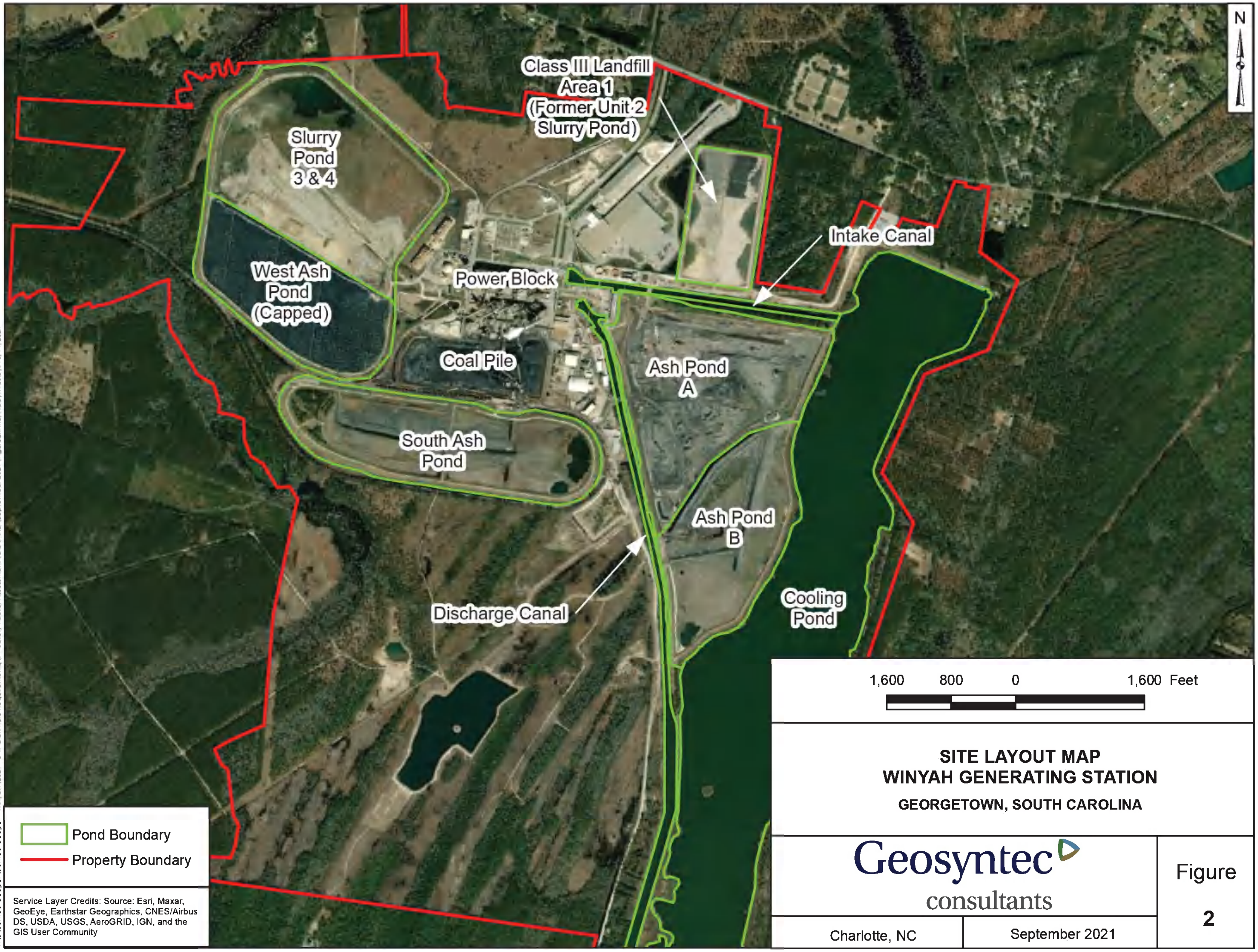

SITE LAYOUT MAP
WINYAH GENERATING STATION

GEORGETOWN, SOUTH CAROLINA

Geosyntec consultants

Charlotte, NC | September 2021

Figure

2

ATTACHMENTS

ATTACHMENT 1

TOPOGRAPHIC SURVEY (SEPTEMBER 2021)

SC GRID NAD 83(2011)

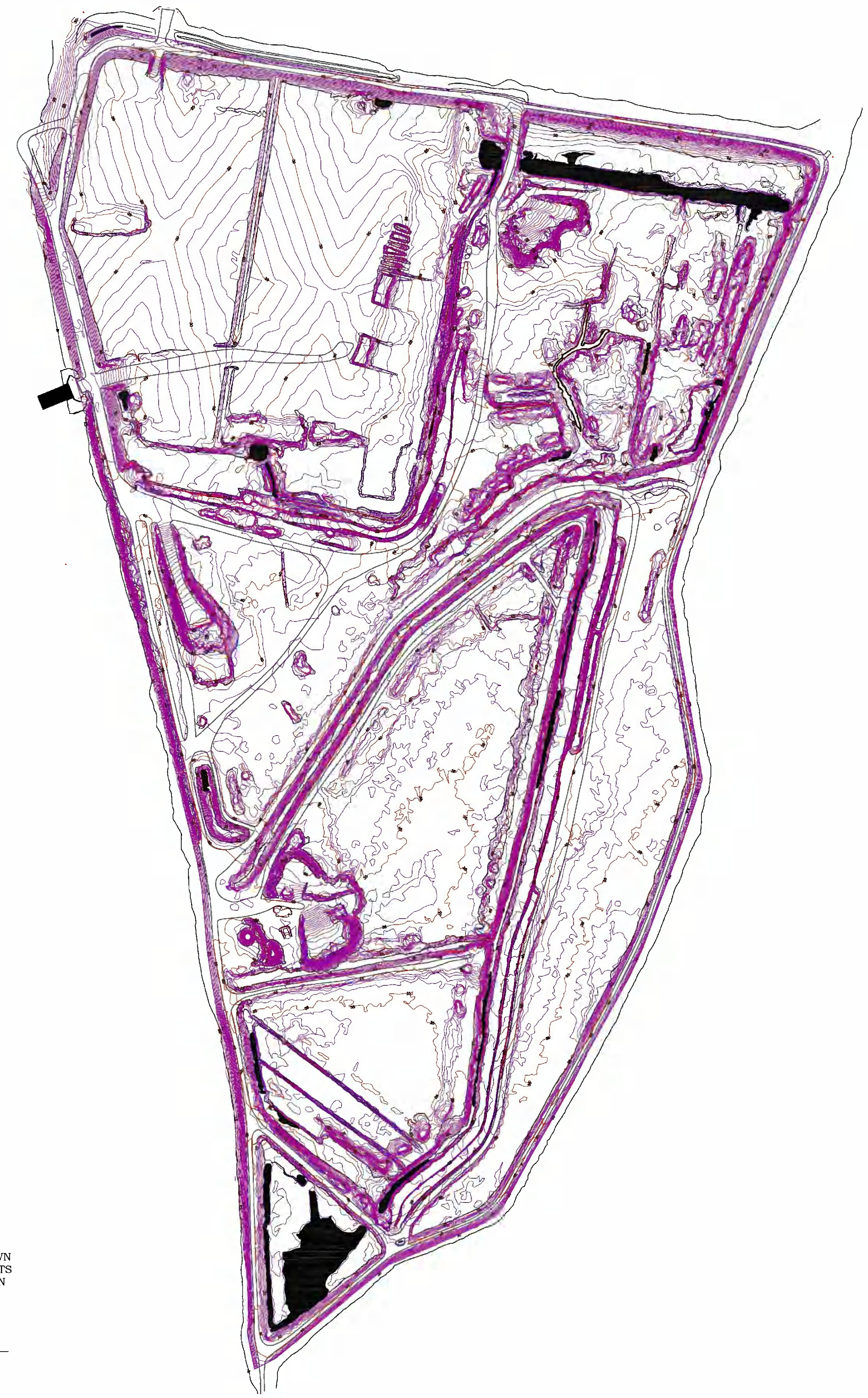

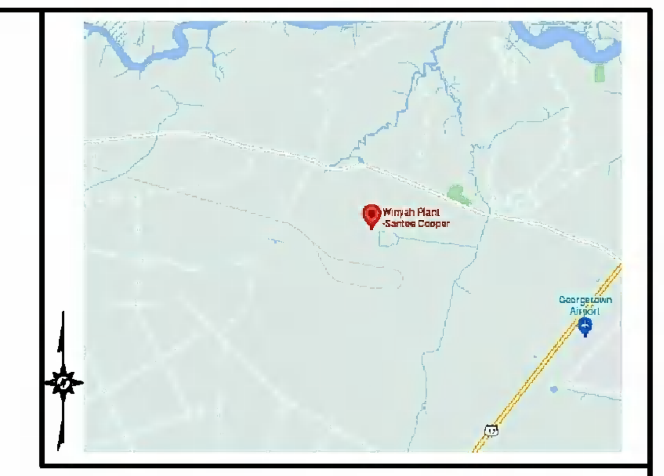

VICINITY MAP – NOT TO SCALE

SURVEYOR'S NOTES

1. ALL DISTANCES ARE HORIZONTAL GROUND IN INTERNATIONAL FEET UNLESS OTHERWISE SHOWN.
2. BEARINGS BASED ON SOUTH CAROLINA NAD83/2011.
3. ELEVATIONS AND CONTOURS SHOWN HERON ARE BASED ON NAVD88. CONTOURS ARE SHOWN AT 1' INTERVALS.
4. SUBSURFACE AND ENVIRONMENTAL CONDITIONS WERE NOT EXAMINED OR CONSIDERED AS A PART OF THIS SURVEY. NO STATEMENT IS MADE CONCERNING THE EXISTENCE OF UNDERGROUND OR OVERHEAD CONTAINERS OR FACILITIES THAT MAY AFFECT THE USE OR DEVELOPMENT OF THIS TRACT.
5. THE EXISTENCE OR NONEXISTENCE OF WETLANDS ON SUBJECT PROPERTY HAS NOT BEEN DETERMINED BY THIS SURVEY.
6. SUBJECT TO ALL EASEMENTS, RIGHT OF WAYS, AND OR ENCUMBRANCES THAT MAY EFFECT THIS PROPERTY.

SIMULTANEOUS AERIAL LIDAR ('50PPSM, AND IMAGERY (~5.7CM GSD) WAS COLLECTED ON 07–24–2021 WITH A FIXED–WING AIRCRAFT EQUIPPED WITH A REIGL 1560II LIDAR SENSOR (SERIAL # S2224887) AND PHASE ONE CAMERA (SERIAL # MM010158). TOPOGRAPHIC MAPPING WAS PERFORMED TO PRODCUE 1"=50' SCALE PLANIMETRICS AND A DIGITAL TERRAIN MODEL (DTM) SUITABLE FOR 1' CONTOURS ALONG WITH 3–INCH PIXEL ORTHOPHOTOS. GROUND CONTROL VALUES CHECKED AGAINS THE LIDAR SURFACE RESULTED IN AN RMSEZ OF 0.088 FT. PHOTO TRIANGULATION RESULTED IN RMS CONTROL OF X: 0.009, Y: 0.012, Z: 0.011,XY: 0.010

" I HEREBY STATE THAT TO THE BEST OF MY PROFESSIONAL KNOWLEDGE, INFORMATION, AND BELIEF, THE SURVEY SHOWN HEREIN WAS MADE IN ACCORDANCE WITH THE REQUIREMENTS OF THE STANDARDS OF PRACTICE MANUAL FOR SURVEYING IN SOUTH CAROLINA, AND MEETS OR EXCEEDS THE REQUIREMENTS AS SPECIFIED THEREIN."

Raymond B. Dawber 9/2/2021

RAYMOND B. DAWBER
SOUTH CAROLINA PROFESSIONAL LAND SURVEYOR
LICENSE NUMBER NO. 24270

SOUTH CAROLINA PROFESSIONAL LAND SURVEYOR No. 24270 RAYMOND B. DAWBER

SOUTH CAROLINA McKIM & CREED INC. NO. 453 CERTIFICATE OF AUTHORIZATION

SCALE: 1" = 150'

0 75 150 300 450

McKIM&CREED
454 DEANNA LANE SUITE A
CHARLESTON SC, 29492
TELEPHONE: (843) 459-7894
SOUTH CAROLINA FIRM COA NUMBER: 453

TOPOPGRAPHIC SURVEY
FOR
WINYAH GENERATING STATION
Ash Ponds A & B
SANTEE COOPER
LOCATION
07-24-2021

JOB NUMBER:	00633–0014
SCALE:	1" = 150'
CAD NUMBER:	CAD#
PLS:	RD
PARTY CHIEF:	JB
CAD TECH:	SV
FIELD BOOK/PAGE:	FB/PG
DRAWING NUMBER:	DWG

SHEET 1 OF 1

ATTACHMENT 2

HYDROLOGIC AND HYDRAULIC ANALYSIS RESULTS

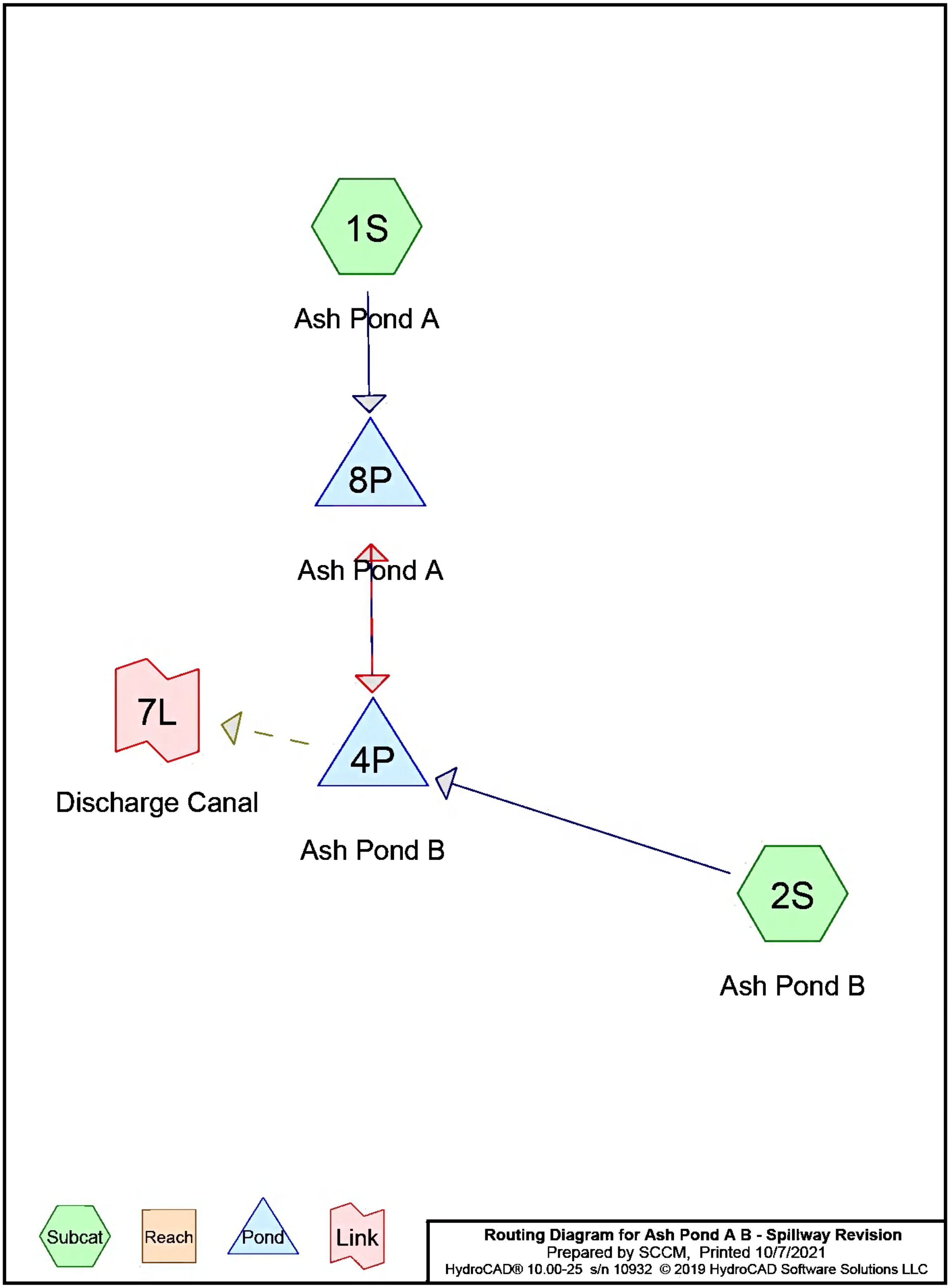

1S
Ash Pond A
8P
Ash Pond A
7L
Discharge Canal
4P
Ash Pond B
2S
Ash Pond B
Subcat
Reach
Pond
Link
Routing Diagram for Ash Pond A B - Spillway Revision
Prepared by SCCM, Printed 10/7/2021
HydroCAD® 10.00-25 s/n 10932 © 2019 HydroCAD Software Solutions LLC

Area Listing (selected nodes)

Area (acres)	CN	Description (subcatchment-numbers)
65.693	87	90% Ash and 10% Water Surface (2S)
88.900	86	CCR (1S)
154.593	**86**	**TOTAL AREA**

Soil Listing (selected nodes)

Area (acres)	Soil Group	Subcatchment Numbers
0.000	HSG A	
0.000	HSG B	
0.000	HSG C	
0.000	HSG D	
154.593	Other	1S, 2S
154.593		**TOTAL AREA**

Ground Covers (selected nodes)

HSG-A (acres)	HSG-B (acres)	HSG-C (acres)	HSG-D (acres)	Other (acres)	Total (acres)	Ground Cover	Subcatchment Numbers
0.000	0.000	0.000	0.000	65.693	65.693	90% Ash and 10% Water Surface	2S
0.000	0.000	0.000	0.000	88.900	88.900	CCR	1S
0.000	**0.000**	**0.000**	**0.000**	**154.593**	**154.593**	**TOTAL AREA**	

Pipe Listing (selected nodes)

Line#	Node Number	In-Invert (feet)	Out-Invert (feet)	Length (feet)	Slope (ft/ft)	n	Diam/Width (inches)	Height (inches)	Inside-Fill (inches)
1	4P	30.21	16.99	113.3	0.1167	0.013	21.6	0.0	0.0
2	4P	35.52	36.50	40.8	-0.0240	0.025	30.0	0.0	0.0
3	4P	34.28	34.49	30.9	-0.0068	0.012	48.0	0.0	0.0
4	4P	34.70	35.20	24.6	-0.0203	0.012	42.0	0.0	0.0
5	8P	36.50	35.52	40.8	0.0240	0.025	30.0	0.0	0.0
6	8P	34.49	34.28	30.9	0.0068	0.012	48.0	0.0	0.0
7	8P	35.20	34.70	24.6	0.0203	0.012	42.0	0.0	0.0

Time span=0.00-900.00 hrs, dt=0.01 hrs, 90001 points
Runoff by SCS TR-20 method, UH=SCS, Weighted-CN
Reach routing by Sim-Route method - Pond routing by Sim-Route method

Subcatchment 1S: Ash Pond A Runoff Area=88.900 ac 0.00% Impervious Runoff Depth=11.03"
Flow Length=2,400' Tc=9.9 min CN=86 Runoff=392.93 cfs 81.747 af

Subcatchment 2S: Ash Pond B Runoff Area=65.693 ac 0.00% Impervious Runoff Depth=11.17"
Flow Length=3,100' Slope=0.0010 '/' Tc=10.8 min CN=87 Runoff=289.00 cfs 61.130 af

Pond 4P: Ash Pond B Peak Elev=35.14' Storage=80.298 af Inflow=289.00 cfs 61.130 af
Primary=2.88 cfs 3.339 af Secondary=0.00 cfs 0.000 af Tertiary=16.95 cfs 46.431 af Outflow=19.84 cfs 49.770 af

Pond 8P: Ash Pond A Peak Elev=24.06' Storage=85.072 af Inflow=393.04 cfs 85.086 af
Primary=0.00 cfs 0.000 af Secondary=0.00 cfs 0.000 af Outflow=0.00 cfs 0.000 af

Link 7L: Discharge Canal Inflow=16.95 cfs 46.431 af
Primary=16.95 cfs 46.431 af

Total Runoff Area = 154.593 ac Runoff Volume = 142.876 af Average Runoff Depth = 11.09"
100.00% Pervious = 154.593 ac 0.00% Impervious = 0.000 ac

Summary for Subcatchment 1S: Ash Pond A

Runoff = 392.93 cfs @ 36.14 hrs, Volume= 81.747 af, Depth=11.03"

Runoff by SCS TR-20 method, UH=SCS, Weighted-CN, Time Span= 0.00-900.00 hrs, dt= 0.01 hrs
Type III 24-hr 72.00 hrs 100-YR, 72-HR Rainfall=12.80"

	Area (ac)	CN	Description
*	88.900	86	CCR
	88.900		100.00% Pervious Area

Tc (min)	Length (feet)	Slope (ft/ft)	Velocity (ft/sec)	Capacity (cfs)	Description
1.0	100	0.0663	1.61		**Sheet Flow, Sheet Flow** n= 0.020 P2= 4.38"
8.9	2,300	0.0010	4.32	634.77	**Channel Flow, Channel Flow** Area= 147.0 sf Perim= 59.0' r= 2.49' n= 0.020
9.9	2,400	Total			

Subcatchment 1S: Ash Pond A

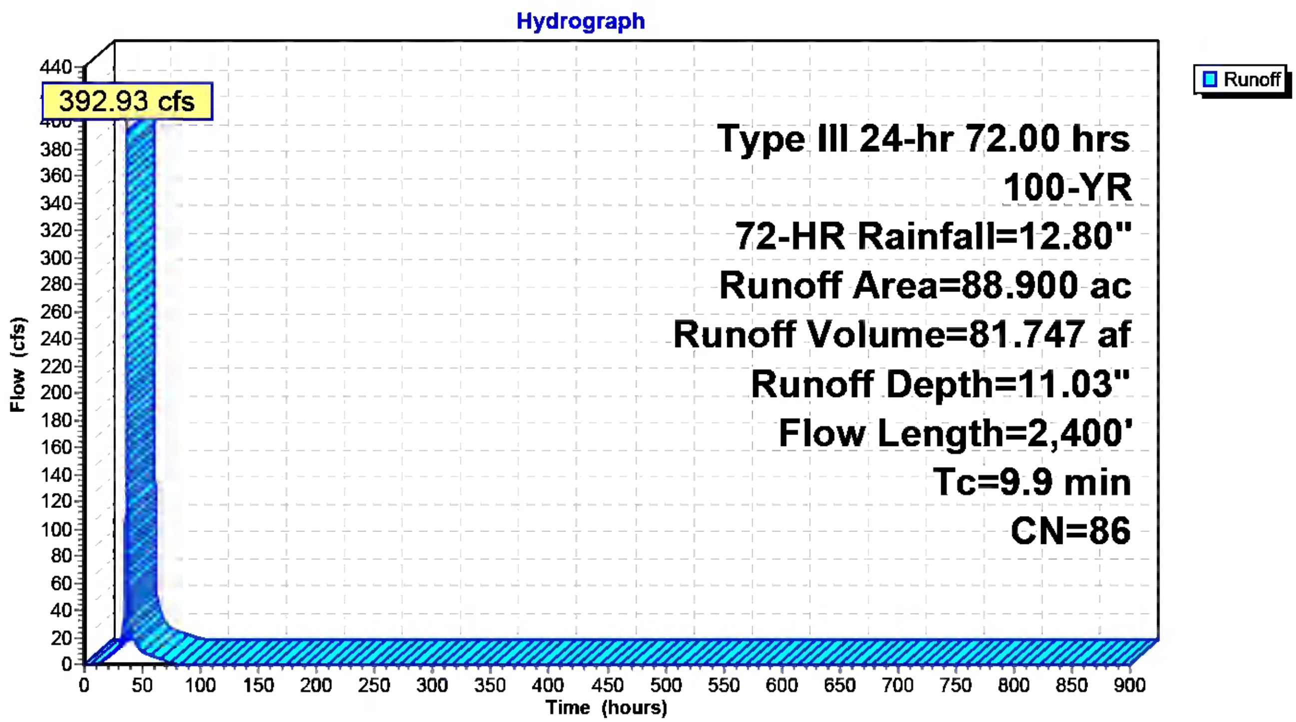

Summary for Subcatchment 2S: Ash Pond B

Runoff = 289.00 cfs @ 36.15 hrs, Volume= 61.130 af, Depth=11.17"

Runoff by SCS TR-20 method, UH=SCS, Weighted-CN, Time Span= 0.00-900.00 hrs, dt= 0.01 hrs
Type III 24-hr 72.00 hrs 100-YR, 72-HR Rainfall=12.80"

	Area (ac)	CN	Description
*	65.693	87	90% Ash and 10% Water Surface
	65.693		100.00% Pervious Area

Tc (min)	Length (feet)	Slope (ft/ft)	Velocity (ft/sec)	Capacity (cfs)	Description
10.8	3,100	0.0010	4.77	510.30	**Channel Flow, Channel Flow** Area= 107.0 sf Perim= 37.0' r= 2.89' n= 0.020

Subcatchment 2S: Ash Pond B

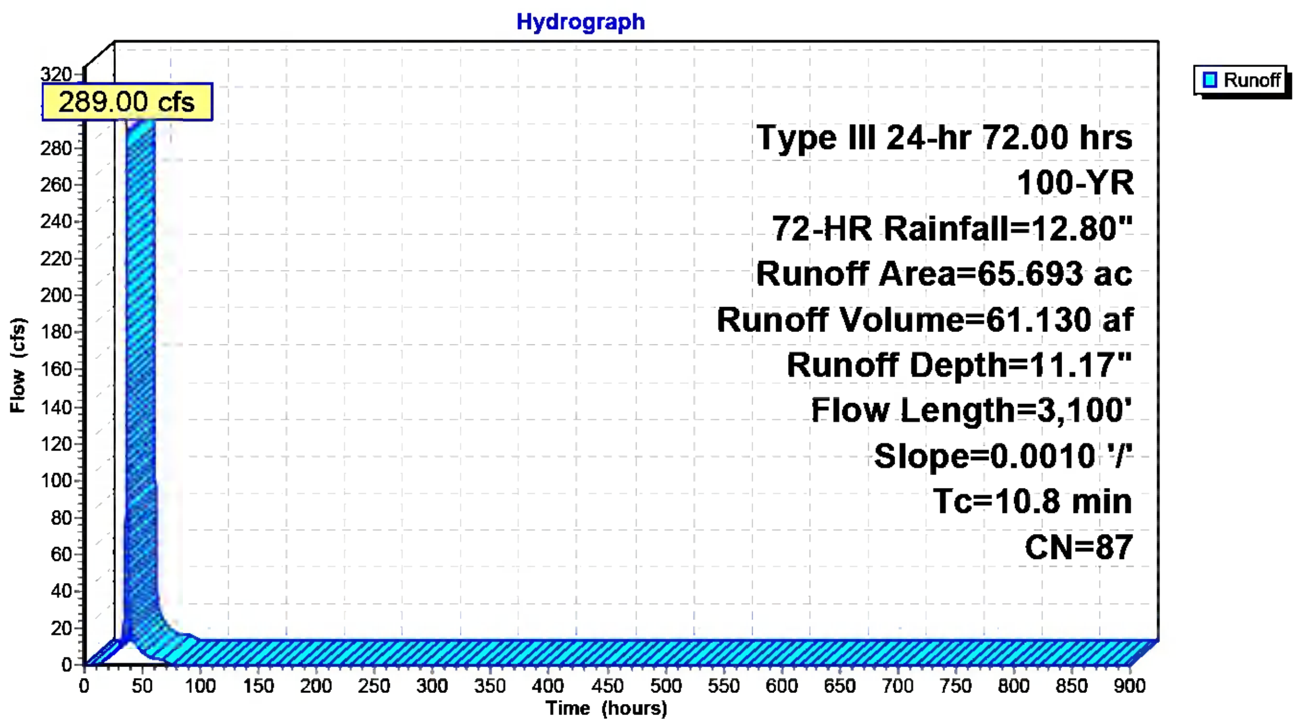

Summary for Pond 4P: Ash Pond B

Inflow =	289.00 cfs @	36.15 hrs,	Volume=	61.130 af
Outflow =	19.84 cfs @	39.36 hrs,	Volume=	49.770 af, Atten= 93%, Lag= 192.3 min
Primary =	2.88 cfs @	39.36 hrs,	Volume=	3.339 af
Secondary =	0.00 cfs @	0.00 hrs,	Volume=	0.000 af
Tertiary =	16.95 cfs @	39.36 hrs,	Volume=	46.431 af

Routing by Sim-Route method, Time Span= 0.00-900.00 hrs, dt= 0.01 hrs
Starting Elev= 33.14' Surf.Area= 12.744 ac Storage= 41.153 af
Peak Elev= 35.14' @ 39.36 hrs Surf.Area= 27.906 ac Storage= 80.298 af (39.145 af above start)

Plug-Flow detention time= 5,856.7 min calculated for 8.617 af (14% of inflow)
Center-of-Mass det. time= 1,574.5 min (3,880.9 - 2,306.3)

Volume	Invert	Avail.Storage	Storage Description
#1	21.00'	235.686 af	**Custom Stage Data (Prismatic)** Listed below (Recalc)

Elevation (feet)	Surf.Area (acres)	Inc.Store (acre-feet)	Cum.Store (acre-feet)
21.00	0.110	0.000	0.000
22.00	0.174	0.142	0.142
23.00	0.482	0.328	0.470
24.00	0.975	0.728	1.198
25.00	1.245	1.110	2.308
26.00	1.474	1.359	3.668
27.00	1.800	1.637	5.305
28.00	2.451	2.125	7.430
29.00	3.866	3.159	10.589
30.00	5.289	4.577	15.166
31.00	6.338	5.813	20.980
32.00	9.304	7.821	28.801
33.00	11.944	10.624	39.425
34.00	17.658	14.801	54.226
35.00	26.792	22.225	76.451
36.00	34.713	30.752	107.203
37.00	41.359	38.036	145.239
38.00	45.093	43.226	188.465
39.00	49.349	47.221	235.686

Device	Routin	Invert	Outlet Devices
#1	Tertiary	30.21'	**21.6" Round Culvert** L= 113.3' CPP, projecting, no headwall, Ke= 0.900 Inlet / Outlet Invert= 30.21' / 16.99' S= 0.1167 '/' Cc= 0.900 n= 0.013 Corrugated PE, smooth interior, Flow Area= 2.54 sf
#2	Device 1	33.90'	**4.0' long Sharp-Crested Rectangular Weir** 2 End Contraction(s)
#3	Primary	36.50'	**30.0" Round Culvert 1** L= 40.8' CMP, projecting, no headwall, Ke= 0.900 Inlet / Outlet Invert= 35.52' / 36.50' S= -0.0240 '/' Cc= 0.900 n= 0.025 Corrugated metal, Flow Area= 4.91 sf
#4	Primary	34.49'	**48.0" Round Culvert 2** L= 30.9' CMP, projecting, no headwall, Ke= 0.900

			Inlet / Outlet Invert= 34.28' / 34.49' S= -0.0068 '/' Cc= 0.900 n= 0.012 Steel, smooth, Flow Area= 12.57 sf
#5	Primary	35.20'	**42.0" Round Culvert 3** L= 24.6' CMP, projecting, no headwall, Ke= 0.900 Inlet / Outlet Invert= 34.70' / 35.20' S= -0.0203 '/' Cc= 0.900 n= 0.012 Steel, smooth, Flow Area= 9.62 sf
#6	Secondary	36.00'	**85.0' long x 11.5' breadth Broad-Crested Rectangular Weir** Head (feet) 0.20 0.40 0.60 0.80 1.00 1.20 1.40 1.60 Coef. (English) 2.55 2.60 2.70 2.67 2.67 2.67 2.66 2.64

Primary OutFlow Max=2.88 cfs @ 39.36 hrs HW=35.14' TW=23.03' (Dynamic Tailwater)
3=Culvert 1 (Controls 0.00 cfs)
4=Culvert 2 (Inlet Controls 2.88 cfs @ 2.17 fps)
5=Culvert 3 (Controls 0.00 cfs)

Secondary OutFlow Max=0.00 cfs @ 0.00 hrs HW=33.14' TW=17.00' (Dynamic Tailwater)
6=Broad-Crested Rectangular Weir (Controls 0.00 cfs)

Tertiary OutFlow Max=16.95 cfs @ 39.36 hrs HW=35.14' TW=23.15' (Dynamic Tailwater)
1=Culvert (Passes 16.95 cfs of 19.42 cfs potential flow)
2=Sharp-Crested Rectangular Weir (Weir Controls 16.95 cfs @ 3.64 fps)

Pond 4P: Ash Pond B

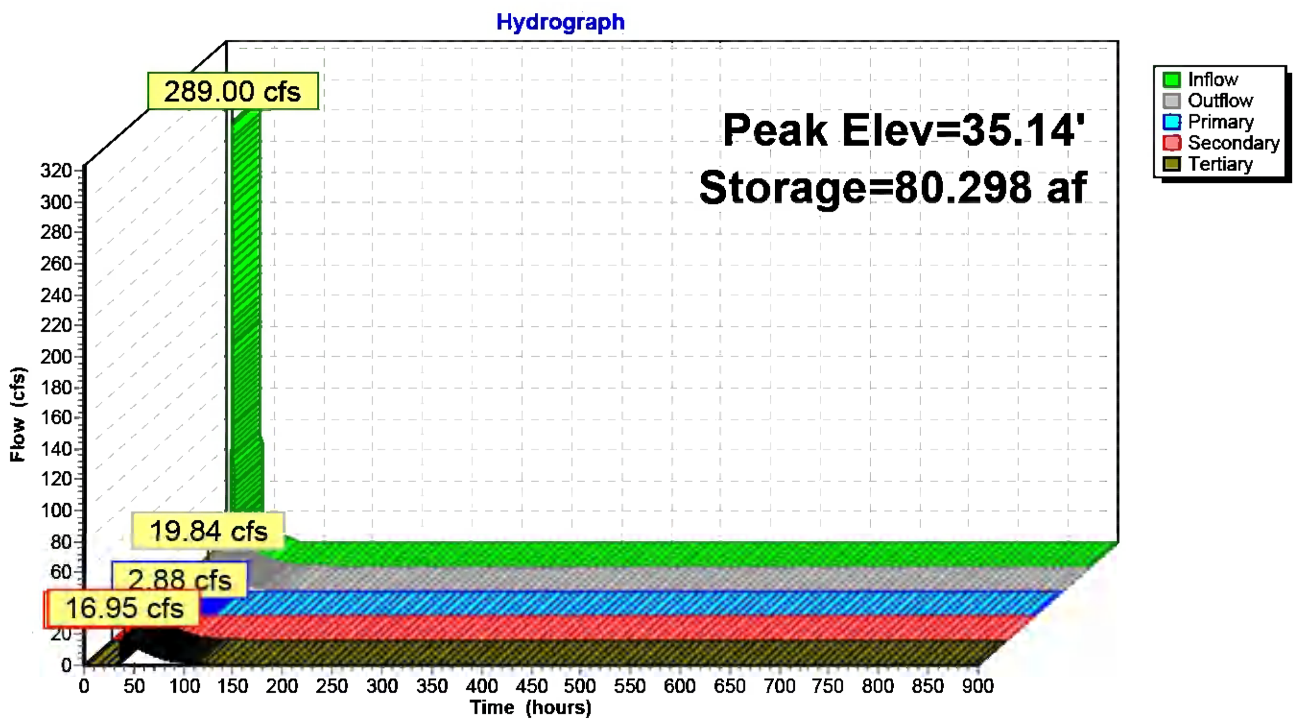

Elevation in NAVD 88

Summary for Pond 8P: Ash Pond A

Inflow =	393.04 cfs @	36.14 hrs,	Volume=	85.086 af
Outflow =	0.00 cfs @	0.00 hrs,	Volume=	0.000 af, Atten= 100%, Lag= 0.0 min
Primary =	0.00 cfs @	0.00 hrs,	Volume=	0.000 af
Secondary =	0.00 cfs @	0.00 hrs,	Volume=	0.000 af

Routing by Sim-Route method, Time Span= 0.00-900.00 hrs, dt= 0.01 hrs
Peak Elev= 24.06' @ 73.10 hrs Surf.Area= 26.727 ac Storage= 85.072 af

Plug-Flow detention time= (not calculated: initial storage exceeds outflow)
Center-of-Mass det. time= (not calculated: no outflow)

Volume	Invert	Avail.Storage	Storage Description
#1	17.00'	837.990 af	**Custom Stage Data (Prismatic)**Listed below (Recalc)

Elevation (feet)	Surf.Area (acres)	Inc.Store (acre-feet)	Cum.Store (acre-feet)
17.00	1.463	0.000	0.000
18.00	2.653	2.058	2.058
19.00	5.950	4.301	6.359
20.00	8.019	6.984	13.344
21.00	12.211	10.115	23.459
22.00	17.713	14.962	38.421
23.00	23.002	20.357	58.778
24.00	26.325	24.664	83.442
25.00	32.861	29.593	113.035
26.00	34.797	33.829	146.864
27.00	37.477	36.137	183.001
28.00	41.370	39.424	222.425
29.00	48.989	45.179	267.604
30.00	53.062	51.026	318.629
31.00	56.826	54.944	373.573
32.00	61.765	59.295	432.869
33.00	69.069	65.417	498.286
34.00	68.844	68.957	567.242
35.00	69.304	69.074	636.317
36.00	72.249	70.776	707.093
37.00	72.617	72.433	779.526
38.00	44.312	58.465	837.990

Device	Routing	Invert	Outlet Devices
#1	Primary	36.50'	**30.0" Round Culvert 1** L= 40.8' CMP, projecting, no headwall, Ke= 0.900 Inlet / Outlet Invert= 36.50' / 35.52' S= 0.0240 '/' Cc= 0.900 n= 0.025 Corrugated metal, Flow Area= 4.91 sf
#2	Primary	34.49'	**48.0" Round Culvert 2** L= 30.9' CMP, projecting, no headwall, Ke= 0.900 Inlet / Outlet Invert= 34.49' / 34.28' S= 0.0068 '/' Cc= 0.900 n= 0.012 Steel, smooth, Flow Area= 12.57 sf
#3	Primary	35.20'	**42.0" Round Culvert 3** L= 24.6' CMP, projecting, no headwall, Ke= 0.900

			Inlet / Outlet Invert= 35.20' / 34.70' S= 0.0203 '/' Cc= 0.900 n= 0.012 Steel, smooth, Flow Area= 9.62 sf
#4	Secondary	36.00'	**86.5' long x 11.0' breadth Broad-Crested Rectangular Weir** Head (feet) 0.20 0.40 0.60 0.80 1.00 1.20 1.40 1.60 Coef. (English) 2.53 2.59 2.70 2.68 2.67 2.68 2.66 2.64

Primary OutFlow Max=0.00 cfs @ 0.00 hrs HW=17.00' TW=33.14' (Dynamic Tailwater)
1=Culvert 1 (Controls 0.00 cfs)
2=Culvert 2 (Controls 0.00 cfs)
3=Culvert 3 (Controls 0.00 cfs)

Secondary OutFlow Max=0.00 cfs @ 0.00 hrs HW=17.00' TW=33.14' (Dynamic Tailwater)
4=Broad-Crested Rectangular Weir (Controls 0.00 cfs)

Pond 8P: Ash Pond A

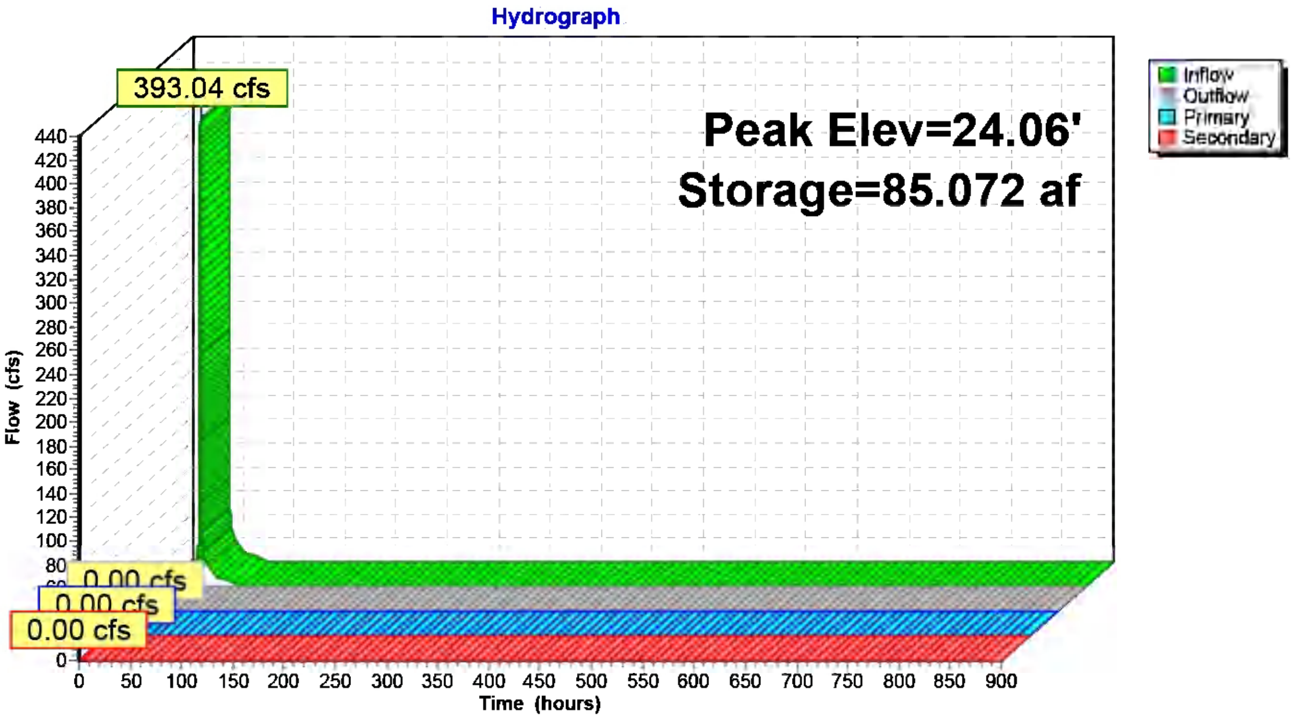

Summary for Link 7L: Discharge Canal

Inflow	=	16.95 cfs @	39.36 hrs,	Volume=	46.431 af
Primary	=	16.95 cfs @	39.37 hrs,	Volume=	46.431 af, Atten= 0%, Lag= 0.6 min

Primary outflow = Inflow, Time Span= 0.00-900.00 hrs, dt= 0.01 hrs

Fixed water surface Elevation= 23.15'

Link 7L: Discharge Canal

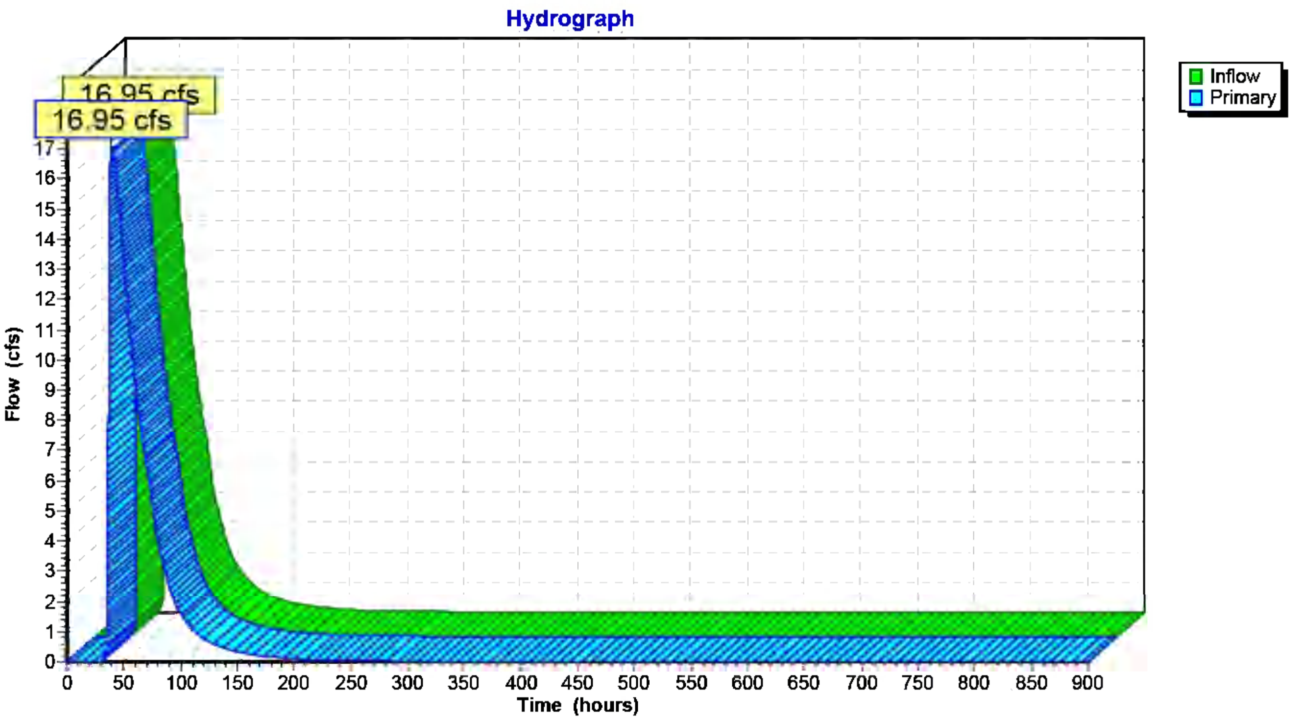

ATTACHMENT 3

SEISMIC HAZARD EVALUATION AND SITE RESPONSE ANALYSIS

SEISMIC HAZARD EVALUATION AND SITE RESPONSE ANALYSIS: ASH POND B

PURPOSE

The purpose of this calculation package is to present the results of the seismic hazard evaluation and site response analyses performed for Ash Pond B at the Winyah Generating Station (WGS or Site). This calculation package is provided as Attachment 3 to the *2021 Periodic Safety Factor Assessment* (2021 Safety Factor Assessment Report). Seismic hazard analysis for the Site includes the selection of an appropriate hazard level and associated hazard parameters. Based on the selected hazard level and associated hazard parameters, site response analyses were performed to evaluate the local site effects on the selected time history records propagated from the hypothetical firm ground outcrop to the ground surface of the Site. The objective of this site response analysis is to calculate accelerations and shear stresses within the critical representative soil profile of the Ash Pond B perimeter dikes. Cyclic shear stresses will be used to evaluate liquefaction potential for dike fill and foundation soils and to calculate the seismic coefficient for seismic slope stability analyses presented in Attachments 4 and 5 of the 2021 Safety Factor Assessment Report, respectively.

SEISMIC HAZARD EVALUATION

Seismic hazard analysis for the Site includes the selection of: (i) appropriate hazard level; and (ii) associated hazard parameters. The appropriate hazard level is often expressed in probabilistic terms as a specific hazard level that has a certain probability of exceedance in a given time period. Selecting the hazard parameters includes developing an understanding of the seismic sources, ground motion attenuation, and site response. The goals of this section are to: (i) develop the target response spectrum, including the peak ground acceleration (PGA), at a hypothetical firm ground outcrop at WGS corresponding to the appropriate seismic hazard level; (ii) select the earthquake magnitude that contributes predominantly to the seismic hazard at WGS; and (iii) select a set of ground motion time histories that envelope the target spectrum, and are generally consistent with the source and path characteristics of ground motions at WGS.

Seismic Hazard Level

On 17 April 2015, the United States Environmental Protection Agency (USEPA) published the CCR Rule (40 Code of Federal Regulations [CFR] Parts 257 and 261). §257.63(a) of the CCR Rule states that:

"New CCR landfills, existing and new CCR surface impoundments, and all lateral expansions of CCR units must not be located in seismic impact zones, unless the owner or operator demonstrates

by the dates specified in paragraph (c) of this section that all structural components including liners, leachate collection and removal systems, and surface water control systems, are designed to resist the maximum horizontal acceleration in lithified earth material for the site."

§257.53 of the CCR Rule defines the maximum horizontal acceleration in lithified earth material as:

"... the maximum expected horizontal acceleration at the ground surface as depicted on a seismic hazard map, with a 98 percent or greater probability that the acceleration will not be exceeded in 50 years, or the maximum expected horizontal acceleration based on a site-specific seismic risk assessment."

A 98 percent or greater probability of not being exceeded in 50 years (or 2 percent probability of exceedance in 50 years) corresponds to a return period of approximately 2,500 years. The Preamble of the CCR Rule indicates that USEPA selected this return period by considering a typical operating life for CCR surface impoundments (i.e., 50 years) and its common use in seismic design criteria throughout engineering (e.g., American Society of Civil Engineers [ASCE] 7-16 [2016]). For the CCR surface impoundments at WGS, closure was initiated in 2021 and is expected to be complete in less than 15 years. Therefore, an earthquake return period of approximately 750 years was conservatively selected for the 2021 Safety Factor Assessment of Ash Pond B (i.e., two percent probability of exceedance in 15 years) following the basis for selecting the return period of approximately 2,500 years for typical CCR surface impoundments. A 750-year return period is approximately equivalent to an annual frequency of exceedance of 1.33E-03.

Peak Ground Acceleration (PGA)

PGA values corresponding to different hazard levels and different site conditions, including firm ground outcrops, are published as seismic hazard maps or curves. The 2016 Safety Factor Assessment Report (Geosyntec, 2016) referenced seismic hazard maps presented in the South Carolina Department of Transportation (SCDOT) Geotechnical Design Manual (GDM) (SCDOT, 2010) for selection of a PGA to incorporate local site effects for the Charleston Seismic Zone researched by Chapman and Talwani (2006). The GDM was updated in 2019 (SCDOT, 2019) and does not present the seismic hazard maps referenced in the 2016 Safety Factor Assessment Report. Moreover, SCDOT is updating seismic hazard maps at the time of this seismic hazard evaluation.

As an alternative, United States Geological Survey (USGS) hazard curves for two percent probability of exceedance in 15 year ground motion (i.e., approximately 750-year return period event) at the BC boundary (i.e., boundary between National Earthquake Hazard Reduction Program [NEHRP] site classes B and C with a mean shear wave velocity of 2,500 ft/s) were used to estimate the PGA and spectral accelerations for a hypothetical firm ground outcrop, similar to "geologically realistic" site conditions, at the Site. The data available at the USGS website (Petersen et al., 2019) use pre-calculated hazard values at nearby grid locations and interpolate the hazard value for a given site location. As presented in Figure 1, the interpolated PGA from USGS hazard curves is 0.15g for the Site.

Earthquake Magnitude

In a probabilistic seismic hazard analysis, the PGA cannot be associated with a single earthquake event due to the hazard contribution from multiple possible events. An earthquake moment magnitude (M_W) value is required to conduct liquefaction potential analyses and select earthquake time histories. A process called deaggregation can be performed for sites that have multiple hazard sources using the most up-to-date USGS (2014) deaggregation tool.

Figure 2 presents the deaggregation for the PGA at the Site. A 7.3 moment magnitude earthquake event at a source-to-site distance of approximately 70 km is the modal event contributing to the hazard at the Site. Thus, a 7.3 moment magnitude was selected for liquefaction potential analyses and time history selection for WGS.

Target Acceleration Response Spectra

Using the USGS hazard curves, the uniform hazard spectrum (UHS) was developed for an approximately 750-year return period event at the BC boundary to represent the "geologically realistic" target acceleration response spectrum for WGS (Figure 3). The "geologically realistic" target acceleration response spectrum has a PGA (represented by a spectral period of 0.005 seconds) of 0.15g and a peak spectral acceleration of 0.40g at a spectral period of 0.075 seconds.

Time Histories

Time histories of ground motions are used as input for site response analysis and are selected such that their response spectra match or exceed the target spectrum. While use of recorded ground motion time histories from earthquakes with similar source characteristics is preferred, synthetic motions may be used if recordings are not available for a particular tectonic setting. Earthquake events with a moment magnitude, M_W, 7.0 or greater have not occurred in the stable continental tectonic environment of the Central and Eastern United States since the Charleston earthquake in 1886, so ground motion time history records matching the seismic source characteristics for the WGS are generally not available. Two synthetic acceleration time histories were selected from the six synthetic acceleration time histories developed for the Site using the USGS Interactive Deaggregation tool (USGS, 2002). These time histories are referred to herein as Winyah1 and Winyah2, and provide a reasonable match to the short-period portion of the "geologically realistic" target acceleration response spectrum. Three time histories, BOS-T1, DEL090, and YER360, were selected to provide a conservative envelope for the long-period portion of the "geologically realistic" target acceleration response spectrum. The three time histories were developed by McGuire et al. (2001) as part of a study for the Nuclear Regulatory Commission to provide time histories representative of expected earthquake events in the Central and Eastern United States. Also, one time history (RSN8529-HNE) from the Next Generation Attenuation – East (NGA East) database (Goulet et al., 2014), which provides a database of time histories recorded for earthquake events in the Central and Eastern United States, was selected to also provide a conservative envelope for the long-period portion of the "geologically realistic" target acceleration response spectrum. As shown in Figure 4, this suite of six time histories provides a reasonable envelope of the "geologically realistic" target spectrum for the Site over a broad range of periods. Time histories were scaled in the site response evaluation computer program to match the target PGA of 0.15g. These scaled acceleration time histories are presented in Appendix 1. Additional details of the time histories are presented in Table 1.

SITE RESPONSE ANALYSIS

Site response analyses were performed to evaluate the effect of local site conditions on the propagation of earthquake ground motions at the Site. The objective of the site response analysis for the 2021 Safety Factor Assessment Report is to calculate updated accelerations and shear stresses at the critical profile observed in the 2016 Safety Factor Assessment (Geosyntec, 2016). Calculated shear stresses are used to evaluate the liquefaction potential (Attachment 4 of the 2021 Safety Factor Assessment Report) and seismic stability (Attachment 5 of the 2021 Safety Factor Assessment Report) for the Ash Pond B perimeter dikes.

Methodology for Site Response Analysis

Site response analyses presented herein were conducted using DEEPSOIL® (Hashash et al., 2020), a one-dimensional nonlinear site response analysis program. The program assumes that all the soil layers are perfectly horizontal (i.e., "layer cake") and that ground response is mainly caused by vertically-propagating, horizontally polarized shear waves. This assumption is valid for many geotechnical cases including the analyses of the Site. Under these assumptions, the subsurface stratigraphy is modeled as a one-dimensional column of soil layers for the analyses.

DEEPSOIL® employs a viscoelastic material model, described by its shear modulus (G), mass density (ρ) or unit weight (γ), and material damping ratio (D). Preliminary equivalent-linear site response analyses yielded calculated maximum shear strains greater than five percent in some layers, which is greater than the shear strains for which equivalent-linear analyses are considered applicable (i.e., one to two percent) (Kaklamanos et al., 2013). Therefore, nonlinear site response analyses were performed.

Input Parameters for Site Response Analysis

Input Motions

As discussed in the Time Histories subsection, six acceleration time histories were selected and scaled to match the target PGA of 0.15g. These ground motions were applied as outcrop motions in DEEPSOIL® at the top of the half space.

Representative Soil Profile

Santee Cooper personnel indicated that no changes were made to the Ash Pond B perimeter dikes and adjacent areas outside the dikes since preparation of the 2016 Safety Factor Assessment Report. Also, no additional geotechnical subsurface investigations have been conducted since 2016. Therefore, the subsurface stratigraphy developed in the 2016 Safety Factor Assessment is still valid and was also used for the 2021 Safety Factor Assessment. A detailed description of the subsurface stratigraphy is presented in the 2016 Safety Factor Assessment Report (Geosyntec, 2016). Information specific to the site response analysis is presented herein.

To develop representative soil profiles, the Ash Pond B perimeter dike was divided into two sections depending on the depth of the dike fill and the V_s profile of the subsurface as shown in Figure 5. The top of the dike is roughly at the same elevation by the intake/discharge canals (West) and the cooling pond (East). However, the dike fill extends to greater depths near the cooling pond. Two representative profiles to 100 ft below ground surface (bgs) were developed for the perimeter dike: (i) one by the intake/discharge canals (Profile 1); and (ii) one by the cooling pond (Profile 2). The 2016 Safety Factor Assessment identified a section with lower calculated factors for slope stability along the Cooling Pond (Geosyntec, 2016). Therefore, site response analyses were only performed for Profile 2, which contains the critical section identified in the 2016 Safety Factor Assessment, for the 2021 Safety Factor Assessment Report to provide an updated evaluation of the critical area of Ash Pond B. The representative profile is shown in Figure 6.

A review of the topographic survey data from August 2021 (McKim & Creed, 2021) indicated the top of ash surface adjacent to Profile 2 of Ash Pond B is similar to the surface used for the 2016 Safety Factor Assessment Report . Santee Cooper provided available water level measurements from wells in the area of Ash Pond B. The recorded water levels in these wells have generally been steady over the last five years. Based on the review of the topographic survey and available water level measurements adjacent to Profile 2, the water level within the perimeter dike is expected to be similar to the water level used for the 2016 Safety Factor Assessment Report. The site response analyses for Ash Pond B in the 2016 Safety Factor Assessment Report considered a water table 15 ft bgs. Therefore, site response analyses for the 2021 Safety Factor Assessment were performed with the water table modeled at 15 ft bgs.

Profile 2 was extended to a depth of 500 ft bgs using information on deep V_s profiles derived from URS (2001) and S&ME (2001). At that depth, the deep V_s profiles indicate the presence of firm Coastal Plain sediments with V_s of approximately 2,300 ft/s, which is consistent with the definition of "geologically realistic" soil conditions and approximately represents the BC boundary. The site response analysis presented in this package thus considers the full depth of the soil column (i.e., 500 ft bgs), but results are presented for the soil column to a depth of approximately 100 ft bgs to emphasize the near-surface response.

Dynamic Soil Properties

Shear Modulus Reduction and Damping Curves

The modified Kondner-Zelasko model implemented in DEEPSOIL® is described in Matasovic (1993). The shear modulus reduction and damping curves are required as input parameters to the constitutive soil model, and were developed with consideration of regional soil characteristics based on guidance presented in the SCDOT GDM (2019) and previous geotechnical reports of the Site. Adopting relationships proposed by Stokoe et al. (1995 and 1999), Andrus et al. (2003) developed regression equations for shear modulus reduction and damping curves suitable for South Carolina soils. The regression equations are presented in the SCDOT GDM (2019). These region-specific curves are a function of the plasticity index (PI) of the soil, effective mean stress, and geologic age and location of soil deposits. Geologic interpretation of the foundation soil at WGS by Paul C. Rizzo Associates (PCRA) (PCRA, 1999) and the SC Department of Natural Resources (DNR) (2012) indicates the native foundation soils above the Chicora and Williamsburg Formation strata are Pleistocene deposits. The dike fill soils were considered to be a Holocene deposit because the perimeter dikes were constructed of compacted earthen fill in 1979-1980. The shear modulus reduction and damping curves were calculated for the dike fill and foundation soils located above the Chicora and Williamsburg Formation strata. Soft rock curves (Silva et al., 1997) were selected for the Chicora and Williamsburg Formation strata to be consistent with the V_s-based classification indicating soft rock conditions. Pacific Engineering (S&ME, 2001) also used these soft rock shear modulus reduction and damping curves to perform the site response analysis of an ammonia tank building onsite. Figure 7 presents shear modulus reduction and damping curves used for these analyses. An example of the development of the dynamic curves and the references are provided in Appendix 2.

Representative Shear Wave Velocity Profile

Geosyntec developed representative V_s profiles of the dike fill and foundation soils using both direct measurements from Seismic Cone Penetration Tests (SCPTs) and estimates using Cone Penetration Tests (CPTs) and associated correlations. Upon evaluation of several correlations, the Mayne (2006) correlation was found to agree most closely with results of site-specific V_s measurements. This correlation is as follows:

$$V_s = 118.8 \log (f_s) + 18.5$$

where,

V_s = shear wave velocity (m/sec); and
f_s = sleeve friction from CPT (kPa).

Appendix 3 presents SCPT measurements, estimated values, and the selected V_s profile. Figure 8 shows the shallow (depths less than 100 ft bgs) V_s profile used for the site response analyses presented herein. As described previously, the profile was extended to a greater depth to layers with V_s of approximately 2,300 ft/s to be consistent with the definition of "geologically realistic" soil conditions.

Unit Weight

Unit weights of the dike fill and foundation soils were selected predominantly based on laboratory measured values as presented in the 2016 Safety Factor Assessment Report (Geosyntec, 2016). The selected unit weight of the dike fill was 125 pcf. The selected unit weight of the foundation soils was 115 pcf. Unit weights of the Chicora and Williamsburg Formation soils were assumed to be 130 pcf and 105 pcf, respectively, based on Standard Penetration Test (SPT) N-values and material descriptions presented in the PCRA (1999) report. Williamsburg Formation soils at depths greater than approximately 110 feet bgs were assumed to have unit weights of 125 pcf.

Site Response Analysis Results

Figure 9 shows calculated maximum shear strain and shear stress profiles for Profile 2. The maximum shear strains produced by one of the motions (BOS-T1) is relatively large in the foundation soils, supporting the use of nonlinear site response analyses. Calculated accelerations within the soil profile are presented in Appendix 4. The envelopes of maximum shear strain and shear stress for the six motions for Profile 2 are presented in Figure 10. The calculated envelope of maximum shear stress (τ_{max}) values at different depths is presented in Table 2. These values were used to calculate cyclic stress ratios for the evaluation of liquefaction potential (Attachment 4 to the

2021 Safety Factor Assessment Report) and to calculate the seismic coefficient for seismic stability analyses (Attachment 5 to the 2021 Safety Factor Assessment Report).

CONCLUSIONS

- The design PGA was conservatively selected to be 0.15g. This firm ground PGA corresponds to an event with a probability of exceedance of two percent in 15 years (i.e., event with a 750-year return period) and is representative of a motion expected for the "geologically realistic" site condition presented in the SCDOT GDM (2019).

- The design earthquake was assumed to have an M_w of 7.3 based on the deaggregation of the probabilistic seismic hazard analysis. This M_w was used for soil liquefaction analysis and time history selection.

- A target response spectrum for "geologically realistic" site conditions was developed using the USGS seismic hazard curves (Petersen et al., 2019) and is presented in Figure 3.

- Six time history recordings were used for the site response analyses. Two synthetic time histories were obtained using the USGS Interactive Deaggregation tool (USGS, 2002), three of the time histories were selected from the McGuire et al. (2001) database, and one of the time histories was selected from the NGA East database (Goulet et al., 2014). The time histories were scaled to match the design PGA of 0.15g for site response analyses.

- Nonlinear site response analyses were conducted using DEEPSOIL® (Hashash et al., 2020). The critical soil profile identified in the 2016 Safety Factor Assessment was used for the site response analyses. The analyses used region-specific shear modulus reduction and damping curves. The shear wave velocity profile was estimated from measured SCPT values and correlations between V_s and measured CPT sleeve frictions. The inputs used for the profile in DEEPSOIL® are shown in Appendix 5.

- The site response analysis results are presented in Figures 9 and 10. The calculated maximum shear stresses are presented in Table 2 and are used for evaluation of soil liquefaction potential and calculation of the seismic coefficient for seismic stability analyses.

REFERENCES

American Society of Civil Engineers (ASCE), (2017), "Minimum Design Loads and Associated Criteria for Buildings and Other Structures (ASCE 7-16)", American Society of Civil Engineers, Reston, Virginia.

Andrus, R.D., Zhang, J., Ellis, B.S., and Juang, C.H. (2003), "Guide for Estimating the Dynamic Properties of South Carolina Soils for Ground Response Analysis", South Carolina Department of Transportation, SC-DOT Research Project No. 623, FHWA-SC-03-07.

Chapman, M.C. and Talwani, P. (2006), “Seismic Hazard Mapping for Bridge and Highway Design in South Carolina”, South Carolina Department of Transportation, FHWA-SC-06-09.

Geosyntec Consultants, Inc. (2016), “2016 Surface Impoundment Periodic Safety Factor Assessment Report: Ash Pond B, Winyah Generating Station, Georgetown, South Carolina”, submitted to Santee Cooper.

Goulet, C.A., Kishida, T., Ancheta, T.D., Cramer, C.H., Darragh, R.B., Silva, W.J., Hashash, Y.M.A., Harmon, J., Stewart, J.P., Wooddell, K.E., and Youngs, R.R. (2014), “PEER NGA-East Database”, Pacific Earthquake Engineering Research Center, PEER 2014/17.

Hashash, Y.M.A., Musgrove, M.I., Harmon, J.A., Ilhan, O., Xing, G., Numanoglu, O., Groholski, D.R., Phillips, C.A., and Park, D. (2020), “DEEPSOIL 7.0, User Manual”, Board of Trustees of University of Illinois at Urbana-Champaign, Urbana, Illinois.

Kaklamanos, J., Bradley, B.A., Thompson, E.M., and Baise, L.G. (2013). "Critical parameters affecting bias and variability in site response analyses using KiK-net downhole array data." Bulletin of the Seismological Society of America, Vol. 103, No. 3, pp. 1733-1749.

Matasovic, N. (1993), “Seismic Response of Composite Horizontally-Layered Soil Deposits”, Ph.D. Dissertation, University of California, Los Angeles, California.

Mayne, P.W. (2006), “The 2nd James K. Mitchell Lecture: Undisturbed Sand Strength from Seismic Cone Tests”, Geomechanics and Geoengineering, Vol. 1, No. 4, 2006, pp.239–247.

McGuire, R.K., Silva, W.J., and Constantino, C.J. (2001), “Technical Basis for Revision of Regulatory Guidance on Design Ground Motions: Hazard- and Risk-consistent Ground Motion Spectra Guidelines”, United States Nuclear Regulatory Commission, NUREG/CR-6728.

McKim & Creed (2021), “Topographic Survey for Winyah Generating Station.”

Paul C. Rizzo Associates (1999), “Geotechnical/Hydrogeologic Investigation Winyah Generating Station”, Georgetown, South Carolina, submitted to Santee Cooper.

Petersen, M.D., Shumway, A.M., Powers, P.M., Mueller, C.S., Moschetti, M.P., Frankel, A.D., Rezaeian, S., McNamara, D.E., Luco, N., Boyd, O.S., Rukstales, K.S., Jaiswal, K.S., Thompson, E.M., Hoover, S.M., Clayton, B.S., Field, E.H., and Zeng, Y. (2019), "The 2018 update of the US national seismic hazard model: Overview of model and implications", Earthquake Spectra, Vol. 36, No. 1, 2019, pp. 5-41.

S&ME, Inc. (2001), "Report of Geotechnical Exploration Winyah Generating Station Units 1&2 Ammonium Sulfate FGD System", Georgetown, South Carolina, submitted to Marsulex Environmental Technologies.

Silva, W.J., N. Abrahamson, G. Toro, and C Costantino (1997), "Description and validation of the stochastic ground motion model", Submitted to Brookhaven National Laboratory, Associated Universities, Inc. Upton, New York.

South Carolina Dept. of Transportation (SCDOT) (2010), Geotechnical Design Manual, available: http://www.scdot.org/doing/structural_Geotechnical.aspx

South Carolina Dept. of Transportation (SCDOT) (2019), Geotechnical Design Manual Version 2.0, available: https://www.scdot.org/business/pdf/geotech/SCDOT-Geotechnical-Design-Manual.pdf

South Carolina Department of Natural Resources: Geologic Survey, (2012). "Geologic Map of the Georgetown South Quadrangle, Georgetown County, South Carolina", 2012.

Stokoe, K. H., II, Hwang, S. K., Darendeli, M. B., and Lee, N. J. (1995), "Correlation Study of Nonlinear Dynamic Soils Properties", final report to Westinghouse Savannah River Company, The University of Texas at Austin, Austin, TX.

Stokoe, K. H., II, Darendeli, M. B., Andrus, R. D., and Brown, L. T. (1999), "Dynamic Soil Properties: Laboratory, Field and Correlation Studies", Proceedings, 2nd International Conference on Earthquake Geotechnical Engineering, Vol. 3, Lisbon, Portugal, 811-845.

URS Corporation, Durham Technologies, Inc., Image Cat, Inc., Pacific Engineering and Analysis, S&ME, Inc. (2001), "Comprehensive Seismic Risk and Vulnerability Study for the State of South Carolina", prepared for South Carolina Emergency Preparedness Division, 51-D0111027.00, Final Report, 10 September 2001.

USGS (2002), "2002 Interactive Deaggregation", 2002. https://geohazards.usgs.gov/deaggint/2002/index.php

U.S. Geological Survey (USGS), (2014), "Dynamic: Conterminous U.S. 2014 (v4.2.0) Interactive Deaggregations", 2014. https://earthquake.usgs.gov/hazards/interactive/

Tables

Table 1. Summary of Hazard Parameters of the Time Histories Selected for Site Response Analysis

Name	**Site Class**	**M_w**	**R (km)**	**PGA (g)**	**T_p (s)**
BOS-T1	-	7.40	26.1	0.14	0.36
DEL090	C	6.70	59.3	0.27	0.22
RSN8529-HNE	C	5.74	124.1	0.09	0.26
Winyah1	A	7.04	30.2	0.56	0.08
Winyah2	A	7.04	30.2	0.56	0.10
YER360	C	7.30	24.9	0.22	0.22

Note:

1. All accelerations are scaled within DEEPSOIL® to match the target PGA of 0.15g.

Table 2. Calculated Maximum Shear Stress Envelope

Profile 2	
Depth (ft)	τ_{max} (psf)
1.5	19
5.0	57
9.0	87
13.0	111
17.0	140
20.5	166
24.5	190
29.5	206
34.5	215
39.5	221
44.5	233
49.5	295
57.0	380
67.0	474
77.0	601
87.0	738
97.0	873
107.0	1026

Figures

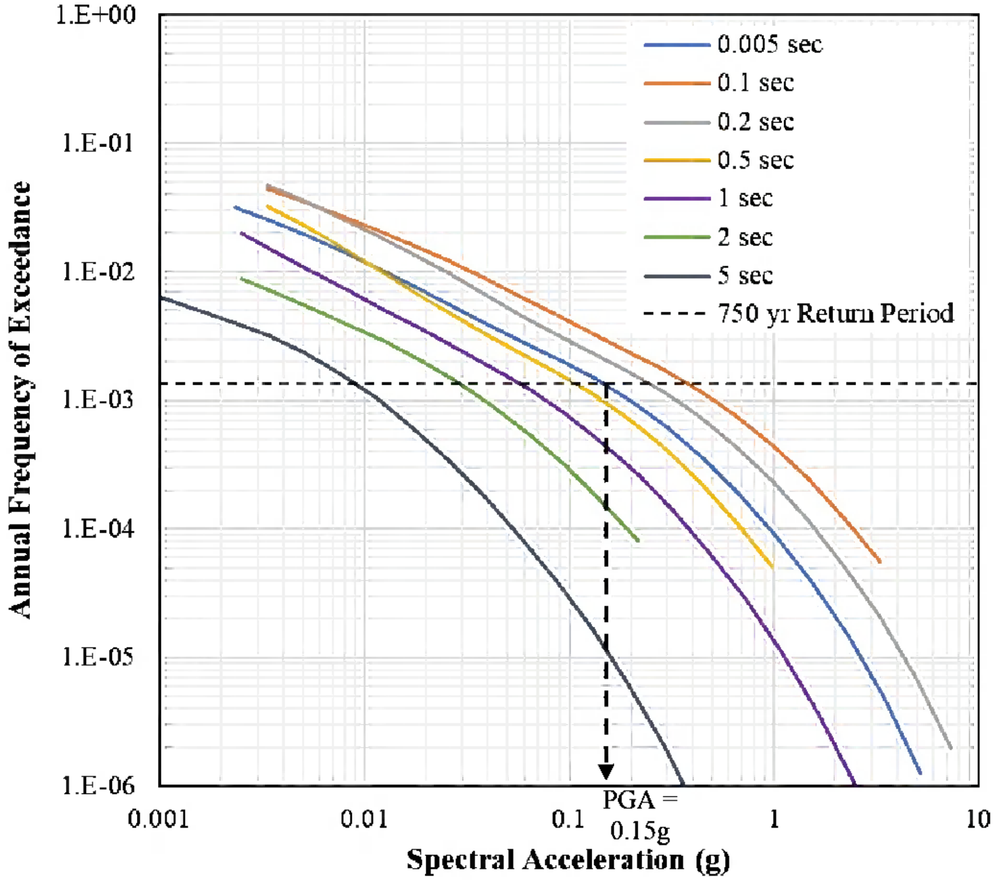

Figure 1. USGS Hazard Curves for Geologically Realistic Conditions (BC Boundary) at the Site (Petersen et al., 2019)

Notes:

1. The different hazard curves represent different spectral periods. USGS provides hazard curves for 22 spectral periods; however, hazard curves are only shown for 7 spectral periods in the figure for clarity.
2. The dashed line represents a hazard with a 750-year return period (i.e., approximately annual frequency of exceedance of 1.33E-03). The intersections of the dashed lines and curves for the different spectral periods were used to develop the UHS for the Site shown in Figure 3.
3. PGA is approximated by a spectral period of 0.005 seconds. As illustrated, PGA for WGS was selected as 0.15g.

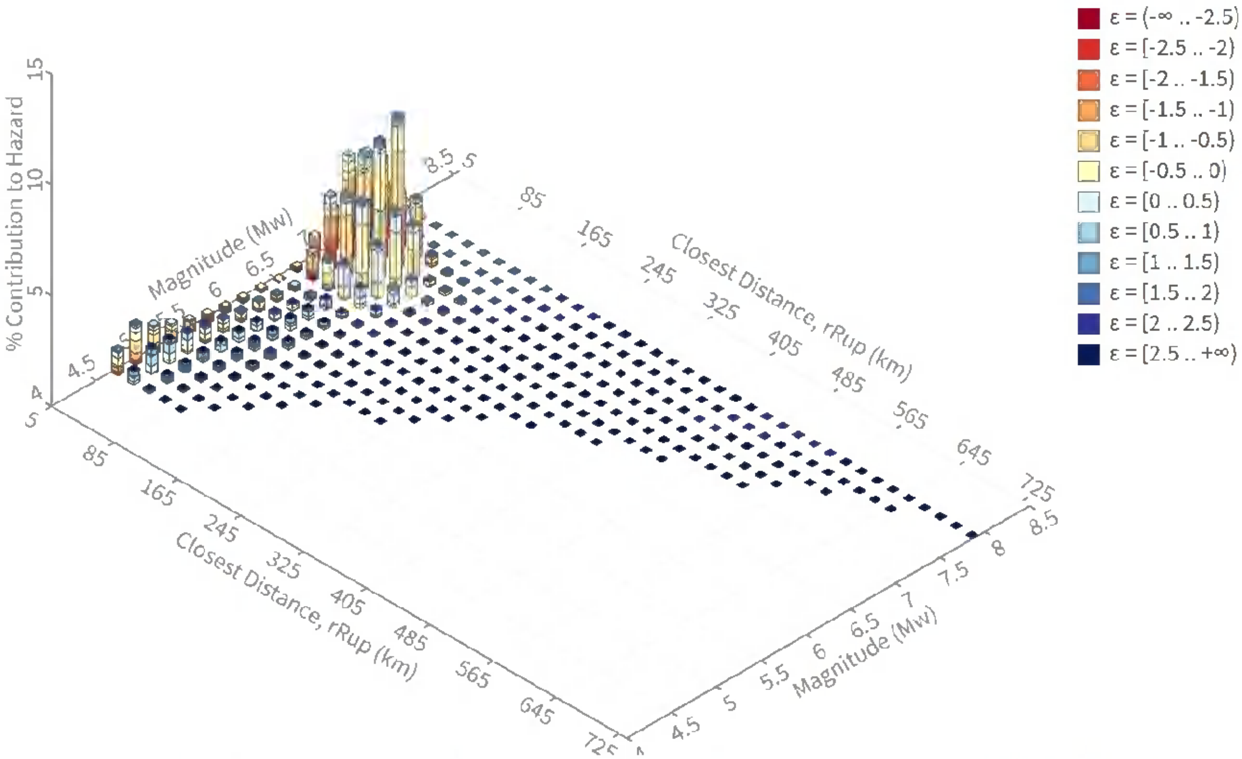

Deaggregation targets

Return period: 750 yrs
Exceedance rate: 0.0013333333 yr^{-1}
PGA ground motion: 0.12257412 g

Recovered targets

Return period: 748.46717 yrs
Exceedance rate: 0.0013360639 yr^{-1}

Totals

Binned: 100 %
Residual: 0 %
Trace: 0.93 %

Mean (over all sources)

m: 6.76
r: 52.82 km
ε_0: -0.76 σ

Mode (largest m-r bin)

m: 7.3
r: 68.52 km
ε_0: -0.68 σ
Contribution: 6.82 %

Mode (largest m-r-ε_0 bin)

m: 7.3
r: 70.16 km
ε_0: -0.76 σ
Contribution: 3.14 %

Discretization

r: min = 0.0, max = 1000.0, Δ = 20.0 km
m: min = 4.4, max = 9.4, Δ = 0.2
ε: min = -3.0, max = 3.0, Δ = 0.5 σ

Epsilon keys

ε0: [-∞ .. -2.5)
ε1: [-2.5 .. -2.0)
ε2: [-2.0 .. -1.5)
ε3: [-1.5 .. -1.0)
ε4: [-1.0 .. -0.5)
ε5: [-0.5 .. 0.0)
ε6: [0.0 .. 0.5)
ε7: [0.5 .. 1.0)
ε8: [1.0 .. 1.5)
ε9: [1.5 .. 2.0)
ε10: [2.0 .. 2.5)
ε11: [2.5 .. +∞]

Figure 2. Deaggregation of Two Percent Probability of Exceedance in 15 Years at the BC Boundary of the Site

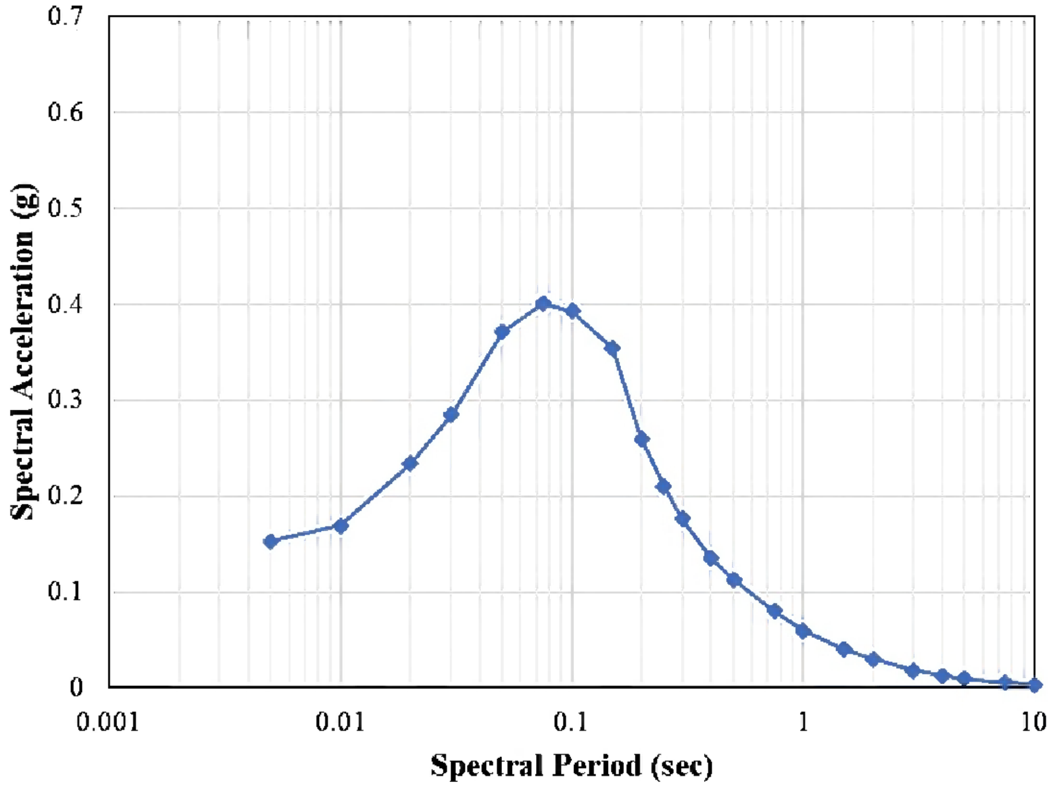

Figure 3. “Geologically Realistic” Target Response Spectrum for WGS

Note:

1. Target response spectrum shown for “geologically realistic” conditions was developed using USGS seismic hazard curves (see Figure 1).

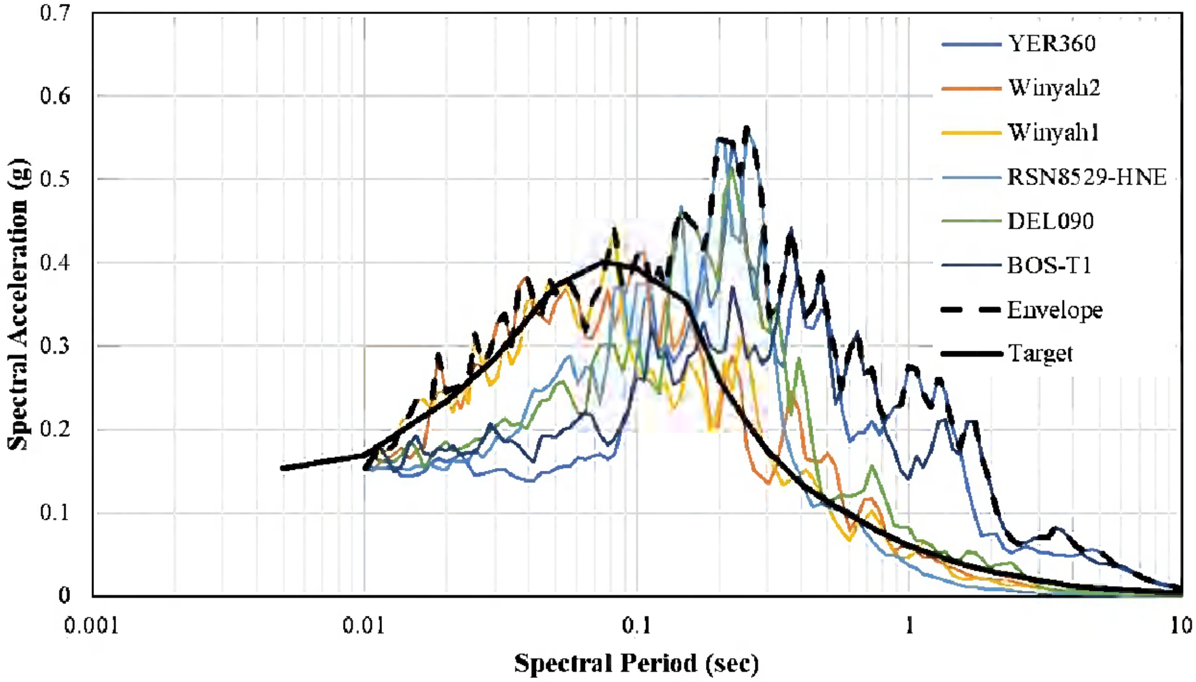

Figure 4. Response Spectra of Scaled Time Histories Selected for Site Response Analyses

Note:

1. Time histories were scaled to match the target PGA = 0.15g (represented by a period of 0.005 seconds).

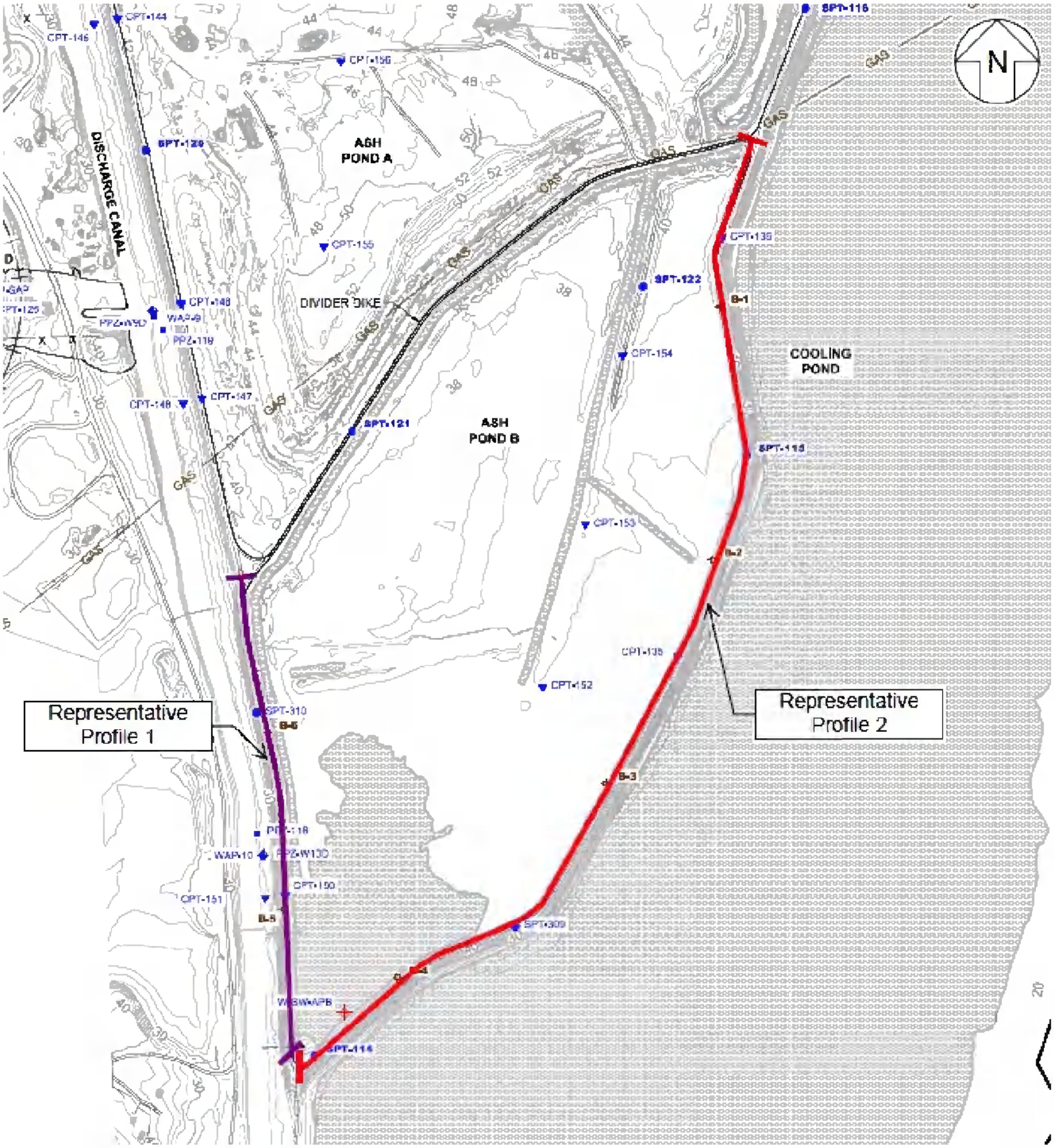

Figure 5. Locations of Representative Soil Profiles

Note:

1. The site responses analyses were performed for Profile 2 only.

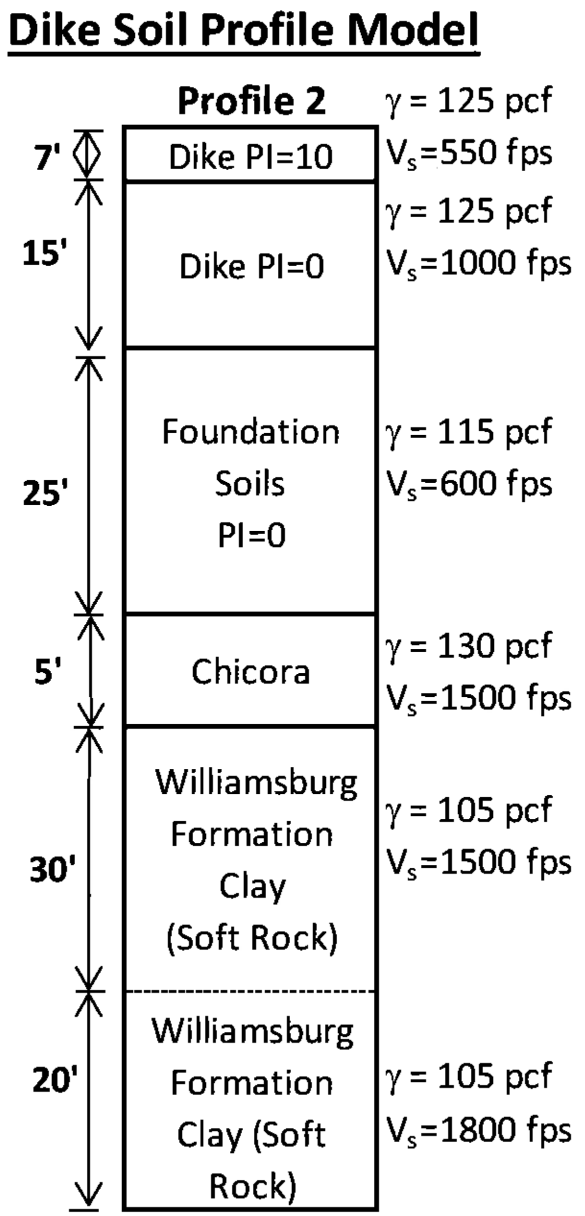

Figure 6. DEEPSOIL® Soil Profile

Note:

[1] The water table was modeled at 15 ft below ground surface.

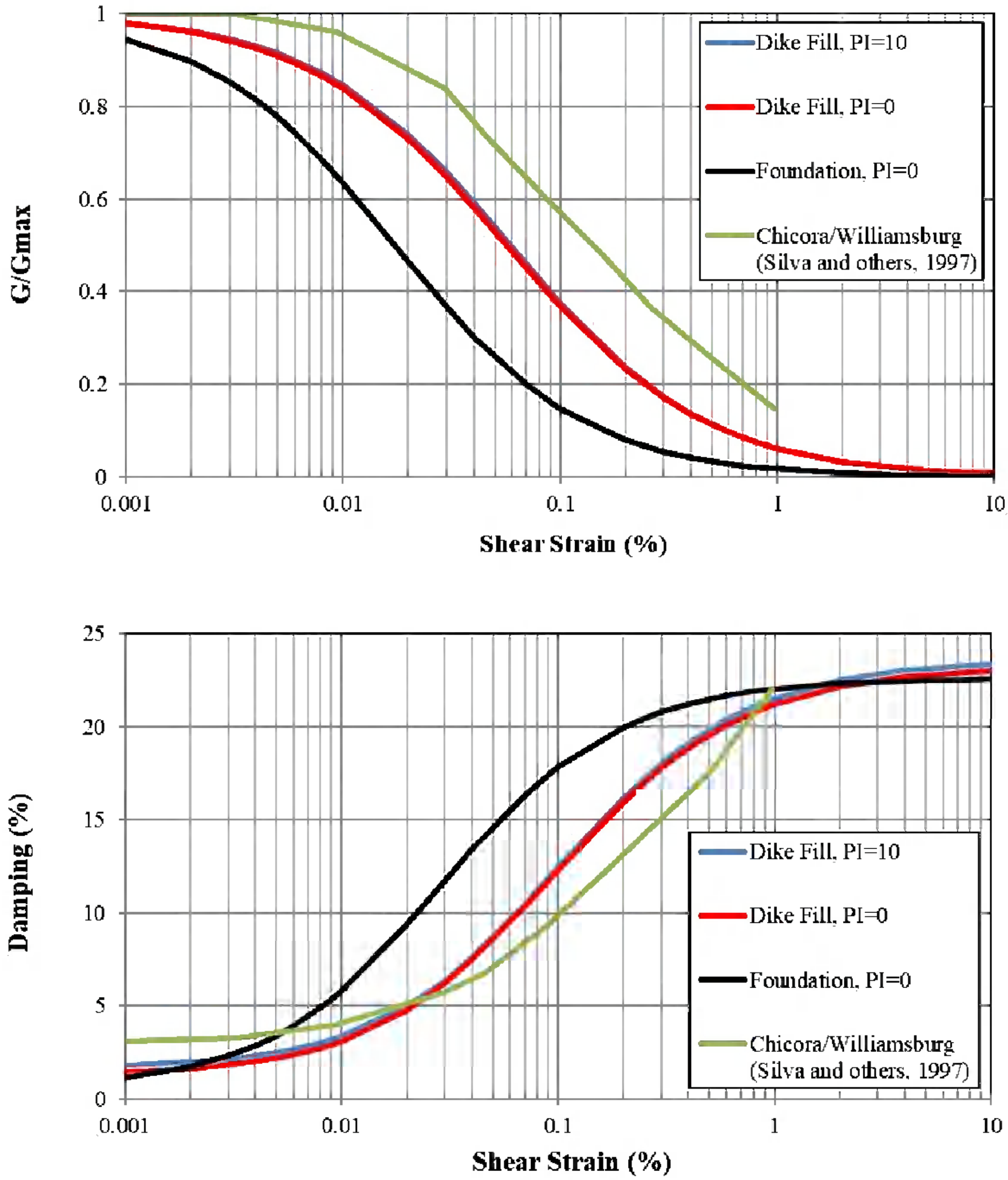

Figure 7. Shear Modulus Reduction (G/G_{max}) and Damping Curves for Soils Used in Site Response Analyses

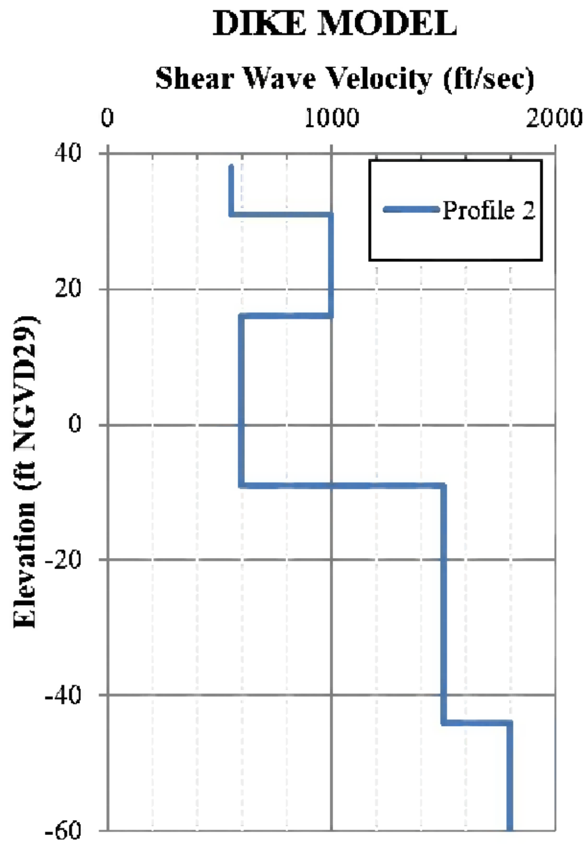

Figure 8. Selected Shear Wave Velocity (V_s) Profile for Site Response Analyses

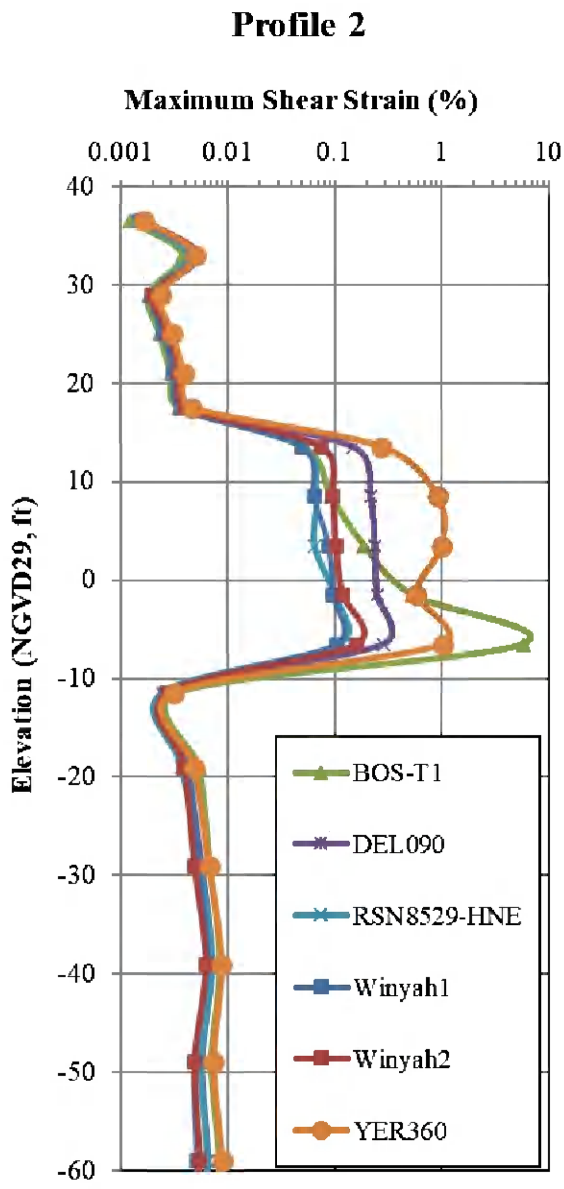

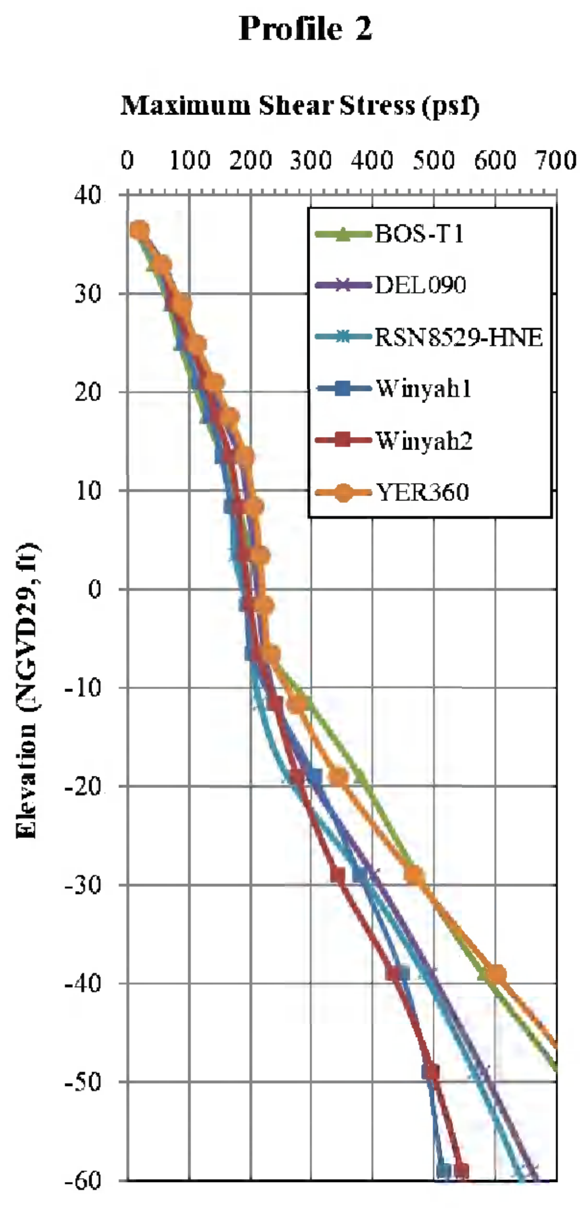

Figure 9. Site Response Analysis Results for Profile 2

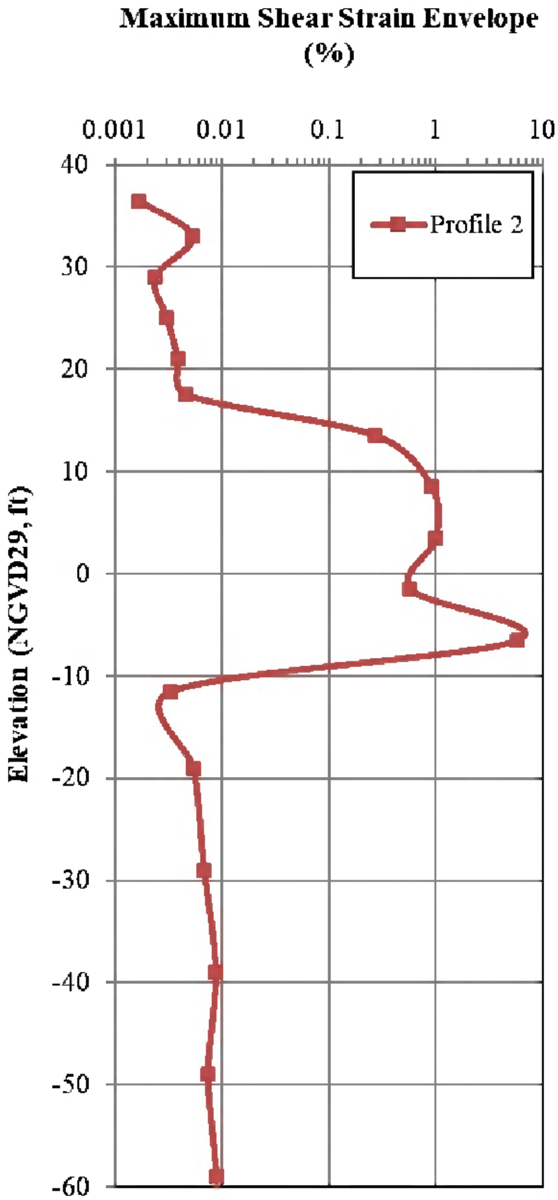

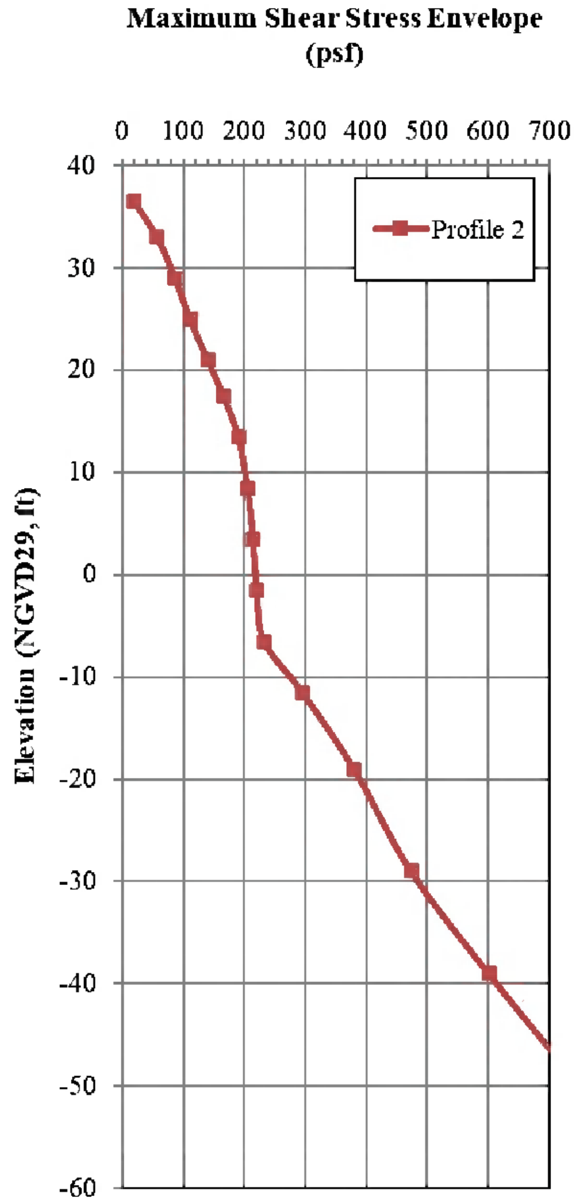

Figure 10. Maximum Shear Strain and Shear Stress Envelopes for Profile 2

Appendix 1

Selected Time Histories

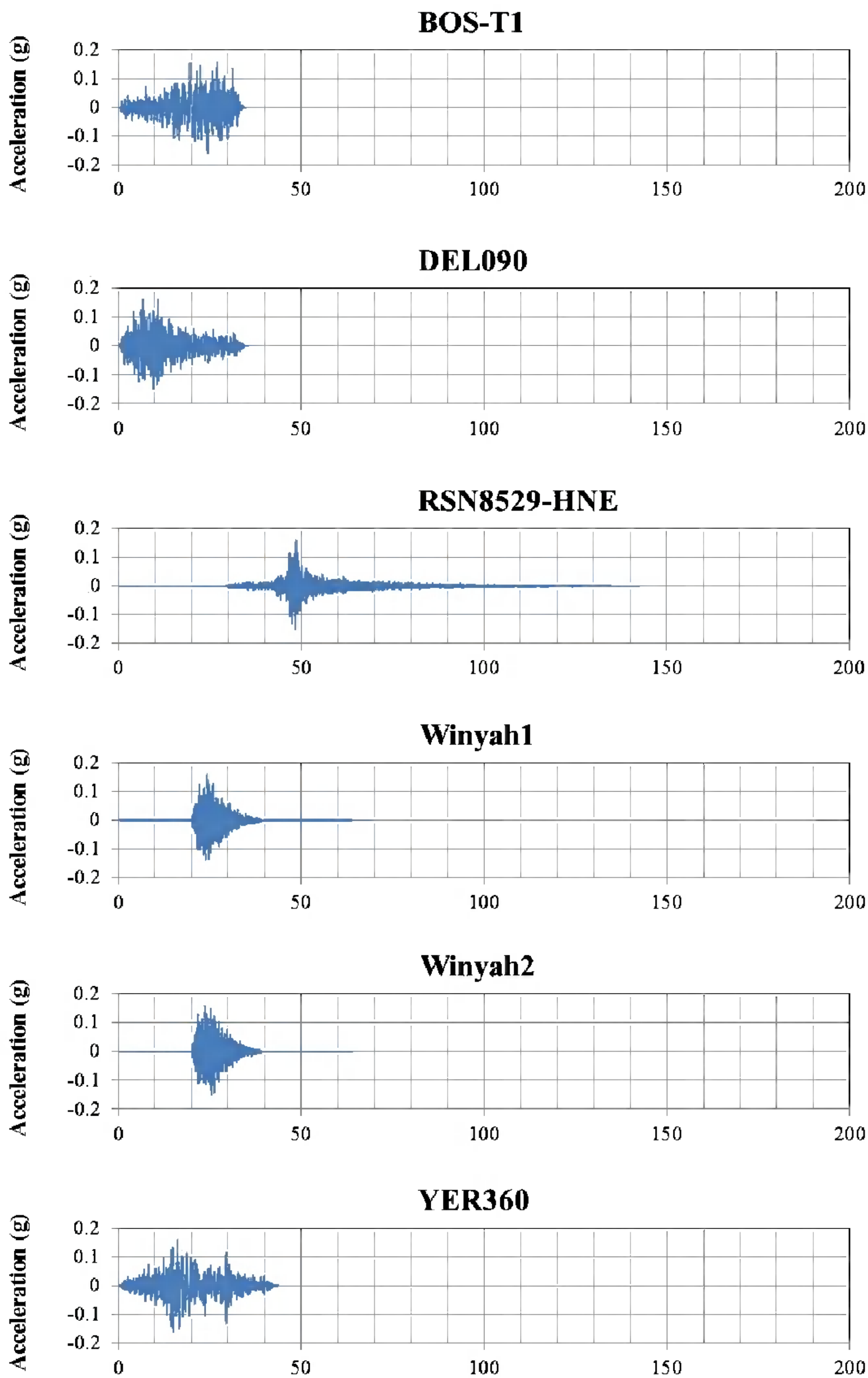

Figure 1-1. Acceleration Time Histories of Selected Earthquake Motions Scaled to PGA of 0.15g

Appendix 2

Shear Modulus Reduction and Damping Curve Selection

As indicated in the package, Geosyntec developed region-specific shear modulus reduction and damping curves based on the procedures presented in SCDOT GDM (2019). Figures 2-1 and 2-5 show the procedures. An example calculation following these procedures is presented as follows.

Shear Modulus Reduction Curve for the foundation soil in Profile 2

(see Figure 2-1 for description on each step; see Figure 2-2 for the profile)

Step 1 – age of the soil layer: Pleistocene deposit.

Step 2 – soil type: sandy soils with PI=0; groundwater table @ 15 ft bgs.

Step 3 – calculate σ_m'@ mid-depth of the layer (34.5 ft bgs)

$\sigma_v' = \gamma H - \gamma_w H_w = 125\times22 + 115\times12.5 - 62.4\times19.5 = 2970.7$ psf

$\sigma_m' = \sigma_v' (1+2K'_o)/3 = 2970.7\times(1+2\times0.47)/3 = 1921.2$ psf

$(K_o' = 1\text{- } \sin\phi' = 1\text{- } \sin(32) = 0.47)$

Step 4 – σ_m' for the upper and lower native soils are within ±50% σ_m' value calculated above. The modulus reduction curve developed here can be used for the entirety of the foundation soils in Profile 2.

Step 5 – select the parameters α, γ_{r1}, k from Figure 2-4.

$\gamma_{r1} = 0.018\%$, $\alpha = 1.00$, $k = 0.454$

Step 6 – compute the reference strain using SCDOT GDM Equation 7-135 (see Figure 2-3 for the equation).

$\gamma_r = \gamma_{r1} (\sigma_m'/P_a)^k = 0.018\times(1921.1/2089)^{0.454} = 0.0173\%$

Step 7 – compute shear modulus reduction curve using SCDOT GDM Equation 7-134 (see Figure 2-3 for the equation)

$$\frac{G}{G_{max}} = \frac{1}{1+(\frac{\gamma}{\gamma_r})^\alpha}$$

If $\gamma = 0.001\%$, $G/G_{max} = 1/[1+(0.001/0.0173)] = 0.945$

If $\gamma = 0.01\%$, $G/G_{max} = 1/[1+(0.01/0.0173)] = 0.634$

If $\gamma = 0.1\%$, $G/G_{max} = 1/[1+(0.1/0.0173)] = 0.148$

Damping Curve for the foundation soil in Profile 2

(see Figure 2-5 for description on each step; see Figure 2-2 for the profile)

Steps 1 through 4 are the same as those for modulus reduction curve development.

Step 5 – select small-strain material damping @ σ_m' = 1 atm, D_{min1} from Figure 2-6.

$D_{min1} = 0.59\%$

Step 6 – compute the small strain material damping, D_{min}, using SCDOT GDM Equation 7-137 (see Figure 2-7 for the equation).

$D_{min} = D_{min1}\ (\sigma_m'/P_a)^{-0.5k} = 0.59\times(1921.1/2089)^{-0.5\times0.454} = 0.601\%$

Step 7-9 – instead of taking Steps 7 through 9, use SCDOT GDM Equation 7-138 to compute damping ratio curve (D).

$D = 12.2\ (G/G_{max})^2 - 34.2\ (G/G_{max}) + 22.0 + D_{min}$

If $\gamma = 0.001\%$, $D = 12.2\times(0.945)^2 - 34.2\times(0.945) + 22.0 + 0.601 = 1.17\%$

If $\gamma = 0.01\%$, $D = 12.2\times(0.634)^2 - 34.2\times(0.634) + 22.0 + 0.601 = 5.82\%$

If $\gamma = 0.1\%$, $D = 12.2\times(0.147)^2 - 34.2\times(0.147) + 22.0 + 0.601 = 17.82\%$

Shear Modulus Reduction and Damping Curves for Chicora / Williamsburg Formation

Figure 2-8 presents shear modulus reduction and damping curves used for Pacific Engineering's site response analyses of the Ammonia tank building located at the WGS.

Table 7-30, Procedure for Computing G/G_{max}

Step	Procedure Description
1	Perform a geotechnical subsurface exploration and identify subsurface soil geologic units, approximate age, and formation.
2	Develop soil profiles based on geologic units, soil types, average PI, and soil density. Subdivide major geologic units to reflect significant changes in PI and soil density. Identify design ground water table based on seasonal fluctuations and artesian pressures.
3	Calculate the average σ'_m and determine the corresponding ±50% range of σ'_m for each major geologic unit using Equation 7-136.
4	Calculate σ'_m for each layer within each major geologic unit. If the values for σ'_m of each layer are within a geologic unit's ±50% range of σ'_m (Step 3) then assign the average σ'_m for the major geologic unit (Step 3) to all layers within it. If the σ'_m of each layer within a geologic unit is not within the ±50% range of σ'_m for the major geologic unit, then the geologic unit needs to be "subdivided" and more than one average σ'_m needs to be used, provided the σ'_m remain within the ±50% range of σ'_m for the "subdivided" geologic unit.
5	Select the appropriate values for each layer of cyclic reference strain, γ_{cr1}, at 1 tsf (1 atm), curvature coefficient, α, and k exponent from Table 7-29. These values may be selected by rounding to the nearest PI value in the table or by interpolating between listed PI values in the table.
6	Compute the cyclic reference strain, γ_{cr}, based on Equation 7-135 for each geologic unit (or "subdivided" geologic unit) that has a corresponding average σ'_m.
7	Compute the design shear modulus reduction curves (G/G_{max}) for each layer by substituting cyclic reference strain, γ_{cr}, and curvature coefficient, α, for each layer using Equation 7-134. Tabulate values of normalized shear modulus, G/G_{max} with corresponding cyclic shear strain, γ_c, for use in a site-specific response analysis.

Figure 2-1. Procedure for Development of Region-specific Modulus Reduction Curve (SCDOT, 2019)

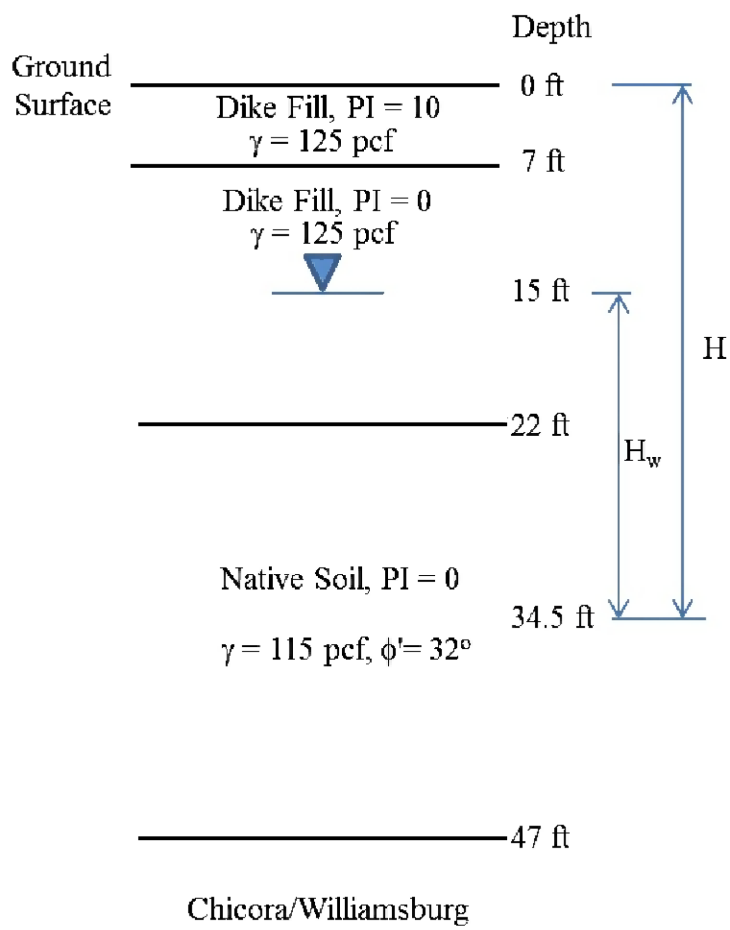

Figure 2-2. Profile 2 for the Example Calculations

$$G/G_{max} = \frac{1}{1+\left(\frac{\gamma_c}{\gamma_{cr}}\right)^{\alpha}}$$ Equation 7-134

Where,

α = Curvature coefficient

γ_c = Cyclic shear strain

γ_{cr} = Cyclic reference shear strain

$$\gamma_{cr} = \gamma_{cr1} * \left(\frac{\sigma'_m}{P_a}\right)^{k}$$ Equation 7-135

$$\sigma'_m = \sigma'_v * \left(\frac{1+2*K_o}{3}\right)$$ Equation 7-136

Where,

σ'_v = Vertical effective pressure, kPa

K_o = At-rest earth pressure coefficient

Figure 2-3. Equations Needed for Shear Modulus Reduction Curve Development (SCDOT, 2019)

Table 7-29, Recommended Values γ_{cr1}, α, and k for SC Soils (Andrus, et al. (2003))

Geologic Age and Location of Deposits [1]	Variable	Soil Plasticity Index, PI (%)					
		0	15	30	50	100	150
Holocene	γ_{cr1} (%)	0.073	0.114	0.156	0.211	0.350	0.488
	α	0.95	0.96	0.97	0.98	1.01	1.04 [2]
	k	0.385	0.202	0.106	0.045	0.005	0.001 [2]
Pleistocene (Wando)	γ_{cr1} (%)	0.018	0.032	0.047	0.067	0.117	0.166
	α	1.00	1.02	1.04	1.06	1.13	1.19
	k	0.454	0.402	0.355	0.301	0.199	0.132
Tertiary Ashley Formation (Cooper Marl)	γ_{cr1} (%)	—	—	0.030 [2]	0.049	0.096 [2]	—
	α	—	—	1.10 [2]	1.15	1.28	—
	k	—	—	0.497 [2]	0.455	0.362 [2]	—
Tertiary (Stiff Upland Soils)	γ_{cr1} (%)	—	—	0.023	0.041 [2]	—	—
	α	—	—	1.00	1.00 [2]	—	—
	k	—	—	0.102	0.045 [2]	—	—
Tertiary (All soils at SRS except Stiff Upland Soils)	γ_{cr1} (%)	0.038	0.058	0.079	0.106	0.174 [2]	—
	α	1.00	1.00	1.00	1.00	1.00 [2]	—
	k	0.277	0.240	0.208	0.172	0.106 [2]	—
Tertiary (Tobacco Road, Snapp)	γ_{cr1} (%)	0.029	0.056	0.082	0.117	0.205 [1]	—
	α	1.00	1.00	1.00	1.00	1.00 [1]	—
	k	0.220	0.185	0.156	0.124	0.070 [1]	—
Tertiary (Soft Upland Soils, Dry Branch, Santee, Warley Hill, Congaree)	γ_{cr1} (%)	0.047	0.059	0.071	0.086	0.125 [1]	—
	α	1.00	1.00	1.00	1.00	1.00 [1]	—
	k	0.313	0.299	0.285	0.268	0.229 [1]	—
Residual Soil and Saprolite	γ_{cr1} (%)	0.040	0.066	0.093 [1]	0.129 [1]	—	—
	α	0.72	0.80	0.89	1.01 [1]	—	—
	k	0.202	0.141	0.099	0.061 [2]	—	—

[1] SRS = Savannah River Site
[2] Tentative Values – Andrus et al. (2003)

Figure 2-4. Recommended Parameters for South Carolina Soils (SCDOT, 2019)

Table 7-32, Procedure for Computing Damping Ratio

Step	Procedure Description
1	Perform a geotechnical subsurface exploration and identify subsurface soil geologic units, approximate age, and formation.
2	Develop soil profiles based on geologic units, soil types, average PI, and soil density. Subdivide major geologic units to reflect significant changes in PI and soil density. Identify design ground water table based on seasonal fluctuations and artesian pressures.
3	Calculate the average σ'_m and determine the corresponding ±50% range of σ'_m for each major geologic unit using Equation 7-136.
4	Calculate σ'_m for each layer within each major geologic unit. If the values for σ'_m of each layer are within a geologic unit's ±50% range of σ'_m (Step 3) then assign the average σ'_m for the major geologic unit (Step 3) to all layers within it. If the σ'_m of each layer within a geologic unit is not within the ±50% range of σ'_m for the major geologic unit, then the geologic unit needs to be "subdivided" and more than one average σ'_m needs to be used, provided the σ'_m remain within the ±50% range of σ'_m for the "subdivided" geologic unit.
5	Select appropriate small-strain material Damping @ σ'_m = 1 atm, λ_{min1}, from Table 7-31 for each layer within a geologic unit.
6	Compute the small-strain material Damping, λ_{min}, for each layer within a geologic unit using Equation 7-137.
7	Select the appropriate values for each layer of cyclic reference strain, γ_{cr1}, @ σ'_m = 1atm , curvature coefficient, α, and k exponent from Table 7-29. These values may be selected by rounding to the nearest PI value in the table or by interpolating between listed PI values in the table.
8	Compute the cyclic reference strain, γ_{cr}, based on Equation 7-135 for each geologic unit that has a corresponding average σ'_m.
9	Compute the design equivalent viscous damping ratio curves (λ) for each layer by substituting cyclic reference strain, γ_{cr}, and curvature coefficient, α, and small-strain material Damping, λ_{min}, for each layer using Equation 7-139. Tabulate values of Soil Damping Ratio, λ, with corresponding cyclic shear strain, γ_c, for use in a site-specific site response analysis.

Figure 2-5. Procedure for Development of Region-Specific Damping Curve (SCDOT, 2019)

Table 7-31, Recommended Value λ_{min1} (%) for SC Soils (Andrus, et al. (2003))

Geologic Age and Location of Deposits	Soil Plasticity Index, PI (%)					
	0	15	30	50	100	150
Holocene	1.09	1.29	1.50	1.78	2.48	3.18 [1]
Pleistocene (Wando)	0.59	0.66	0.73	0.83	1.08	1.32
Tertiary Ashley Formation (Cooper Marl)	—	—	1.14 [1]	1.52 [1]	2.49 [1]	—
Tertiary (Stiff Upland Soils)	—	—	0.98	1.42 [1]	—	—
Tertiary (All soils at SRS except Stiff Upland Soils)	0.68	0.94	1.19	1.53	2.37 [1]	—
Tertiary (Tobacco Road, Snapp)	0.68	0.94	1.19	1.53	2.37 [1]	—
Tertiary (Soft Upland Soils, Dry Branch, Santee, Warley Hill, Congaree)	0.68	0.94	1.19	1.53	2.37 [1]	—
Residual Soil and Saprolite	0.56 [1]	0.85 [1]	1.14 [1]	1.52 [1]	—	—

[1] Tentative Values – Andrus, et al. (2003)

Figure 2-6. Recommended D_{min1} for South Carolina Soils (SCDOT, 2019)

$$\lambda_{min} = \lambda_{min1} * \left(\frac{\sigma'_m}{P_a}\right)^{-0.5*k}$$ **Equation 7-137**

Where λ_{min1} is the small-strain damping at σ'_m of 1 tsf (1 atm). The mean confining pressure,

Equation 7-137 represents a best-fit equation (UTA Correlation) of the observed relationship of $(\lambda - \lambda_{min})$ vs. (G/G_{max}) indicated below:

Equation 7-138

$$\lambda - \lambda_{min} = 12.2 * \left(\frac{G}{G_{max}}\right)^2 - 34.2 * \left(\frac{G}{G_{max}}\right) + 22.0$$

If we substitute Equation 7-134 into Equation 7-138 and solve for the damping ratio, λ, the Equivalent Viscous Damping Ratio curves can be generated using the following equation.

Equation 7-139

$$\lambda = \lambda_{min} + 12.2 * \left[\frac{1}{1 + \left(\frac{\gamma_c}{\gamma_{cr}}\right)^{\alpha}}\right]^2 - 34.2 * \left[\frac{1}{1 + \left(\frac{\gamma_c}{\gamma_{cr}}\right)^{\alpha}}\right] + 22.0$$

Where values of reference strain, γ_{cr}, are computed using Equation 7-135.

Figure 2-7. Equations Needed for Damping Curve Development (SCDOT, 2019)

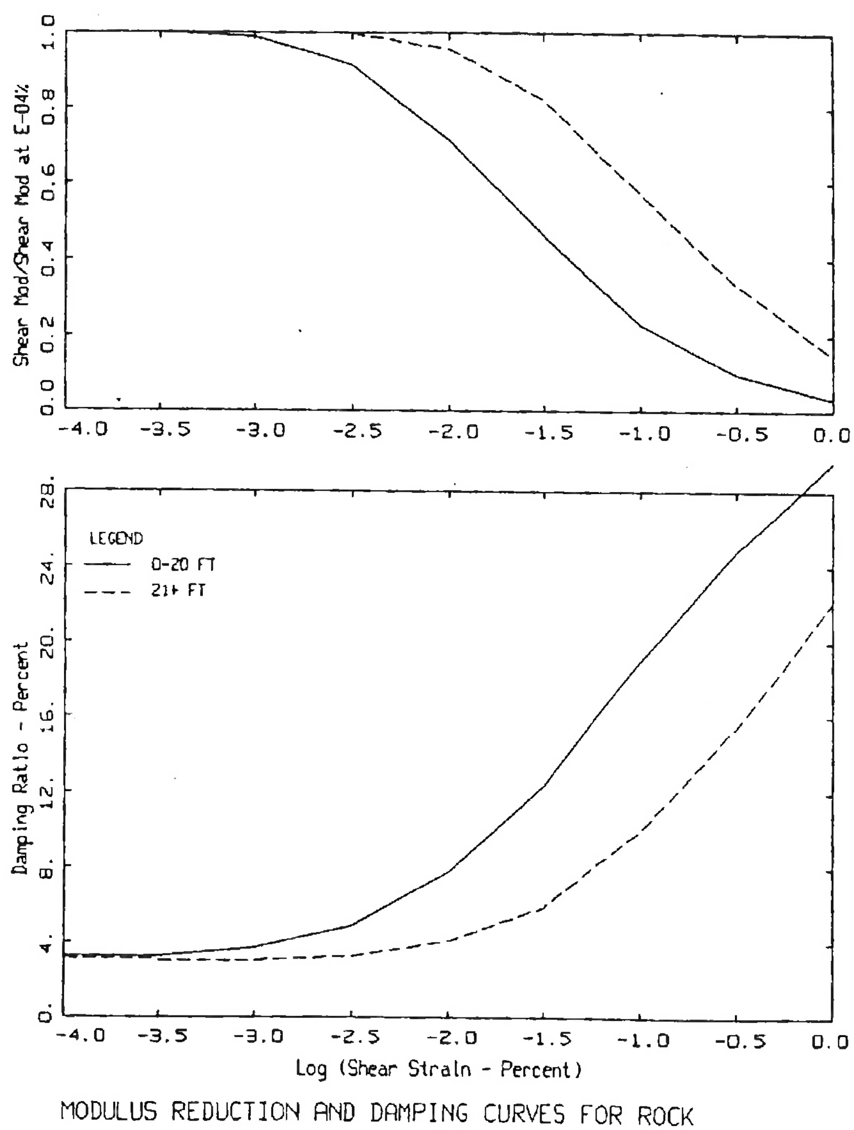

Figure 5b. Generic G/Gmax and hysteretic damping curves for soft rock (Silva et al., 1997).

Figure 2-8. Shear Modulus Reduction and Damping Curves for Chicora/Williamsburg Formation (S&ME, 2001)

Appendix 3
Shear Wave Velocity Profile Selection

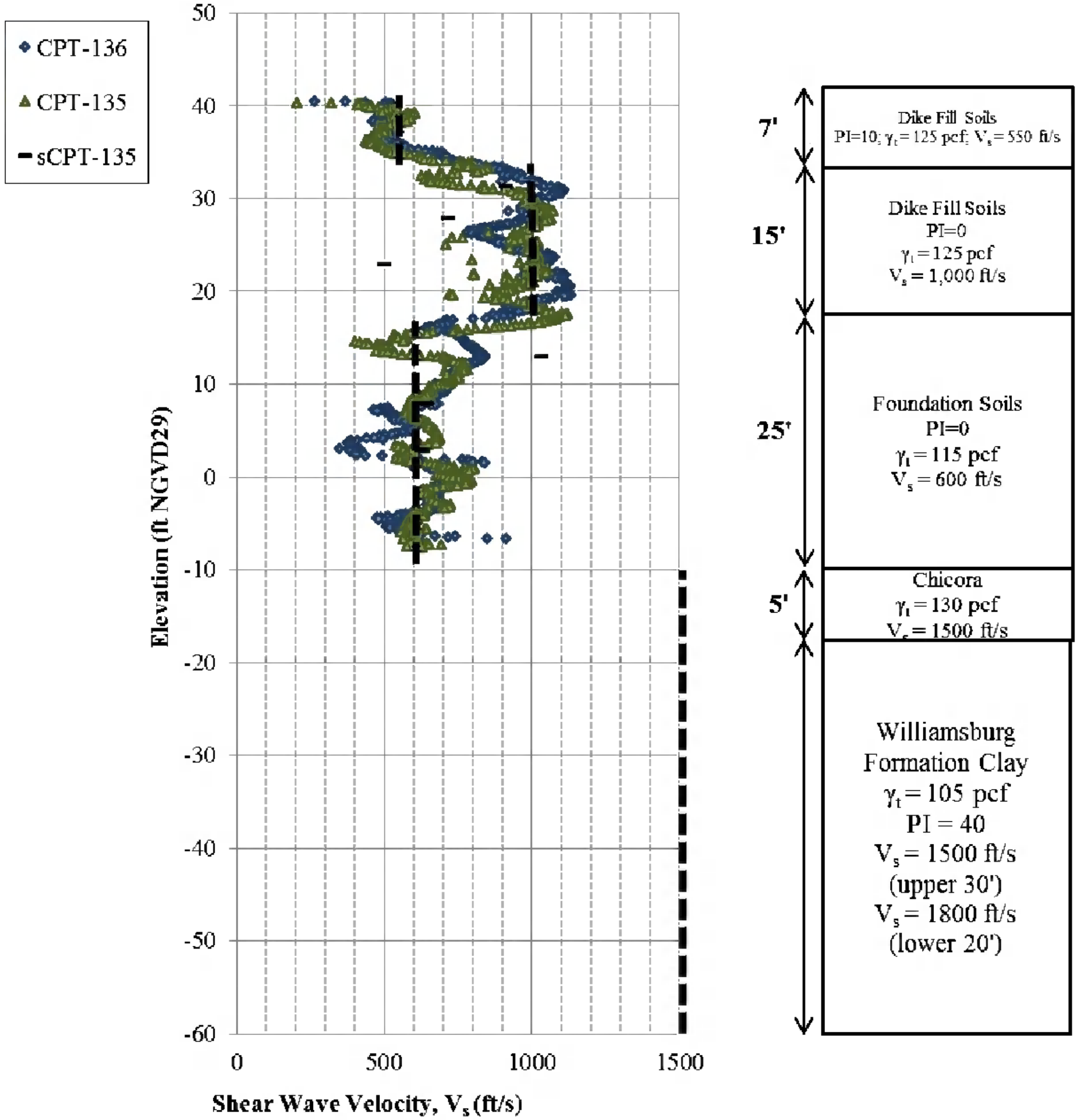

Figure 3-1. Selected V_s Profile for the Ash Pond B Dike Model (Profile 2)

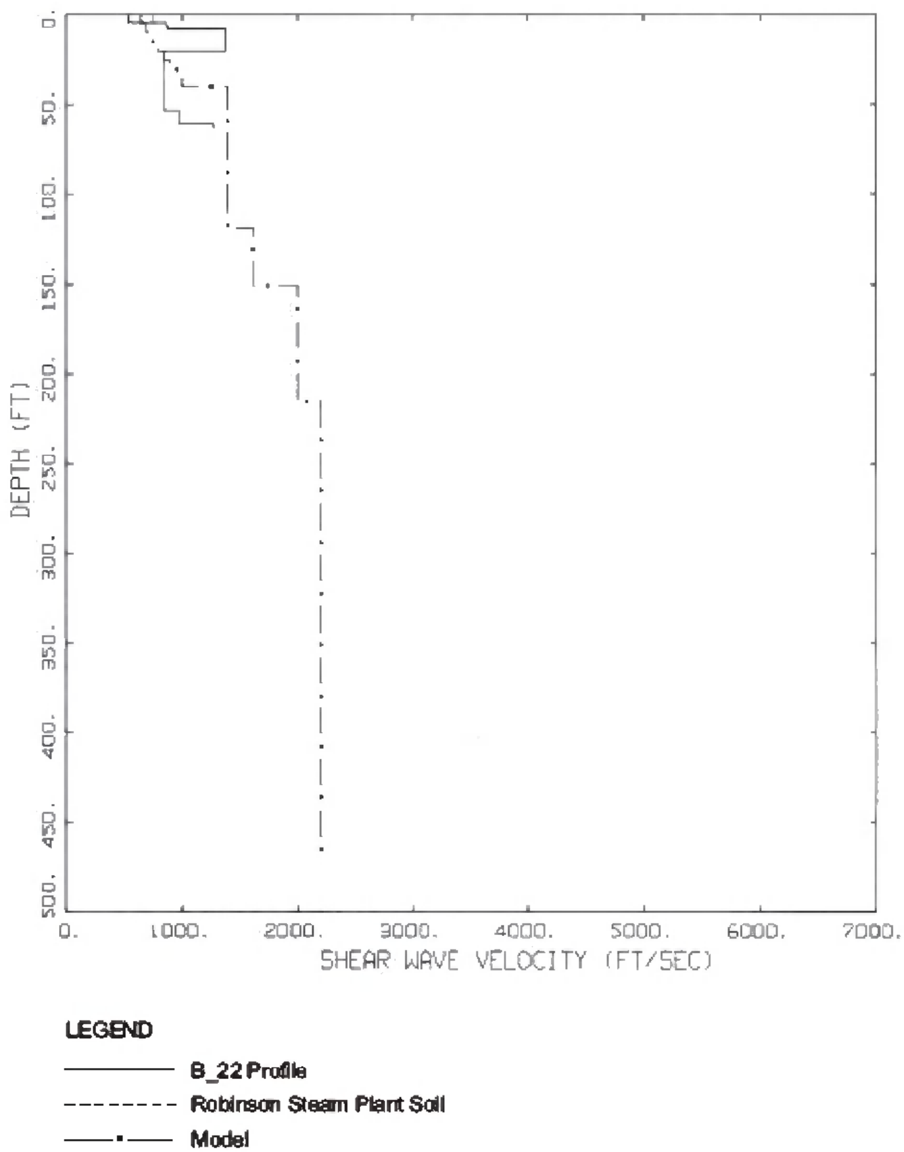

Figure 3-9. Base case shear-wave velocity profile for the Myrtle Beach site response category along with available profiles.

Figure 3-2. Reference V_s Profile for Chicora/Williamsburg Formation (URS, 2001)

Appendix 4

Calculated Acceleration Profiles

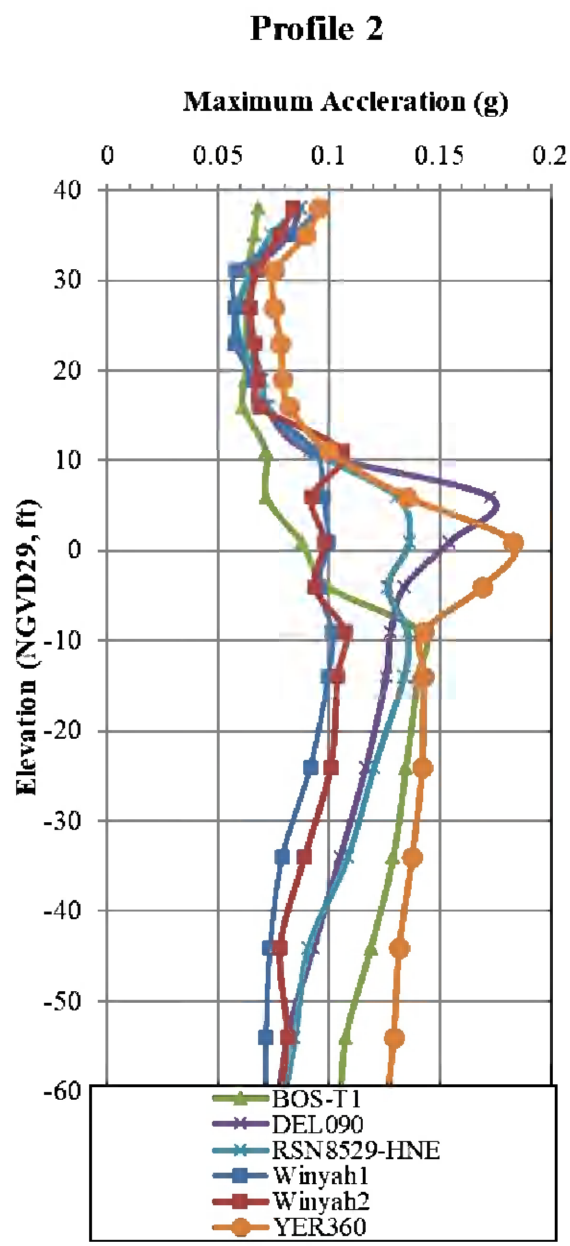

Figure 4-1. Calculated Maximum Acceleration for Profile 2

Note:

1. The input motions were applied as an outcrop motion with a PGA of 0.15g.

Appendix 5

DEEPSOIL® Input

Analysis Type Definition

Analysis Method

Nonlinear

Pore Pressure Options

- [ ] Generate Excess Porewater Pressure
  - [ ] Enable Dissipation
  - [x] Make Top of Profile Permeable
  - [x] Make Bottom of Profile Permeable

Solution Type

Time Domain

Default Soil Model

Note: The selected default soil model will be assigned to all newly generated layers.

Pressure-Dependent Modified Kondner Zelasko (MKZ)

Default Hysteretic Re/Unloading Formulation

Non-Masing Re/Unloading

Automatic Profile Generation

○ On ◉ Off

Unit System

◉ English ○ Metric

Complementary Analyses

- [x] Equivalent Linear - Frequency Domain
- [ ] Linear - Frequency Domain (Under development)
- [ ] Linear - Time Domain (Under development)

Analysis Tag

DS-NL2

Layer Properties | Advanced Table View

Layer Number	Layer Name	Thickness (ft)	Unit Weight (pcf)	Shear Wave Velocity (ft/s)	Shear Strength (psf)	Soil Model	Dmin (%)	Ref. Strain (%)	Reference Stress (MPa)	β	s
1	Dike	3	125	550		MKZ	1.76653025803	0.07440000000	0.18	1.545	0.96
2	Dike	4	125	550		MKZ	1.50871098731	0.1032	0.18	1.56	0.96
3	Dike	4	125	1000		MKZ	1.34541686587	0.07640000000	0.18	1.575	0.945
4	Dike	4	125	1000		MKZ	1.25395921560	0.08620000000	0.18	1.545	0.945
5	Dike	4	125	1000		MKZ	1.20507222121	0.09340000000	0.18	1.545	0.945
6	Dike	3	125	1000		MKZ	1.18132113586	0.09920000000	0.18	1.575	0.945
7	Foundation Soil	5	115	600		MKZ	0.61296896129	0.0254	0.18	1.605	1.005
8	Foundation Soil	5	115	600		MKZ	0.59924942300	0.0266	0.18	1.605	1.005
9	Foundation Soil	5	115	600		MKZ	0.58709032480	0.0262	0.18	1.515	1.005
10	Foundation Soil	5	115	600		MKZ	0.57622210377	0.0294	0.18	1.635	1.005
11	Foundation Soil	5	115	600		MKZ	0.56626037016	0.0296	0.18	1.59	1.005
12	Chicora	5	130	1500		MKZ	3.01770846178	0.234	0.18	1.575	0.96
13	Williamsburg Fc	10	105	1500		MKZ	3.01770846178	0.234	0.18	1.575	0.96
14	Williamsburg Fc	10	105	1500		MKZ	3.01770846178	0.234	0.18	1.575	0.96
15	Williamsburg Fc	10	105	1500		MKZ	3.01770846178	0.234	0.18	1.575	0.96
16	Williamsburg Fc	10	105	1800		MKZ	3.01770846178	0.234	0.18	1.575	0.96
17	Williamsburg Fc	10	105	1800		MKZ	3.01770846178	0.234	0.18	1.575	0.96
18	Williamsburg Fc	10	125	1800		MKZ	3.01770846178	0.234	0.18	1.575	0.96
19	Williamsburg Fc	10	125	1800		MKZ	3.01770846178	0.234	0.18	1.575	0.96
20	Williamsburg Fc	10	125	1800		MKZ	3.01770846178	0.234	0.18	1.575	0.96
21	Williamsburg Fc	10	125	1800		MKZ	3.01770846178	0.234	0.18	1.575	0.96
22	Williamsburg Fc	10	125	1800		MKZ	3.01770846178	0.234	0.18	1.575	0.96

☑ Water table at top of layer: 5 | Add Layer(s) | Remove Layer(s)

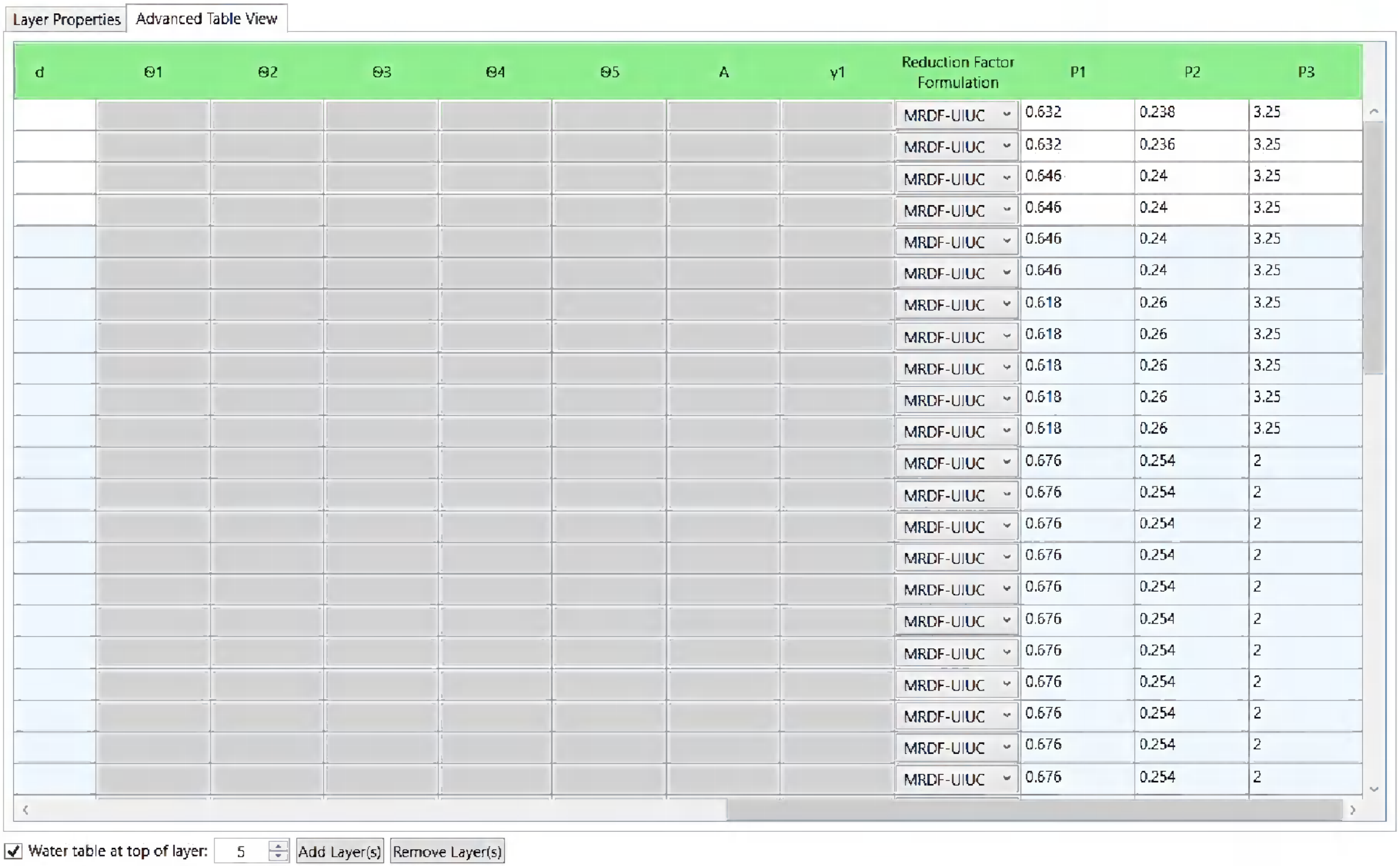

Layer Properties | Advanced Table View

d	Θ1	Θ2	Θ3	Θ4	Θ5	A	γ1	Reduction Factor Formulation	P1	P2	P3
								MRDF-UIUC	0.632	0.238	3.25
								MRDF-UIUC	0.632	0.236	3.25
								MRDF-UIUC	0.646	0.24	3.25
								MRDF-UIUC	0.646	0.24	3.25
								MRDF-UIUC	0.646	0.24	3.25
								MRDF-UIUC	0.646	0.24	3.25
								MRDF-UIUC	0.618	0.26	3.25
								MRDF-UIUC	0.618	0.26	3.25
								MRDF-UIUC	0.618	0.26	3.25
								MRDF-UIUC	0.618	0.26	3.25
								MRDF-UIUC	0.618	0.26	3.25
								MRDF-UIUC	0.676	0.254	2
								MRDF-UIUC	0.676	0.254	2
								MRDF-UIUC	0.676	0.254	2
								MRDF-UIUC	0.676	0.254	2
								MRDF-UIUC	0.676	0.254	2
								MRDF-UIUC	0.676	0.254	2
								MRDF-UIUC	0.676	0.254	2
								MRDF-UIUC	0.676	0.254	2
								MRDF-UIUC	0.676	0.254	2
								MRDF-UIUC	0.676	0.254	2
								MRDF-UIUC	0.676	0.254	2

☑ Water table at top of layer: 5 | Add Layer(s) | Remove Layer(s)

Layer Properties | Advanced Table View

Layer Number	Layer Name	Thickness (ft)	Unit Weight (pcf)	Shear Wave Velocity (ft/s)	Shear Strength (psf)	Soil Model	Dmin (%)	Ref. Strain (%)	Reference Stress (MPa)	β	s
23	Williamsburg Fc	10	125	1800		MKZ	3.01770846178	0.234	0.18	1.575	0.96
24	Williamsburg Fc	10	125	1800		MKZ	3.01770846178	0.234	0.18	1.575	0.96
25	Williamsburg Fc	10	125	1800		MKZ	3.01770846178	0.234	0.18	1.575	0.96
26	Williamsburg Fc	10	125	1800		MKZ	3.01770846178	0.234	0.18	1.575	0.96
27	Williamsburg Fc	10	125	1800		MKZ	3.01770846178	0.234	0.18	1.575	0.96
28	Williamsburg Fc	10	125	2000		MKZ	3.01770846178	0.234	0.18	1.575	0.96
29	Williamsburg Fc	10	125	2000		MKZ	3.01770846178	0.234	0.18	1.575	0.96
30	Williamsburg Fc	10	125	2000		MKZ	3.01770846178	0.234	0.18	1.575	0.96
31	Williamsburg Fc	10	125	2000		MKZ	3.01770846178	0.234	0.18	1.575	0.96
32	Williamsburg Fc	10	125	2000		MKZ	3.01770846178	0.234	0.18	1.575	0.96
33	Williamsburg Fc	10	125	2200		MKZ	3.01770846178	0.234	0.18	1.575	0.96
34	Williamsburg Fc	10	125	2200		MKZ	3.01770846178	0.234	0.18	1.575	0.96
35	Williamsburg Fc	10	125	2200		MKZ	3.01770846178	0.234	0.18	1.575	0.96
36	Williamsburg Fc	10	125	2200		MKZ	3.01770846178	0.234	0.18	1.575	0.96
37	Williamsburg Fc	10	125	2200		MKZ	3.01770846178	0.234	0.18	1.575	0.96
38	Williamsburg Fc	10	125	2200		MKZ	3.01770846178	0.234	0.18	1.575	0.96
39	Williamsburg Fc	10	125	2200		MKZ	3.01770846178	0.234	0.18	1.575	0.96
40	Williamsburg Fc	10	125	2200		MKZ	3.01770846178	0.234	0.18	1.575	0.96
41	Williamsburg Fc	10	125	2200		MKZ	3.01770846178	0.234	0.18	1.575	0.96
42	Williamsburg Fc	10	125	2200		MKZ	3.01770846178	0.234	0.18	1.575	0.96
43	Williamsburg Fc	10	125	2200		MKZ	3.01770846178	0.234	0.18	1.575	0.96
44	Williamsburg Fc	10	125	2200		MKZ	3.01770846178	0.234	0.18	1.575	0.96

☑ Water table at top of layer: 5 | Add Layer(s) | Remove Layer(s)

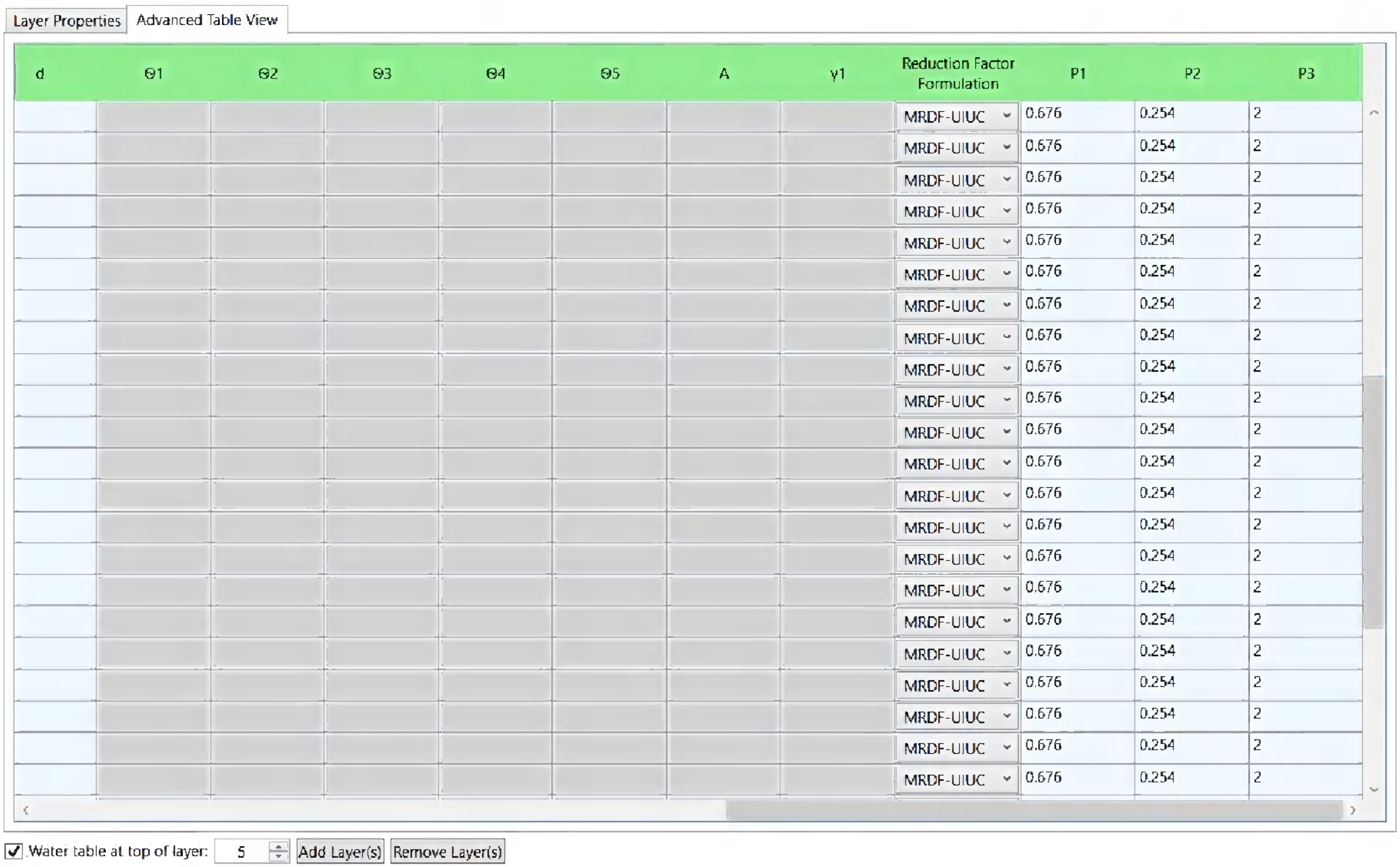
Layer Properties
Advanced Table View
d
Θ1
Θ2
Θ3
Θ4
Θ5
A
γ1
Reduction Factor Formulation
P1
P2
P3
MRDF-UIUC 0.676 0.254 2
MRDF-UIUC 0.676 0.254 2
MRDF-UIUC 0.676 0.254 2
MRDF-UIUC 0.676 0.254 2
MRDF-UIUC 0.676 0.254 2
MRDF-UIUC 0.676 0.254 2
MRDF-UIUC 0.676 0.254 2
MRDF-UIUC 0.676 0.254 2
MRDF-UIUC 0.676 0.254 2
MRDF-UIUC 0.676 0.254 2
MRDF-UIUC 0.676 0.254 2
MRDF-UIUC 0.676 0.254 2
MRDF-UIUC 0.676 0.254 2
MRDF-UIUC 0.676 0.254 2
MRDF-UIUC 0.676 0.254 2
MRDF-UIUC 0.676 0.254 2
MRDF-UIUC 0.676 0.254 2
MRDF-UIUC 0.676 0.254 2
MRDF-UIUC 0.676 0.254 2
MRDF-UIUC 0.676 0.254 2
MRDF-UIUC 0.676 0.254 2
MRDF-UIUC 0.676 0.254 2
Water table at top of layer: 5
Add Layer(s)
Remove Layer(s)

Layer Properties | Advanced Table View

Layer Number	Layer Name	Thickness (ft)	Unit Weight (pcf)	Shear Wave Velocity (ft/s)	Shear Strength (psf)	Soil Model	Dmin (%)	Ref. Strain (%)	Reference Stress (MPa)	β	s
36	Williamsburg Fc	10	125	2200		MKZ	3.01770846178	0.234	0.18	1.575	0.96
37	Williamsburg Fc	10	125	2200		MKZ	3.01770846178	0.234	0.18	1.575	0.96
38	Williamsburg Fc	10	125	2200		MKZ	3.01770846178	0.234	0.18	1.575	0.96
39	Williamsburg Fc	10	125	2200		MKZ	3.01770846178	0.234	0.18	1.575	0.96
40	Williamsburg Fc	10	125	2200		MKZ	3.01770846178	0.234	0.18	1.575	0.96
41	Williamsburg Fc	10	125	2200		MKZ	3.01770846178	0.234	0.18	1.575	0.96
42	Williamsburg Fc	10	125	2200		MKZ	3.01770846178	0.234	0.18	1.575	0.96
43	Williamsburg Fc	10	125	2200		MKZ	3.01770846178	0.234	0.18	1.575	0.96
44	Williamsburg Fc	10	125	2200		MKZ	3.01770846178	0.234	0.18	1.575	0.96
45	Williamsburg Fc	10	125	2200		MKZ	3.01770846178	0.234	0.18	1.575	0.96
46	Williamsburg Fc	10	125	2200		MKZ	3.01770846178	0.234	0.18	1.575	0.96
47	Williamsburg Fc	10	125	2200		MKZ	3.01770846178	0.234	0.18	1.575	0.96
48	Williamsburg Fc	10	125	2200		MKZ	3.01770846178	0.234	0.18	1.575	0.96
49	Williamsburg Fc	10	125	2200		MKZ	3.01770846178	0.234	0.18	1.575	0.96
50	Williamsburg Fc	10	125	2200		MKZ	3.01770846178	0.234	0.18	1.575	0.96
51	Williamsburg Fc	10	125	2200		MKZ	3.01770846178	0.234	0.18	1.575	0.96
52	Williamsburg Fc	10	125	2200		MKZ	3.01770846178	0.234	0.18	1.575	0.96
53	Williamsburg Fc	10	125	2200		MKZ	3.01770846178	0.234	0.18	1.575	0.96
54	Williamsburg Fc	10	125	2200		MKZ	3.01770846178	0.234	0.18	1.575	0.96
55	Williamsburg Fc	10	125	2200		MKZ	3.01770846178	0.234	0.18	1.575	0.96
56	Williamsburg Fc	10	125	2200		MKZ	3.01770846178	0.234	0.18	1.575	0.96
57	Williamsburg Fc	10	125	2200		MKZ	3.01770846178	0.234	0.18	1.575	0.96

☑ Water table at top of layer: 5 | Add Layer(s) | Remove Layer(s)

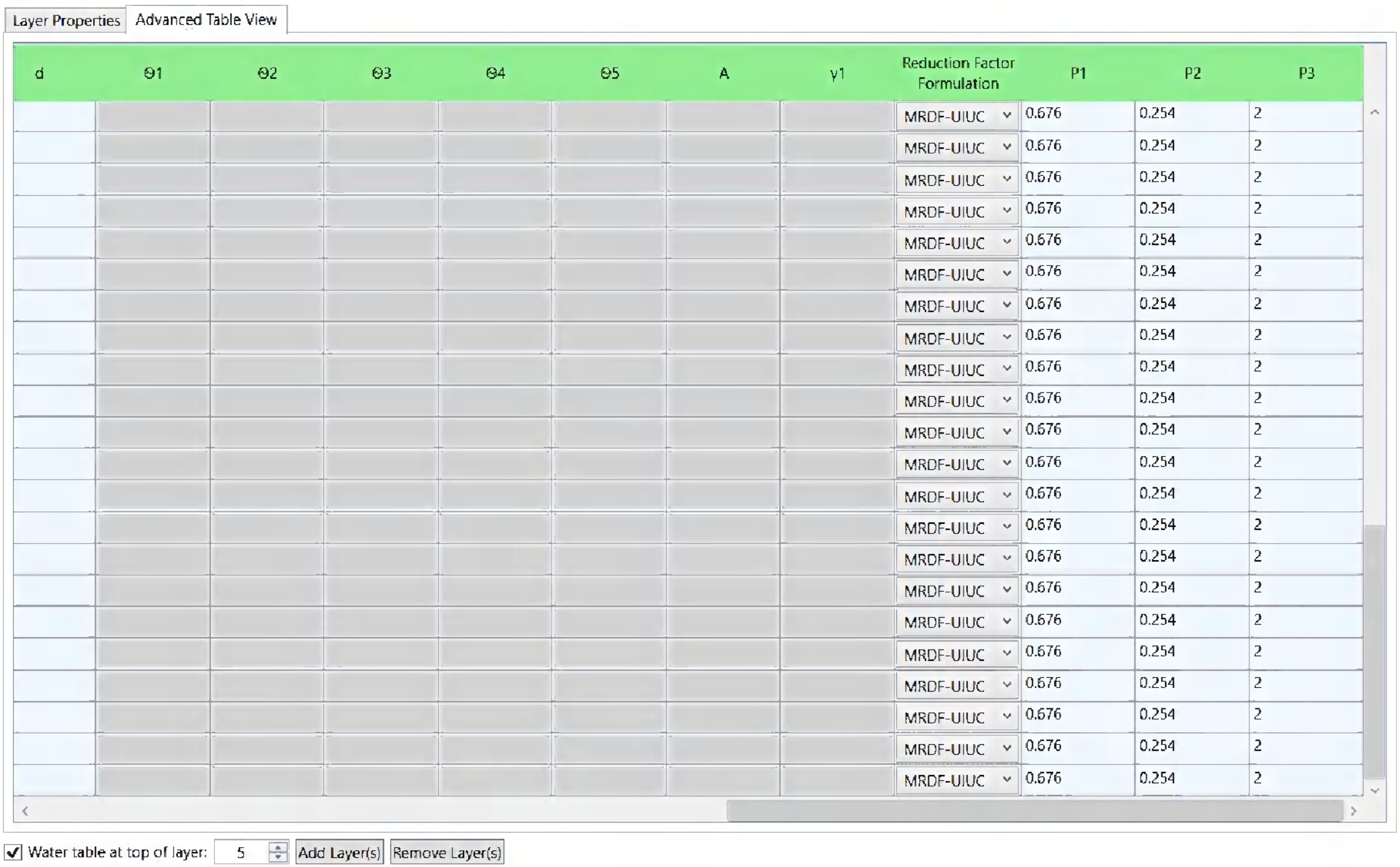

Layer Properties
Advanced Table View
d
Θ1
Θ2
Θ3
Θ4
Θ5
A
γ1
Reduction Factor Formulation
P1
P2
P3
MRDF-UIUC
0.676
0.254
2
Water table at top of layer:
5
Add Layer(s)
Remove Layer(s)

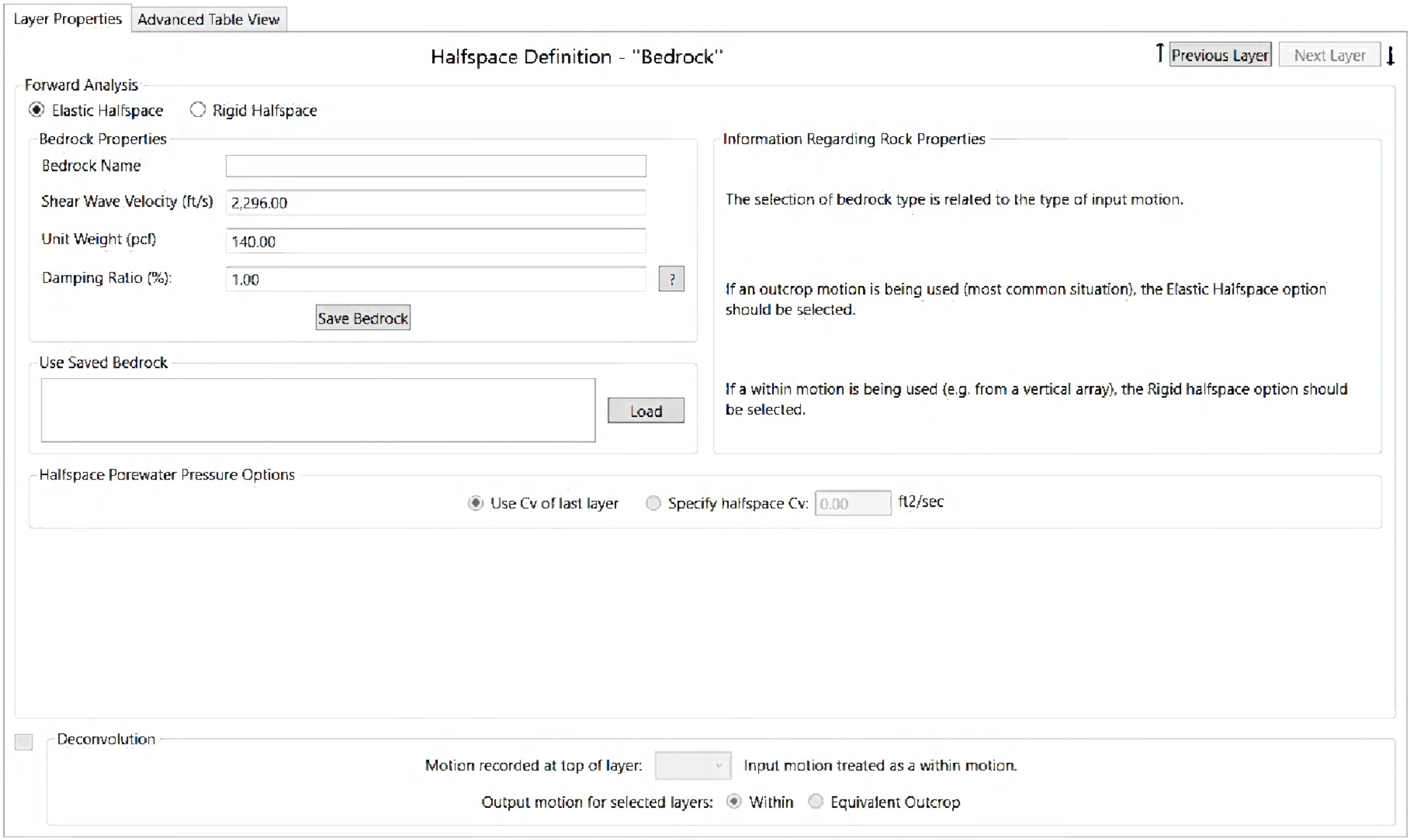
Layer Properties
Advanced Table View
Halfspace Definition - "Bedrock"
Previous Layer
Next Layer
Forward Analysis
Elastic Halfspace
Rigid Halfspace
Bedrock Properties
Bedrock Name
Shear Wave Velocity (ft/s)
2,296.00
Unit Weight (pcf)
140.00
Damping Ratio (%):
1.00
?
Save Bedrock
Use Saved Bedrock
Load
Information Regarding Rock Properties
The selection of bedrock type is related to the type of input motion.
If an outcrop motion is being used (most common situation), the Elastic Halfspace option should be selected.
If a within motion is being used (e.g. from a vertical array), the Rigid halfspace option should be selected.
Halfspace Porewater Pressure Options
Use Cv of last layer
Specify halfspace Cv:
0.00
ft2/sec
Deconvolution
Motion recorded at top of layer:
Input motion treated as a within motion.
Output motion for selected layers:
Within
Equivalent Outcrop

Soil Profile Definition

Soil Profile Plot

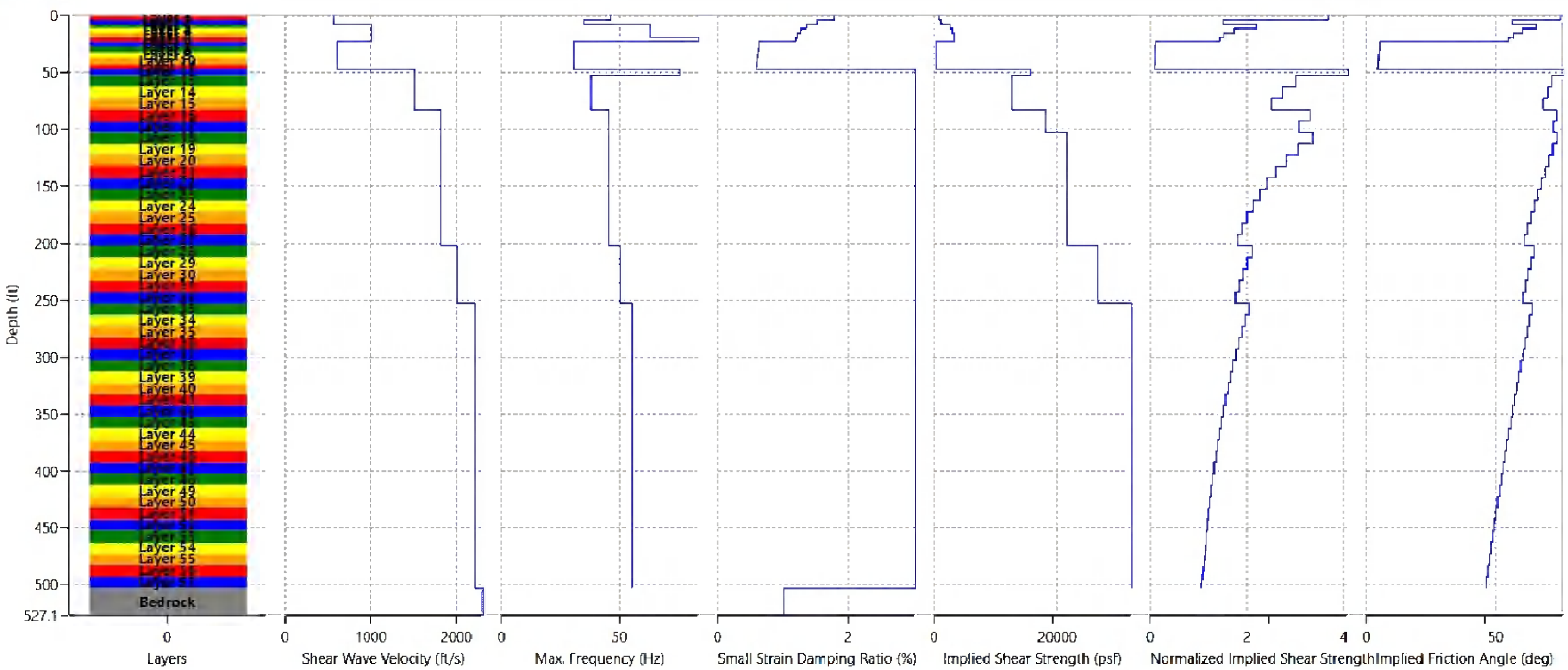

Soil Profile Metrics

Total Profile Depth	502
Profile Natural Frequency (Hz):	0.8388
Profile Natural Period (sec):	1.192

Input Motion Selection

☑ Generate Motion Plots

- ☐ Kocaeli
- ☐ LomaGilroy
- ☐ LomaGilroy2
- ☐ MammothLake
- ☐ Nahanni
- ☐ Northridge
- ☐ Northridge2
- ☐ Parkfield
- ☐ PEL180 - Scaled (
- ☐ PEL180
- ☐ PEL180scaled
- ☑ RSN8529Mineral
- ☐ RSN8529Mineral
- ☐ SED-T1 - Scaled
- ☐ SED-T1
- ☐ SED-T1scaled
- ☐ TAP046-N - Scalc
- ☐ TAP046-N
- ☐ TAP046-Nscaled

Select All

Add New Motion

Remove Selected Motion

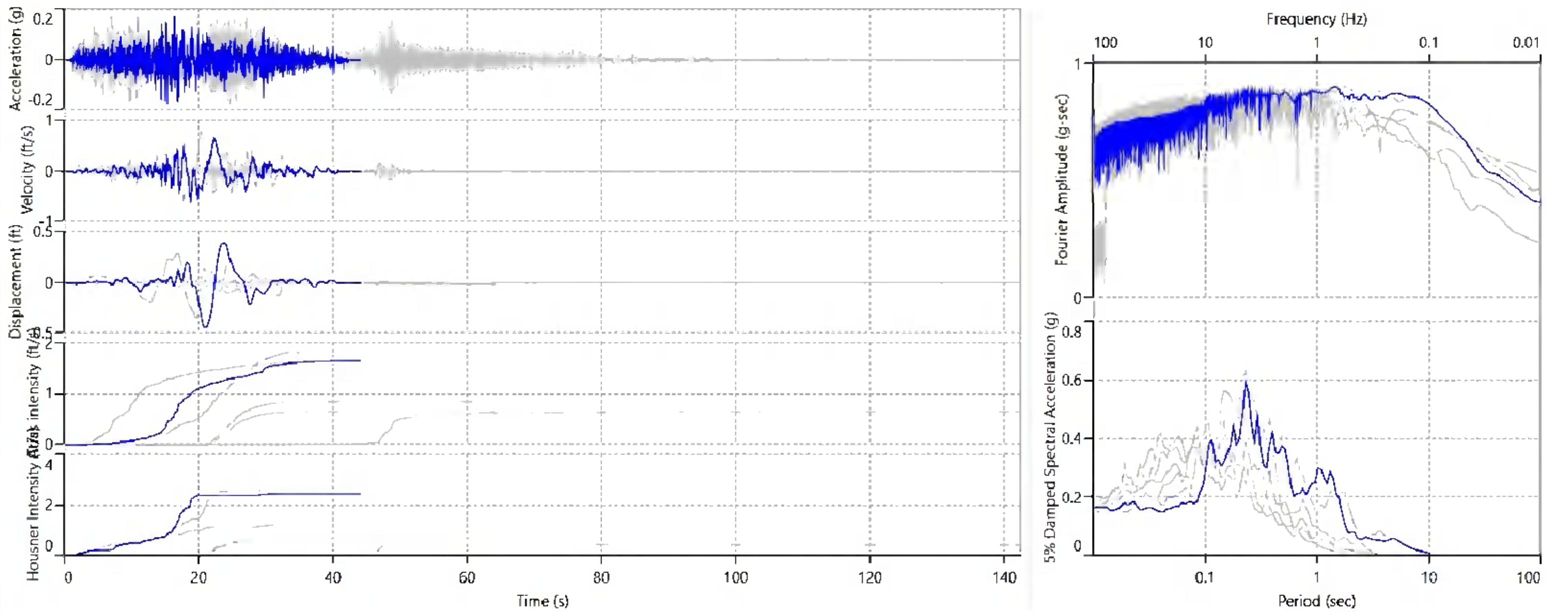

Motion Name :	BOS-T1-015g	DEL090-015g	RSN8529_Mineral-015g	Winyah1-015g	Winyah2-015g	YER360-015g
Number of Points:	6996	7069	28502	12798	12798	8796
Timestep (sec):	0.005	0.005	0.005	0.005	0.005	0.005
Nyquist Freq. (Hz):	100	100	100	100	100	100
PGA (g)	1.5E-1	1.5E-1	1.5E-1	1.5E-1	1.5E-1	1.5E-1
PGV (ft/s)	8E-1	2.5E-1	1.6E-1	1.8E-1	2.6E-1	6.8E-1
PGD (ft)	3.5E-1	5.6E-2	2E-2	8.2E-2	1.1E-1	4.4E-1
Show on Plot :	☑	☑	☑	☑	☑	☑
Tools :	Process ▾	Process ▾	Process ▾	Process ▾	Process ▾	Process ▾

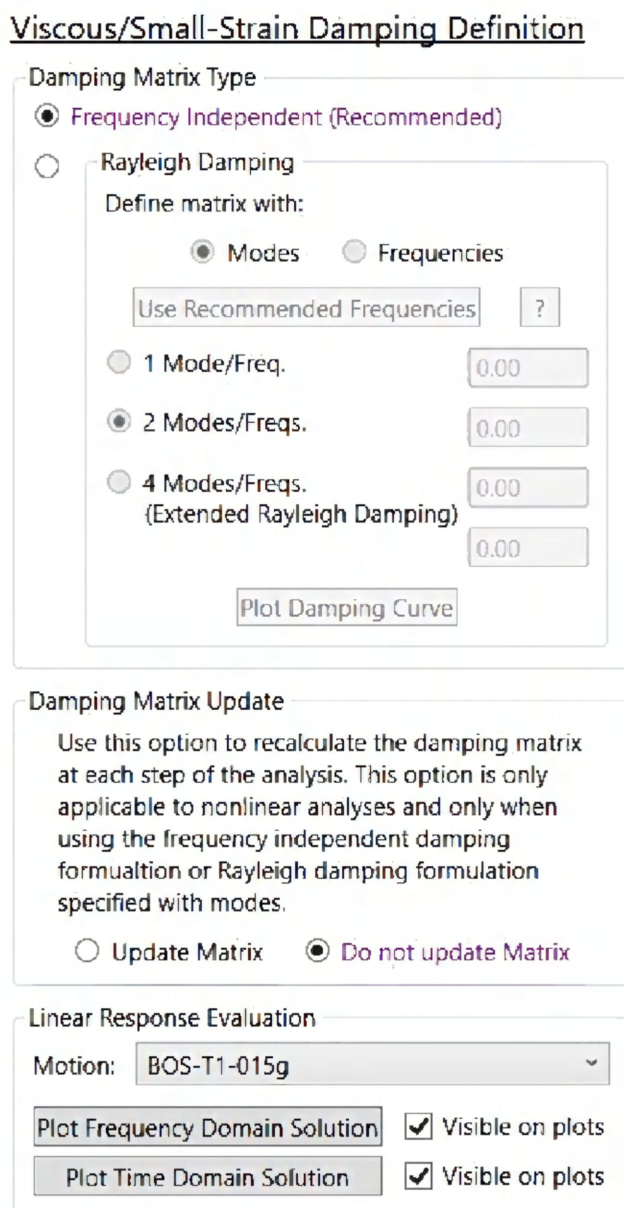
Viscous/Small-Strain Damping Definition
Damping Matrix Type
Frequency Independent (Recommended)
Rayleigh Damping
Define matrix with:
Modes
Frequencies
Use Recommended Frequencies
?
1 Mode/Freq.
0.00
2 Modes/Freqs.
0.00
4 Modes/Freqs.
(Extended Rayleigh Damping)
0.00
0.00
Plot Damping Curve
Damping Matrix Update
Use this option to recalculate the damping matrix at each step of the analysis. This option is only applicable to nonlinear analyses and only when using the frequency independent damping formualtion or Rayleigh damping formulation specified with modes.
Update Matrix
Do not update Matrix
Linear Response Evaluation
Motion:
BOS-T1-015g
Plot Frequency Domain Solution
Visible on plots
Plot Time Domain Solution
Visible on plots

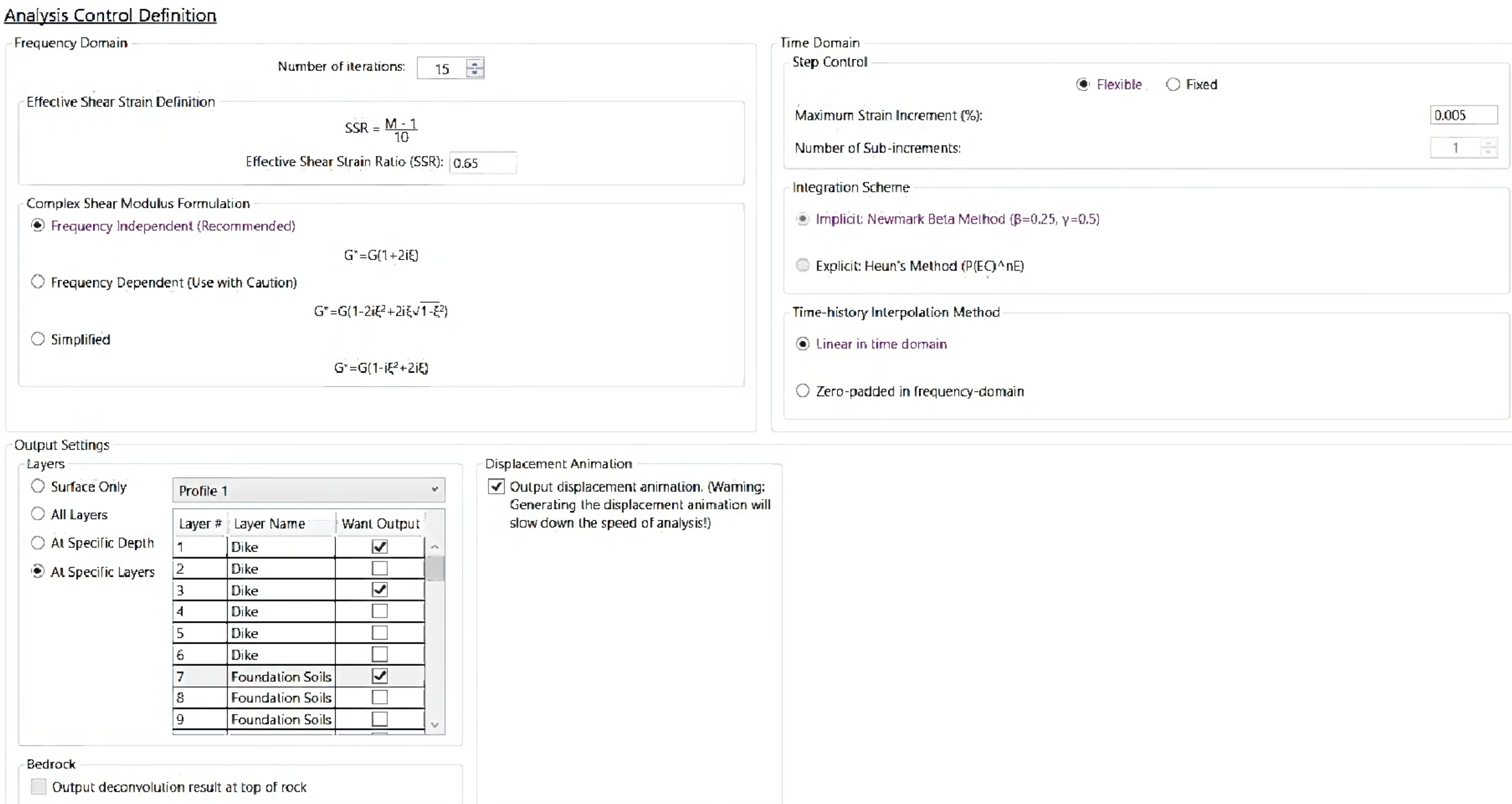
Analysis Control Definition
Frequency Domain
Number of iterations: 15
Effective Shear Strain Definition
SSR = (M - 1)/10
Effective Shear Strain Ratio (SSR): 0.65
Complex Shear Modulus Formulation
Frequency Independent (Recommended)
G*=G(1+2iξ)
Frequency Dependent (Use with Caution)
G*=G(1-2iξ²+2iξ√1-ξ²)
Simplified
G*=G(1-iξ²+2iξ)
Time Domain
Step Control
Flexible
Fixed
Maximum Strain Increment (%): 0.005
Number of Sub-increments: 1
Integration Scheme
Implicit: Newmark Beta Method (β=0.25, γ=0.5)
Explicit: Heun's Method (P(EC)^nE)
Time-history Interpolation Method
Linear in time domain
Zero-padded in frequency-domain
Output Settings
Layers
Surface Only
All Layers
At Specific Depth
At Specific Layers
Profile 1
Layer #
Layer Name
Want Output
1 Dike
2 Dike
3 Dike
4 Dike
5 Dike
6 Dike
7 Foundation Soils
8 Foundation Soils
9 Foundation Soils
Displacement Animation
Output displacement animation. (Warning: Generating the displacement animation will slow down the speed of analysis!)
Bedrock
Output deconvolution result at top of rock

ATTACHMENT 4
LIQUEFACTION POTENTIAL ANALYSIS

Written by:	C. Carlson	Date:	10/14/2021	Reviewed by:	O. Kutlu/W. Shin	Date:	10/14/2021
Client:	Santee Cooper	Project:	Winyah Generating Station	Project/ Proposal No.:	GC8100	Task No.:	03

LIQUEFACTION POTENTIAL ANALYSIS: ASH POND B

INTRODUCTION

This liquefaction potential analysis calculation package (Liquefaction Package) was prepared to present the evaluation for liquefaction potential of the perimeter dike soils forming Ash Pond B and foundation soils beneath the perimeter dike at Winyah Generating Station (WGS or Site). This calculation package is Attachment 4 to *2021 Periodic Safety Factor Assessment: Ash Pond B* (2021 Safety Factor Assessment Report) prepared by Geosyntec Consultants, Inc. (Geosyntec) to demonstrate compliance with the United States Environmental Protection Agency's (USEPA) Coal Combustion Residuals (CCR) Rule with respect to the periodic safety factor assessment criteria presented in 40 Code of Federal Regulations (CFR) 257.73(e). Ground motions and resulting shear stresses for the design seismic event are presented in Attachment 3 *Seismic Hazard Evaluation and Site Response Analysis: Ash Pond B* (Site Response Package) to the 2021 Safety Factor Assessment Report. The liquefaction potential of soils was evaluated using results from soil borings and cone penetration test (CPT) soundings advanced through the Ash Pond B perimeter dike and collected during Geosyntec's 2013 and 2016 geotechnical subsurface investigations and a historical investigation (PCRA, 1993) for which boring logs are available. Details of these investigations are discussed in *2016 Surface Impoundment Periodic Safety Factor Assessment Report: Ash Pond B*(2016 Safety Factor Assessment Report) (Geosyntec, 2016). The remainder of this Liquefaction Package presents: (i) methodology; (ii) analysis cases; (iii) input parameters; (iv) results; (v) conclusions; and (vi) references.

METHODOLOGY

Current state-of-practice procedures for evaluating the liquefaction potential of a soil were developed based on case histories of occurrences and non-occurrences of liquefaction due to past earthquakes. Occurrences (or non-occurrences) of liquefaction were determined by presence (or absence) of surface manifestations of liquefaction such as sand boils, ground cracking, slope movements, and/or flow failures. Surface manifestations were generally present if large excess pore pressures are generated during seismic loading and "liquefaction" is triggered. Therefore, if soils at a particular site are not expected to undergo triggering of liquefaction based on the state-of-practice or regulatory guidance, additional analyses, such as post-liquefaction slope stability or lateral spreading estimations, are not necessary for the anticipated seismic ground motions.

It was assumed that soils classified as Organic Peat, Silt, and Clay, or a combination of these materials, are typically not susceptible to liquefaction. Additionally, soils that exhibit "clay-like" behavior according to data collected during CPT soundings were also screened as not susceptible to liquefaction. "Clay-like" behavior was defined as a soil with a Soil Behavior Index (I_c) greater than

2.60. The interpretation of CPT soundings and the computation of I_c are discussed in the 2016 Safety Factor Assessment Report (Geosyntec, 2016) and reiterated below. If a zone of soil screened as not susceptible to liquefaction by the above criteria, the soil zone was assigned a factor of safety (FS) against liquefaction triggering of 2.0. The criteria recommended by Bray and Sancio (2006) were typically applied at WGS to evaluate the susceptibility of fine-grained soils to cyclic softening. However, fine-grained soils were not encountered except within a few CPT soundings and representative samples were not collected in the vicinity of the Ash Pond B perimeter dikes. Thus, the criteria recommended by Bray and Sancio (2006) were not applicable or applied on samples collected from the Ash Pond B area.

The liquefaction analysis described below was performed based on the simplified procedure recommended by Seed and Idriss (1971) and later updated by Boulanger and Idriss (2014), unless otherwise indicated. Analyses were performed on both the CPT soundings and SPT borings. The methodology to compute the potential of soils to liquefy and the factor of safety against liquefaction are described below.

Cyclic Stress Ratio

The Cyclic Stress Ratio (CSR) is a measure of the shear stresses developed during an earthquake and is normalized with effective overburden stress. The CSR for a depth interval is calculated as follows:

$$CSR_{M,\sigma'_{vo}} = 0.65\,\frac{\tau_{max}}{\sigma'_{vo}} \tag{1}$$

where:

$CSR_{M,\sigma'vo}$ = cyclic stress ratio due to an earthquake with a magnitude, M, for an effective vertical stress, σ'_{vo}, at the depth interval (dimensionless);

τ_{max} = maximum shear stress developed at the depth interval during the seismic loading (psf); and

σ'_{vo} = effective vertical stress at the depth interval (psf).

The CSR represents the loading or demand on a soil unit during an earthquake.

Corrected Normalized CPT Sounding Interpretation

To evaluate the resistance or capacity of the soil against liquefaction, soil data must be interpreted from each boring or CPT sounding. A discussion of the interpretation of the CPT data is provided in the 2016 Safety Factor Assessment Report (Geosyntec, 2016). Equations used in the interpretation are reiterated below.

The normalized cone tip resistance ratio, Q, and normalized friction ratio, F, were calculated by:

$$Q = \left(\frac{q_c - \sigma_{vo}}{P_a}\right)\left(\frac{P_a}{\sigma'_{vo}}\right)^n \quad (2)$$

and,

$$F = \left(\frac{f_s}{q_c - \sigma_{vo}}\right) \times 100\% \quad (3)$$

where:

q_c	=	measured tip resistance (tsf);
σ_{vo}	=	total vertical stress (tsf);
σ'_{vo}	=	effective vertical stress (tsf);
P_a	=	atmospheric pressure ($P_a = 1.058$ tsf);
n	=	varies from 0.5 for sands to 1.0 for clays; and
f_s	=	measured sleeve friction (tsf).

It is noted that the tip resistance (q_c) measured in the field must be adjusted for pore pressure effects on the cone tip if the data collection software does not automatically account for the area ratio of the cone. This correction is discussed within the 2016 Safety Factor Assessment Report (Geosyntec, 2016).

The soil behavior type index, I_c, as derived by Robertson and Wride (1998) is calculated by:

$$I_c = \left[\left(3.47 - \log(Q)\right)^2 + (\log(F) + 1.22)^2\right]^{0.5} \quad (4)$$

The I_c is used to compute the soil behavior type (SBT) index which may be used to infer the type of soil that is present at the depth interval.

To compute the resistance of a soil interval against liquefaction, the overburden-corrected tip resistance, q_{c1}, must be computed for the depth interval. q_{c1} can be computed as follows:

$$q_{c1} = C_N q_c \quad (5)$$

where:

C_N	=	overburden correction factor = $(P_a/\sigma'_{vo})^{1.338-0.249(q_{c1Ncs})^{0.264}}$;
q_{c1N}	=	normalized tip resistance q_{c1}/P_a (dimensionless); and
q_{c1Ncs}	=	equivalent clean sand corrected tip resistance defined in the Cyclic Resistance Ratio (CRR) section.

The computation of C_N was limited to a maximum value of 1.7 and is applicable for values of q_{c1Ncs} between 21 and 254. As evident in the equations above and below, the computation of q_{c1}, q_{c1N}, and

q_{c1Ncs} is an iterative procedure, which was performed using an algorithm developed within the MathCAD® computation software.

Corrected Normalized SPT Blow Count

Interpretation of soil test borings and SPT blow counts is discussed within the 2016 Safety Factor Assessment Report (Geosyntec, 2016) but is briefly reiterated below. The corrected normalized SPT blow count, $(N_1)_{60}$, which is applied in computing resistance of a soil against liquefaction, was calculated by the following equation presented by Idriss and Boulanger (2008).

$$(N_1)_{60} = N_{meas} C_E C_B C_S C_R C_N \tag{6}$$

where:

N_{meas}	=	measured SPT blow count (blows/ft);
C_E	=	correction factor for energy ratio;
C_B	=	correction factor for borehole diameter;
C_R	=	correction factor for rod length;
C_S	=	correction factor for sampler; and
C_N	=	correction factor for overburden pressure.

The correction factor for the applied energy (C_E) is dependent on the type and calibration of the hammer system attached to the drill rig. The correction factor (C_E) converts the measured N-value to a standard value, which assumes a 60 percent efficiency of the hammer system. This correction factor was computed as follows:

$$C_E = \frac{ER}{60} \tag{7}$$

where:

ER	=	energy ratio of the SPT hammer system.

Energy ratios selected for these analyses are discussed later within this Liquefaction Package. The correction factors above (excluding C_N) are given in Table 1. C_N was calculated for equivalent clean sand corrected SPT blow counts, $(N_1)_{60cs}$, (defined in the Cyclic Resistance Ratio (CRR) section) values less than 46 blows per foot, as follows:

$$C_N = \left(\frac{P_a}{\sigma'_{vo}}\right)^{(0.784-0.0768\sqrt{(N_1)_{60cs}})} \tag{8}$$

where:

P_a = atmospheric pressure (2,117 psf); and
σ'_{vo} = effective vertical stress (psf).

The computation of C_N was limited to a maximum value of 1.7. As evident in the equations above and below, the computation of $(N_1)_{60}$ and $(N_1)_{60cs}$ is an iterative procedure, which was performed using an algorithm developed within the MathCAD® computation software.

Cyclic Resistance Ratio (CRR)

The Cyclic Resistance Ratio (CRR) is a measure of a soil's resistance to triggering of liquefaction. The CRR was computed from CPT sounding data based on the corrected tip resistance of clean sand for an earthquake of magnitude = 7.5 and an overburden pressure of one atmosphere, as follows:

$$CRR_{M=7.5,\sigma'_{vo}=1\,atm} = \exp\left(\frac{q_{c1Ncs}}{113} + \left(\frac{q_{c1Ncs}}{1000}\right)^2 - \left(\frac{q_{c1Ncs}}{140}\right)^3 + \left(\frac{q_{c1Ncs}}{137}\right)^4 - 2.8\right) \quad (9)$$

Equation 9 is considered valid for the equivalent clean sand corrected tip resistance (q_{c1Ncs}) with values less than 211. For clean sands, q_{c1Ncs}, is equivalent to q_{c1N}, but for soils with some percentage of fines, $q_{c1Ncs} = q_{c1N} + \Delta q_{c1N}$, where the correction factor, Δq_{c1N}, is given by:

$$\Delta q_{c1N} = \left(11.9 + \frac{q_{c1N}}{14.6}\right) \times \exp\left(1.63 - \frac{9.7}{FC+2} - \left(\frac{15.7}{FC+2}\right)^2\right) \quad (10)$$

where:

FC = percent of fines (by mass).

Using corrected SPT N-values, the CRR was computed similarly for an earthquake of magnitude, M = 7.5, and an overburden pressure of one atmosphere, using corrected SPT N-values, as follows:

$$CRR_{M=7.5,\,\sigma'_{vo}=1\,atm} = \exp\left(\frac{(N_1)_{60cs}}{14.1} + \left(\frac{(N_1)_{60cs}}{126}\right)^2 - \left(\frac{(N_1)_{60cs}}{23.6}\right)^3 + \left(\frac{(N_1)_{60cs}}{25.4}\right)^4 - 2.8\right) \quad (11)$$

For clean sands, the equivalent clean sand value of the SPT penetration resistance $(N_1)_{60cs}$, is equivalent to $(N_1)_{60}$, but for soils with some percentage of fines, $(N_1)_{60cs} = (N_1)_{60} + \Delta(N_1)_{60}$, where the correction factor, $\Delta(N_1)_{60}$, is given by:

$$\Delta(N_1)_{60} = \exp\left(1.63 + \frac{9.7}{FC+0.01} - \left(\frac{15.7}{FC+0.01}\right)^2\right) \quad (12)$$

The selected fines content (FC) values used in these computations are discussed later within this calculation package. It is noted that $\Delta(N_1)_{60}$ is limited to a maximum value of 5.5.

Overburden Correction Factor

The overburden correction factor, K_σ, was introduced by Seed (1983) to adjust the CRR to a reference value of effective overburden stress because the CRR of sands is dependent on the effective overburden stress. The recommended relationship for K_σ is given by:

$$K_\sigma = 1 - C_\sigma \ln\left(\frac{\sigma'_{vo}}{P_a}\right) \leq 1.1 \quad (13)$$

where:

$$C_\sigma = 1 \,/\, (37.3 - 8.27(q_{c1Ncs})^{0.264}) \quad \leq 0.3 \text{ for CPT soundings.} \quad (14)$$

and,

$$C_\sigma = 1 \,/\, (18.9 - 2.55((N_1)_{60cs})^{0.5}) \quad \leq 0.3 \text{ for SPT borings.} \quad (15)$$

Furthermore, Equations 14 and 15 are applicable for q_{c1Ncs} and $(N_1)_{60cs}$ values less than 211 and 37 blows per foot, respectively. The overburden correction factor is used in liquefaction potential computations to adjust the CRR to a common effective overburden stress as shown by the following equation:

$$CRR_{\sigma'_{vo}} = K_\sigma \times CRR_{\sigma'_{vo}=1\,\text{atm}} \quad (16)$$

Magnitude Scaling Factor (MSF)

The magnitude scaling factor (MSF) is applied to adjust the CRR to the design earthquake magnitude, M. For cohesionless soils, the MSF is calculated using the equation below:

$$MSF = 6.9 \times \exp\left(\frac{-M}{4}\right) - 0.058, \text{ and } MSF \leq 1.8 \quad (17)$$

The MSF was calculated as 1.05 for a magnitude 7.3 earthquake, which was selected based on the deaggregation of the probabilistic seismic hazard as described in the Site Response Package.

The CRR for a magnitude M earthquake is calculated as follows:

$$CRR_M = MSF \times CRR_{M=7.5} \quad (18)$$

Age Correction Factor (K_{DR})

Correlations associated with liquefaction potential analysis were developed based on case histories of the presence or absence of liquefaction in relatively young soil deposits (i.e., Holocene age). As described in the South Carolina Department of Transportation (SCDOT) Geotechnical Design Manual (GDM) (2019), the CRR may be adjusted to account for diagenesis and other age-related effects in older soils that have not previously experienced liquefaction. Equation 13-30 of the SCDOT GDM computes the Age Correction Factor (K_{DR}) based on its age (t in years) as:

$$K_{DR} = 0.13\log_{10}(t) + 0.83 \qquad (19a)$$

The K_{DR} in Equation 19a is limited to a maximum value of 2.09. Meanwhile, Andrus et al. (2008) presents a similar equation for the K_{DR} as:

$$K_{DR} = 0.19\log_{10}(t) + 0.68 \qquad (19b)$$

It is noted that "t" is considered based on the "geotechnical age" instead of the "geologic age." Geologic age is the time since initial soil deposition; whereas geotechnical age is the time since the last significant liquefaction event resulting in re-sedimentation of the soil fabric.

The CRR for sand strata was adjusted by the age correction factor to account for this aging effect, and is computed as follows.

$$CRR_{M,K} = K_{DR} \times CRR_M \qquad (20)$$

Factor of Safety

The factors of safety against triggering of liquefaction (FS_{liq}) for both SPT and CPT analyses were computed by:

$$FS_{liq} = \frac{CRR_{M,\sigma'_{vo},Kdr}}{CSR_{M,\sigma'_{vo}}} \qquad (21)$$

where:

- $CRR_{M,\sigma'vo,Kdr}$ = cyclic resistance ratio adjusted for earthquake magnitude, effective overburden stress, and deposit age ($CRR_{M=7.5,\sigma'_{vo}=1\,atm} \times K_\sigma \times MSF \times K_{DR}$); and
- $CSR_{M,\sigma'vo.}$ = cyclic stress ratio for the corresponding design earthquake magnitude and overburden stress at the depth interval.

ANALYSIS CASES

As noted previously, liquefaction potential computations were conducted on soil data collected from soil borings and CPT soundings overseen by Geosyntec in 2013 and 2016 and from field investigation data collected by Paul C. Rizzo Associates (PCRA) (1993). Santee Cooper personnel indicated that no additional geotechnical subsurface investigations have been conducted since 2016. Computations were limited to soil borings and CPT soundings located through the dike centerline into the dike fills and foundation soils immediately underlying the perimeter dikes.

Two representative soil profiles of shear wave velocity (V_s) were developed from the dike crest to the Chicora stratum as presented in the 2016 Safety Factor Assessment Report (Geosyntec, 2016). These profiles were developed from direct measurements of V_s and by means of a correlation with CPT sounding data. As discussed in the 2016 Safety Factor Assessment Report, these representative V_s profiles were supplemented with historical data to extend the V_s profile into the underlying Chicora and Williamsburg Formation Clay strata for the site response analyses of Ash Pond B.

No zones were identified to undergo triggering of liquefaction within Ash Pond B under the design earthquake in the 2016 Safety Factor Assessment. However, the portion of the Ash Pond B perimeter dikes along the Cooling Pond, represented by Profile 2 in the Site Response Package, was observed to have lower calculated FSs for slope stability. Site response analyses were performed only for Profile 2 as part of the 2021 Safety Factor Assessment to support an updated evaluation of liquefaction potential of the subsurface materials in the critical area of Ash Pond B. Therefore, only the investigations along Profile 2 were considered in the liquefaction potential evaluation presented in this calculation package (B-1 through B-4, CPT-135, CPT-136, CPT-226, CPT-227, SPT-114, SPT-115, and SPT-309), as shown on Figure 1.

As described within the Site Response Package, site response analyses of Profile 2 were performed using six ground motions selected for the Site. A profile of the maximum shear stress (τ_{max}) was computed for each ground motion and the maximum value at each depth was calculated to create a single profile of τ_{max} for Profile 2. The τ_{max} profile was used to compute the CSR at every depth for each soil boring or sounding. The maximum shear stress at each computed depth for Profile 2 is provided in Table 2. The τ_{max} for depths between the intervals listed within Table 2 were linearly interpolated.

INPUT PARAMETERS

The following section describes the selection of the input parameters applied for the liquefaction potential analysis.

Total Unit Weight

The total unit weight (γ_T) was used to calculate the total and effective stresses for the soil column for each boring and sounding analyzed. For the purpose of this analysis, CPT intervals were assigned a unit weight based on the ranges presented for soils in the region provided within the SCDOT GDM

(SCDOT, 2019) and the site-specific laboratory data (Geosyntec, 2016). The assigned unit weight is dependent on the measured soil behavior index (I_c) as follows:

- Clays and clayey sand mixtures ($I_c > 2.95$): 100 pcf
- Silt to silty sand mixtures ($2.60 < I_c \leq 2.95$): 100 pcf
- Silty sands to sand mixtures ($2.05 < I_c \leq 2.60$): 110 pcf
- Sands ($1.31 < I_c \leq 2.05$): 120 pcf
- Gravelly sands to sands ($I_c \leq 1.31$): 125 pcf

SPT intervals were assigned total unit weight values based on visual and laboratory observations on the soil type as follows:

- Clays and Silts: 100 pcf
- Loose Sands ($N \leq 10$ blows/foot): 105 pcf
- Medium Dense Sands (10 blows/foot $< N \leq 30$ blows/foot): 115 pcf
- Dense Sands ($N \geq 30$ blows/foot): 120 pcf
- Chicora: 130 pcf
- Williamsburg Formation Clay: 105 pcf

Age Correction Factor

The susceptibility of soil deposits to liquefaction was summarized by type of deposit and geologic age by Youd and Perkins (1978) (Table 3). Youd and Perkins (1978) observed that younger soils (Holocene age) generally are the most susceptible to liquefaction. In the South Carolina (SC) region, the influence of soil age was investigated locally by Arango et al. (2009) and Andrus et al. (2008) based on cyclic strength testing of high-quality samples of sand and in-situ testing on paleoliquefaction sites, respectively. Each researcher compared observations and results in each study with the case-history-based chart for liquefaction triggering developed by Idriss and Boulanger (2008). Andrus (2008) developed a correlation (Equation 19b) relating soil age to a correction factor for CRR. Additionally, Leon et al. (2005) investigated a site nearby to WGS (Sampit, SC) and identified soil ages for sands encountered between 546 to 450,000 years old. Age correction factors (K_{DR}) were computed based on Equations 19a and 19b for the range of soil ages observed in the region presented by Leon et al. (2005) and are provided in Table 4. A K_{DR} was selected from Table 4 and applied to the soils that were evaluated to be of geologic and geotechnical ages older than Holocene age (i.e., foundation soils).

As shown in Figure 2, soils immediately surrounding Ash Pond B perimeter dikes were determined by the SC Department of Natural Resources (2012) to be of Pleistocene age. It was assumed that these soils are located beneath the recompacted dike fill soils, which are considered to be of Holocene age due to the relatively "recent" construction. Based on the range of soil ages presented in Table 4, an age correction factor of 1.2 was selected for Pleistocene-aged, foundation soils at WGS. An age correction factor of 1.0 was applied for dike fill soils, as these structures are approximately 30 to 40 years old. As noted previously, "geologic" age differs from "geotechnical" age. Geologic age refers to the overall age of the soil since deposition. Geotechnical age refers to the age of the soil since the last instance of liquefaction. The geotechnical age was considered in the selection of K_{DR}. Dike base elevations were approximated based on the surface elevation of borings or soundings located at the dike toe or the prevailing ground surface elevation of the Cooling Pond. Information for the investigation points considered in this calculation package are summarized in Table 5.

Fines Content

As shown in Equations 9 through 12, the CRR is influenced by the fines content (percent particles by mass passing a No. 200 sieve). An increase in fines content of the soil results in larger CRR. The 2016 Safety Factor Assessment Report (Geosyntec, 2016) showed the fines content of dike fill and foundation soils is somewhat variable across the Ash Pond B footprint. Physical samples are not collected during CPT soundings and historical borings with laboratory index testing were not available for the 2016 Safety Factor Assessment, so index test data for each CPT sounding was based on the data collected from the nearest available soil boring with laboratory index testing, as provided in the 2016 Safety Factor Assessment Report. Index testing, when available, for soil borings were utilized for each individual SPT N-value. The source of the select fines content for each investigation point is summarized within Table 5.

Phreatic Surface

The phreatic surface through the perimeter dikes to the downstream toe of the dike at the time of the 2016 Safety Factor Assessment (Geosyntec, 2016) was developed for each individual boring or CPT sounding based on depth to water measurements, porewater pressure (u_o) signatures, and dissipation tests. Santee Cooper provided available water level measurements from wells in the Ash Pond B area. The recorded water levels in these wells have generally been steady over the last five years. Based on the review of the available water level measurements, the water level within the perimeter dike and beyond the downstream toe of the perimeter dike is expected to be similar to the water level used for the 2016 Safety Factor Assessment. Therefore, as detailed in the Site Response Package, site response analyses were performed with the water table modeled at 15 ft below ground surface and a maximum shear stress profile was calculated for this water table elevation.

For the liquefaction potential evaluation presented in this calculation package, the phreatic surface assumptions through the Ash Pond B perimeter dikes at the time of the boring (TOB) were used to estimate CRR profiles. CSR profiles were estimated for the time at which the earthquake event occurs using the phreatic surface assumed for the 2016 Safety Factor Assessment. The elevations of the phreatic surface through the Ash Pond B perimeter dikes at the time of the boring (TOB) and at the time of liquefaction analysis (TOA) for this calculation package are summarized in Table 5.

Energy Calibration for SPT N-Values

As described in the 2016 Safety Factor Assessment Report (Geosyntec, 2016), the subcontractor during Geosyntec's 2013 investigation, Soil Consultants, Inc. (SCI), reported that the automatic hammer on the utilized drilling rig had an energy ratio of 88 percent, which was independently evaluated within six months of the investigation. Borings performed by Mid Atlantic Drilling, Inc. along the perimeter dikes (SPT-309 and SPT-310) in 2016 utilized a drilling rig with an energy ratio of 77 percent (Geosyntec, 2016).

Historical Borings

Liquefaction potential of dike fill soils was also evaluated using boring logs provided within a PCRA design report which evaluated the raising of the Ash Pond B perimeter dikes (PCRA, 1993). As stated previously, correlations developed to predict the liquefaction potential of soils are based on empirical observations using a standard procedure or method during drilling activities. PCRA (1993) boring logs indicate that the 4-inch inner diameter, hollow stem auger borings were advanced by a CME-55 drilling rig equipped with rope and cathead hammer. It was assumed that the rope and cathead hammer system contained an energy ratio of 70 percent, which was used for borings B-1 through B-4.

RESULTS

The methodology discussed previously was applied within a MathCAD® algorithm similar to the spreadsheets presented in Idriss and Boulanger (2008). Computations were performed on soil borings (including the historical borings) and CPT soundings located at the dike centerline. FS_{liq} was computed at every depth interval where data were collected for soil test borings (in 2-ft or 5-ft intervals) and CPT soundings (in 0.16-ft intervals). The computed FS_{liq} for the soil borings and CPT soundings within Profile 2 of Ash Pond B are shown on Figures 3 through 7. Figure 3 shows SPT-114 and B-4, which are located at the southern end of Profile 2. Subsequent figures depict calculation results for soil borings and CPT soundings positioned progressively north along Profile 2. Example calculations are provided within Appendix 1.

The computed FS_{liq} typically exceeded 2.0 within dike fill and foundation soils immediately below the Ash Pond B perimeter dikes along the Cooling Pond (Profile 2).

CONCLUSIONS

Based on the liquefaction potential computations presented within this calculation package, the calculated FS_{liq} are greater than 1.7. Therefore, the dike fill soils (i.e., native soils recompacted to form impounding perimeter dikes) and foundation soils beneath the perimeter dikes of Ash Pond B are not expected to undergo triggering of liquefaction during the design earthquake. Given zones expected to undergo triggering of liquefaction were not identified for borings and CPT soundings advanced through the Ash Pond B perimeter dikes, additional post-liquefaction stability and displacement analyses are not warranted for the Ash Pond B perimeter dikes.

REFERENCES

Andrus, R. Gassman, S. L., Talwani, P., Hasek, M., Camp, W. Hayati, H., and Boller, R. (2008), "Characterization of Liquefaction Resistance of Aged Soils: Summary of Selected First Year Findings", *Proceedings of 2008 NSF Engineering Research and Innovation Conference, Knoxville, Tennessee*, NSF Grant # CMS-0556006.

Arango, I., Lewis, M. R., and McHood, M. D. (2009), "Site Characterization Philosophy and Liquefaction Evaluation of Aged Sands", *Bechtel Technology Journal*, Vol. 2, No. 1.

Boulanger, R. W. and Idriss, I. M. (2014), "CPT and SPT Based Liquefaction Triggering Procedures", *Report No. UCD/CGM-14/01*, Center for Geotechnical Monitoring, University of California, Davis, CA.

Bray, J.D. and Sancio, R.B. (2006) "Assessment of the Liquefaction Susceptibility of Fine-Grained Soils". *Journal of Geotechnical and Geoenvironmental Engineering*, Vol. 132, No. 9, pp. 1165-1177.

Geosyntec Consultants, Inc. (2016), "2016 Surface Impoundment Periodic Safety Factor Assessment Report: Ash Pond B, Winyah Generating Station, Georgetown, South Carolina", submitted to Santee Cooper.

Idriss, I. M. and Boulanger, R. W. (2008), "Soil Liquefaction During Earthquakes", *Earthquake Engineering Research Institute*, EERI Publication MNO-12.

Leon, E., Gassman, S. L., and Talwani, P. (2005), "Effect of Soil Aging on Assessing Magnitudes and Accelerations of Prehistoric Earthquakes", *Earthquake Spectra*, Vol. 21, No. 3 pg. 737-759.

Paul C. Rizzo Associates, Inc. (1993), "Report: Ash Pond B Dike Elevation: Winyah Generating Station", December 1993.

Robertson, P.K. and Wride, C.E. (1998), "Evaluating cyclic liquefaction potential using the cone penetration test, *Canadian Geotechnical Journal,* Volume 35, No. 3, pp. 442-59.

Seed, H.B. (1983), "Earthquake Resistant Design of Earth Dams", in *Proceedings, Symposium of Seismic Design of Embankments and Caverns, Pennsylvania,* ASCE, NY, pp. 41-64.

Seed, H.B, and Idriss, I.M. (1971), "Simplified Procedure for Evaluation Soil Liquefaction Potential", *Journal of the Soil Mechanics and Foundations Division,* ASCE, Vol. 107, NO. SM9.

South Carolina Department of Transportation (2019), "Geotechnical Design Manual Version 2.0", available: https://www.scdot.org/business/pdf/geotech/SCDOT-Geotechnical-Design-Manual.pdf

South Carolina Department of Natural Resources: Geologic Survey (2012), "Geologic Map of the Georgetown South Quadrangle, Georgetown County, South Carolina".

Youd, T. L. and Perkins, M. (1978), "Mapping liquefaction-induced ground failure potential", *J. Geotechnical Eng. Div.*, ASCE 104(GT4), 433-46.

Tables

Table 1. Correction Factors for Interpretation of SPT for Liquefaction Potential Analysis (Idriss and Boulanger, 2008)

Factor	Description
Energy ratio	Energy measurements are required to determine the delivered energy ratios or to calibrate the specific equipment being used. The correction factor is then computed as $$C_E = \frac{ER_m}{60}$$ where ER_m is the measured energy ratio as a percentage of the theoretical maximum. Empirical estimates of C_E (for rod lengths of 10 m or more) involve considerable uncertainty, as reflected by the following ranges: Doughnut hammer $C_E = 0.5\text{–}1.0$ Safety hammer $C_E = 0.7\text{–}1.2$ Automatic triphammer $C_E = 0.8\text{–}1.3$ (Seed et al. 1984, Skempton 1986, NCEER 1997)
Borehole diameter	Borehole diameter of 65–115 mm $C_B = 1.0$ Borehole diameter of 150 mm $C_B = 1.05$ Borehole diameter of 200 mm $C_B = 1.15$ (Skempton 1986)
Rod length	Where the ER_m is based on rod lengths of 10 m or more, the ER delivered with shorter rod lengths may be smaller. Recommended values from Youd et al. (2001) are as follows: Rod length < 3 m $C_R = 0.75$ Rod length 3–4 m $C_R = 0.80$ Rod length 4–6 m $C_R = 0.85$ Rod length 6–10 m $C_R = 0.95$ Rod length 10–30 m $C_R = 1.00$
Sampler	Standard split spoon without room for liners (the inside diameter is a constant $1^3/_8$ in.). $C_S = 1.0$. Split-spoon sampler with room for liners but with the liners absent (this increases the inside diameter to $1^1/_2$ in. behind the driving shoe): $C_S = 1.1 \quad \text{for} \quad (N_1)_{60} \le 10$ $C_S = 1 + \frac{(N_1)_{60}}{100} \quad \text{for} \quad 10 \le (N_1)_{60} \le 30$ $C_S = 1.3 \quad \text{for} \quad (N_1)_{60} \ge 30$ (from Seed et al. 1984, equation by Seed et al. 2001)

Table 2. Calculated Maximum Shear Stress Envelope for the Ash Pond B Dike Centerline

Profile 2	
Depth (ft)	τ_{max} (psf)
1.5	19
5	57
9	87
13	111
17	140
20.5	166
24.5	190
29.5	206
34.5	215
39.5	221
44.5	233
49.5	295
57	380
67	474
77	601
87	738
97	873
107	1026

Notes:

1. Profile 2 refers to the perimeter dikes adjacent to the Cooling Pond. Development of the profile is discussed within the Site Response Package.
2. For calculation points located in between the depth intervals listed above, the average τ_{max} was linearly interpolated for liquefaction potential computations.

Table 3. Susceptibility of Soil Deposits to Liquefaction during Strong Seismic Shaking (Youd and Perkins, 1978)

Type of deposit	Distribution of cohesionless sediments in deposit	Likelihood that cohesionless sediments, when saturated, would be susceptible to liquefaction			
		< 500 years	Holocene	Pleistocene	Pre-Pleistocene
Continental					
River channel	Locally variable	Very high	High	Low	Very low
Floodplain	Locally variable	High	Moderate	Low	Very low
Alluvial fan and plains	Widespread	Moderate	Low	Low	Very low
Marine terraces and plains	Widespread	—	Low	Very low	Very low
Delta and fan delta	Widespread	High	Moderate	Low	Very low
Lacustrine and playa	Variable	High	Moderate	Low	Very low
Colluvium	Variable	High	Moderate	Low	Very low
Talus	Widespread	Low	Low	Very low	Very low
Dunes	Widespread	High	Moderate	Low	Very low
Loess	Variable	High	High	High	Unknown
Glacial till	Variable	Low	Low	Very low	Very low
Tuff	Rare	Low	Low	Very low	Very low
Tephra	Widespread	High	High	?	?
Residual soils	Rare	Low	Low	Very low	Very low
Sebkha	Locally variable	High	Moderate	Low	Very low
Coastal zone					
Delta	Widespread	Very high	High	Low	Very low
Estuarine	Locally variable	High	Moderate	Low	Very low
Beach—high wave energy	Widespread	Moderate	Low	Very low	Very low
Beach—low wave energy	Widespread	High	Moderate	Low	Very low
Lagoonal	Locally variable	High	Moderate	Low	Very low
Foreshore	Locally variable	High	Moderate	Low	Very low
Artificial fill					
Uncompacted fill	Variable	Very high	—	—	—
Compacted fill	Variable	Low	—	—	—

Table 4. Age Correction Factor (K_{DR}) based on Soil Age

Soil Age, t (years)	**K_{DR} [1]**	**K_{DR} [2]**
126	1.10	1.08
546	1.19	1.20
5,038	1.31	1.38
10,000	1.35	1.44
450,000	1.56	1.75

Notes:

1. K_{DR} computed by SCDOT Geotechnical Design Manual (SCDOT, 2019), as provided in Equation 19a.
2. K_{DR} computed by Andrus et al (2008) as provided in Equation 19b.

Table 5. Summary of Soil Borings and Soundings Analyzed for Liquefaction Potential

Boring ID	**Northing**	**Easting**	**Elevation at TOB**	**Dike Base Elevation** [2]	**GWT El. at TOB**	**GWT Depth at TOB**	**GWT El. at TOA**	**GWT Depth at TOA**	**FC Basis**	τ_{max} **Profile**
-	**ft**	**ft**	**ft NGVD29**	**ft NGVD29**	**ft NGVD29**	**ft**	**ft NGVD29**	**ft**	-	-
B-1	546477.391	2504902.240	33.6	19.0	22.6	11.0	25.9	15.0	SPT-115	Profile 2
B-2	545661.804	2504880.619	33.7	19.0	20.7	13.0	25.9	15.0	SPT-115	Profile 2
B-3	544942.310	2504538.289	33.8	19.0	20.8	13.0	26.4	14.05	SPT-309	Profile 2
B-4	544316.506	2503866.841	33.8	19.0	21.8	12.0	22.4	19.1	SPT-114	Profile 2
CPT-135	545352.802	2504767.509	40.47	19.0	25.9	14.55	25.9	14.55	SPT-309	Profile 2
CPT-136	546698.537	2504910.337	40.62	19.0	25.0	15.6	25.0	15.6	SPT-115	Profile 2
CPT-226	545328.105	2504766.372	39.69	19.0	23.7	16.0	23.7	16.0	SPT-309	Profile 2
CPT-227	546414.575	2504926.725	39.97	19.0	28.0	12.0	28.0	12.0	SPT-115	Profile 2
SPT-114	544064.630	2503599.466	41.48	19.0	22.4	19.1	22.4	19.1	SPT-114	Profile 2
SPT-115	545998.280	2504990.830	40.90	19.0	25.9	15.0	25.9	15.0	SPT-115	Profile 2
SPT-309	544483.417	2504245.349	40.47	19.0	26.4	14.05	26.4	14.05	SPT-309	Profile 2

Notes:

1. ft NGVD29 - feet National Geodetic Vertical Datum of 1929; TOB - Time of Boring; TOA - Time of Analysis; GWT - Groundwater Table; FC - Fines Content.
2. Dike bottom elevation was estimated based on the elevation of the ground surface in the Cooling Pond (19.0 ft NGVD29).
3. Borings B-1 through B-4 were conducted in 1993 by PCRA to design the raising of dike structures. It was assumed that the dike was raised to the elevation of the nearest SPT-series or CPT-series boring performed recently. It was also assumed that the depth to groundwater was similar to that of a nearby boring or sounding at the time of analysis.
4. FC Basis refers to the source of the fines content profile for each investigation point. Fines content data are provided in the 2016 Safety Factor Assessment Report (Geosyntec, 2016).

Figures

N

LEGEND

W-SW-APB	EXISTING STAFF GAUGE
CPT-144	GEOSYNTEC CONE PENETRATION TEST
PPZ-5	PIEZOMETER
SPT-111	GEOSYNTEC SOIL BORING
B-1	HISTORICAL BORING
WAP-9	GROUNDWATER MONITORING WELL
	POND BOUNDARY
	PROPERTY BOUNDARY
	EXISTING GAS LINE
	EXISTING RAILROAD

NOTES:
1. Aerial imagery was obtaied from ESRI online database.
2. The position of underground utilities shown should be considered approximate.

600 300 0 600 Feet

ASH POND B WINYAH GENERATING STATION

GEORGETOWN, SOUTH CAROLINA

Geosyntec consultants

Charlotte, NC

October 2021

Figure 1

Y:\S\Santee Cooper\Santee Cooper - Winyah\2021 - 5 Yr CCR Rule Requirements\7 - Safety Factor Assessment\GIS\MXD\September 2021\FigureX_Ash Pond B_No X-Sections.mxd; Abby.Wesley; 10/12/2021

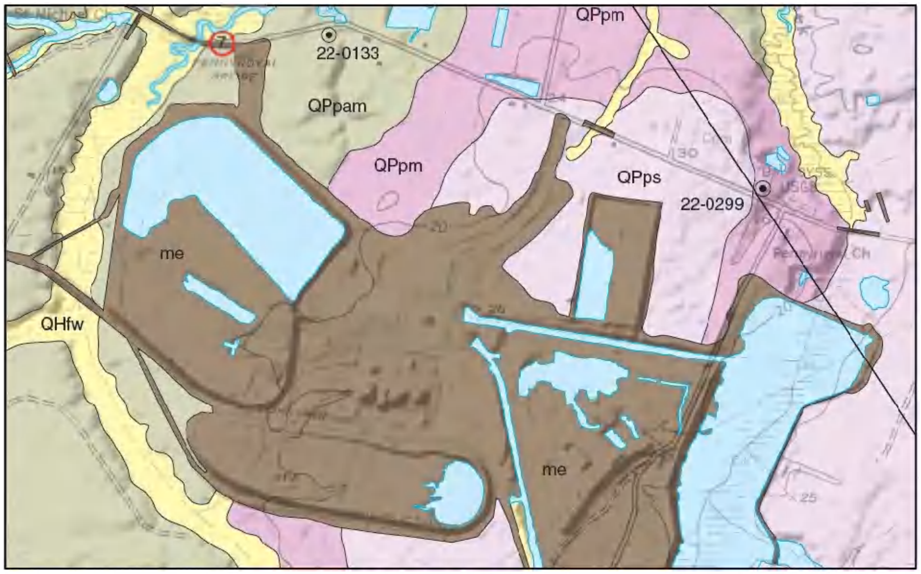

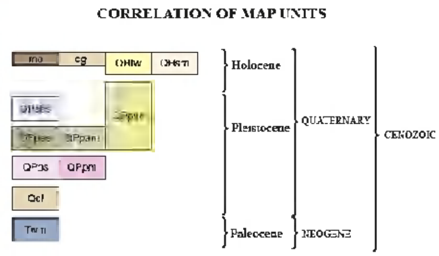

QPpam **Estuarine deposits or marine deposits or both (Pleistocene)** – In its lower part, quartz and phosphatic sand, medium bluish-gray (5B 5/1), poorly sorted, subrounded to very angular, fine to very coarse grained with trace amounts of very fine grained heavy minerals. Lower part 10 to 20 feet thick. In upper part, muddy sand to sandy mud, clay, silt, silty sand, clayey sand, phosphatic sand and quartz sand and shells, medium light-gray (N6) to medium bluish-gray (5B 5/1). Some zones contain broken and intact *Oliva, Polinices, Terebra, Mercenaria and Dosinia*. Upper part 1 to 10 feet thick.

Figure 2. Geologic Map of Areas Surrounding Ash Pond B
(Map taken from SC Department of Natural Resources: Geological Survey, 2012)

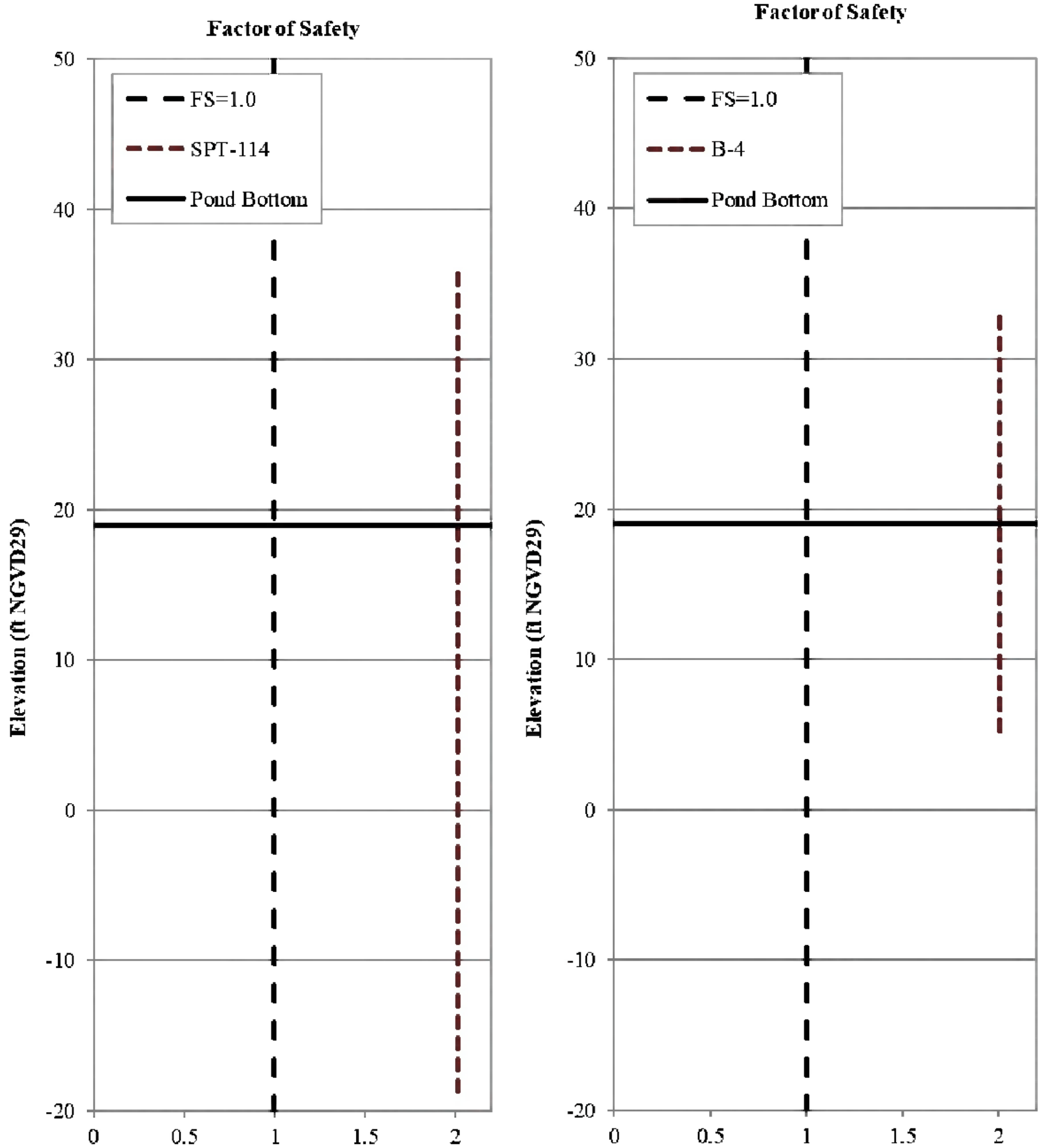

Figure 3. Liquefaction Results for Dike and Foundation Soils for SPT-114 and B-4

Notes:

1. Foundation soils were assumed to begin at the dike bottom, which was selected based on the surface elevation of the Cooling Pond.
2. Soil boring B-4 (PCRA, 1993) was not advanced to refusal at the top of the Chicora stratum.

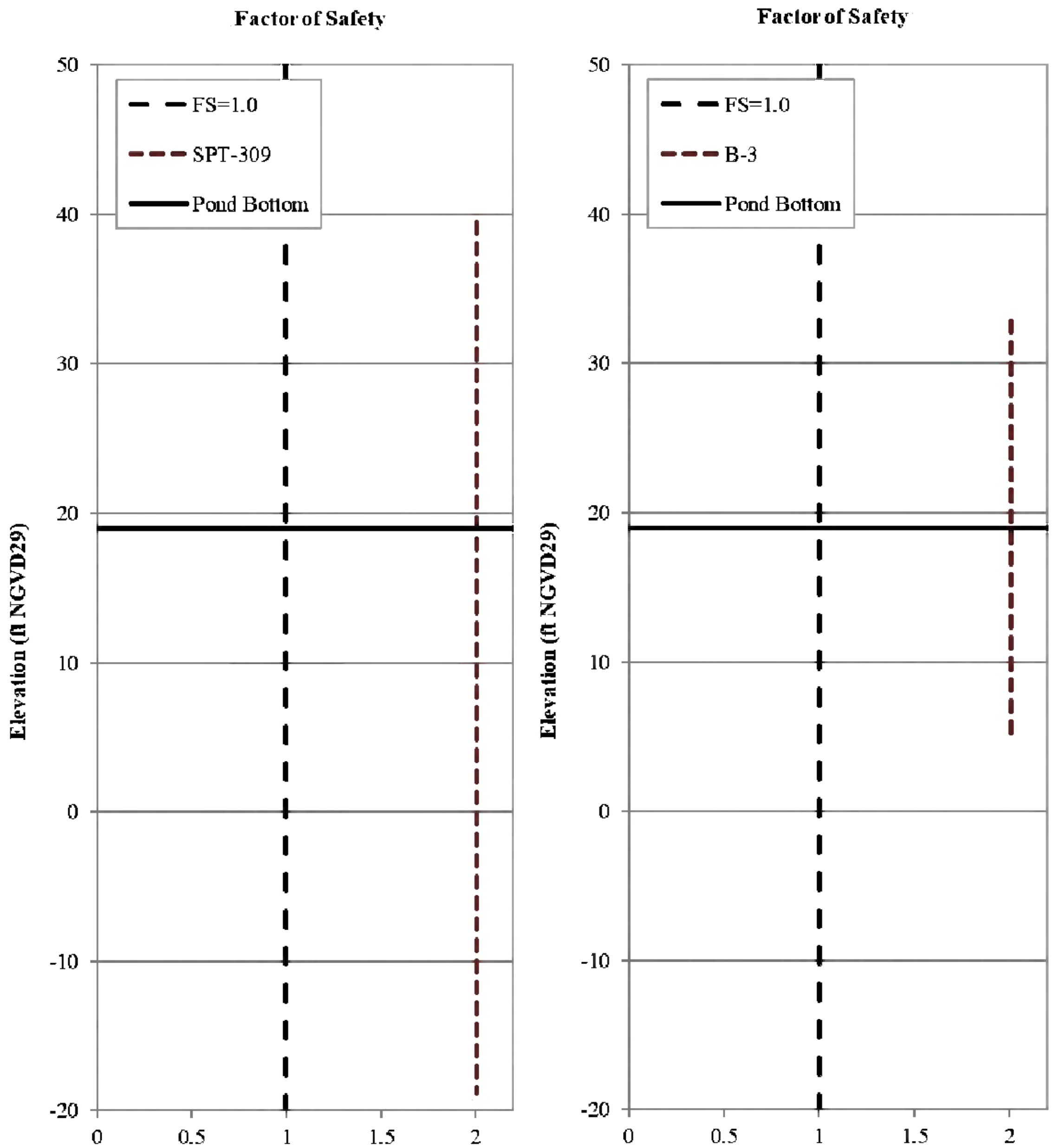

Figure 4. Liquefaction Results for Dike and Foundation Soils for SPT-309 and B-3

Notes:

1. Foundation soils were assumed to begin at the dike bottom, which was selected based on the surface elevation of the Cooling Pond.
2. Soil boring B-3 (PCRA, 1993) was not advanced to refusal at the top of the Chicora stratum.

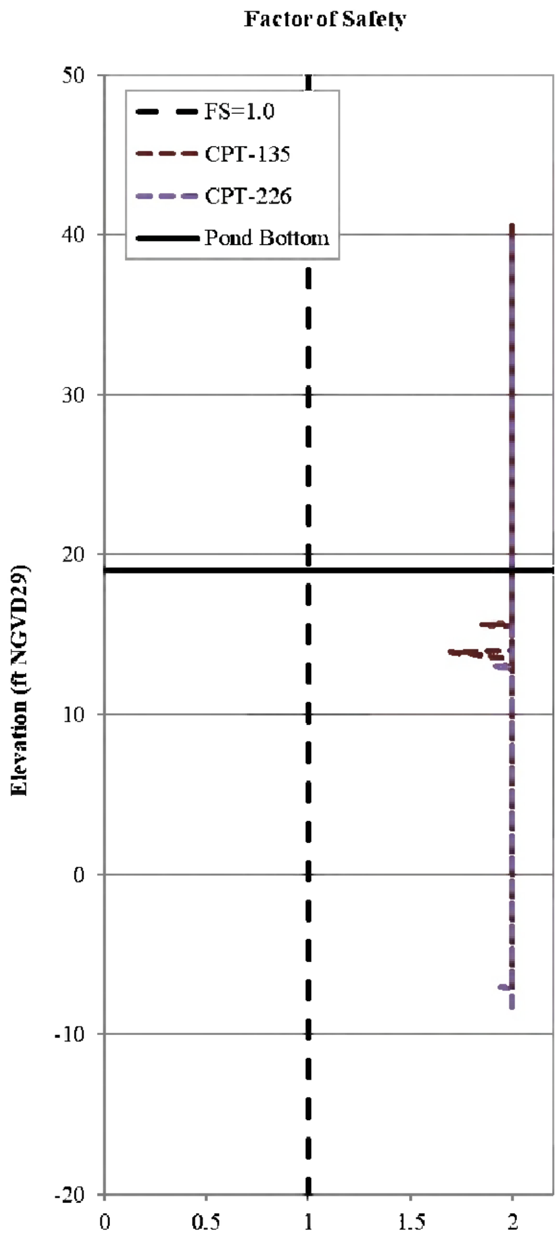

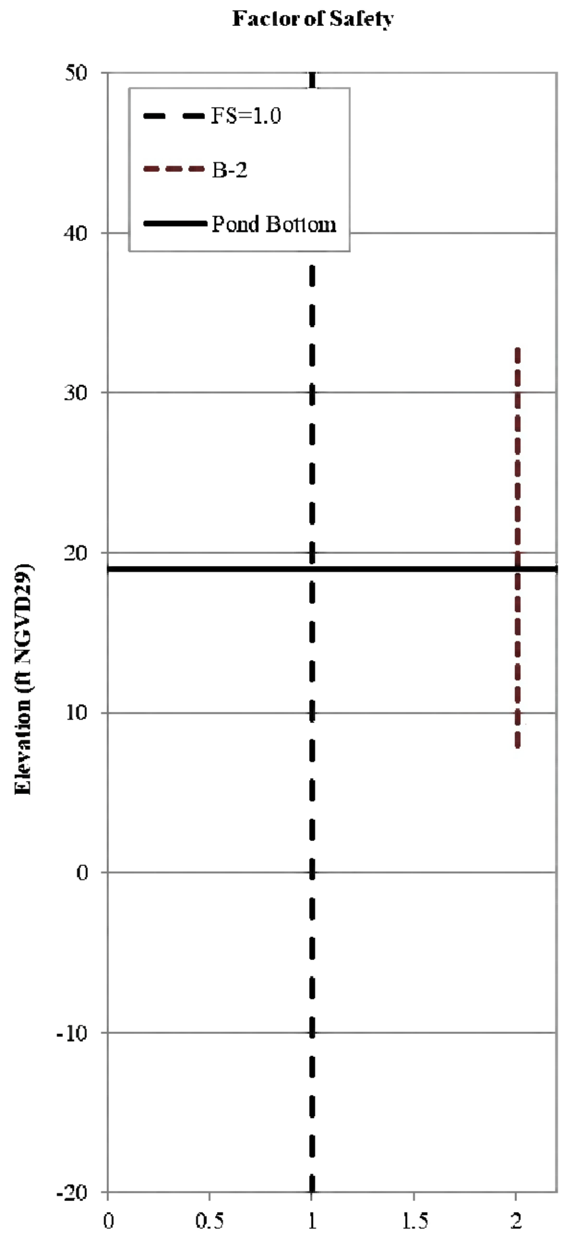

Figure 5. Liquefaction Results for Dike and Foundation Soils for CPT-135, CPT-226, and B-2

Notes:

1. Foundation soils were assumed to begin at the dike bottom, which was selected based on the surface elevation of the Cooling Pond.
2. Soil boring B-2 (PCRA, 1993) was not advanced to refusal at the top of the Chicora stratum.
3. CPT-135 and CPT-226 were plotted together as the two locations are positioned within 50-ft of each other.

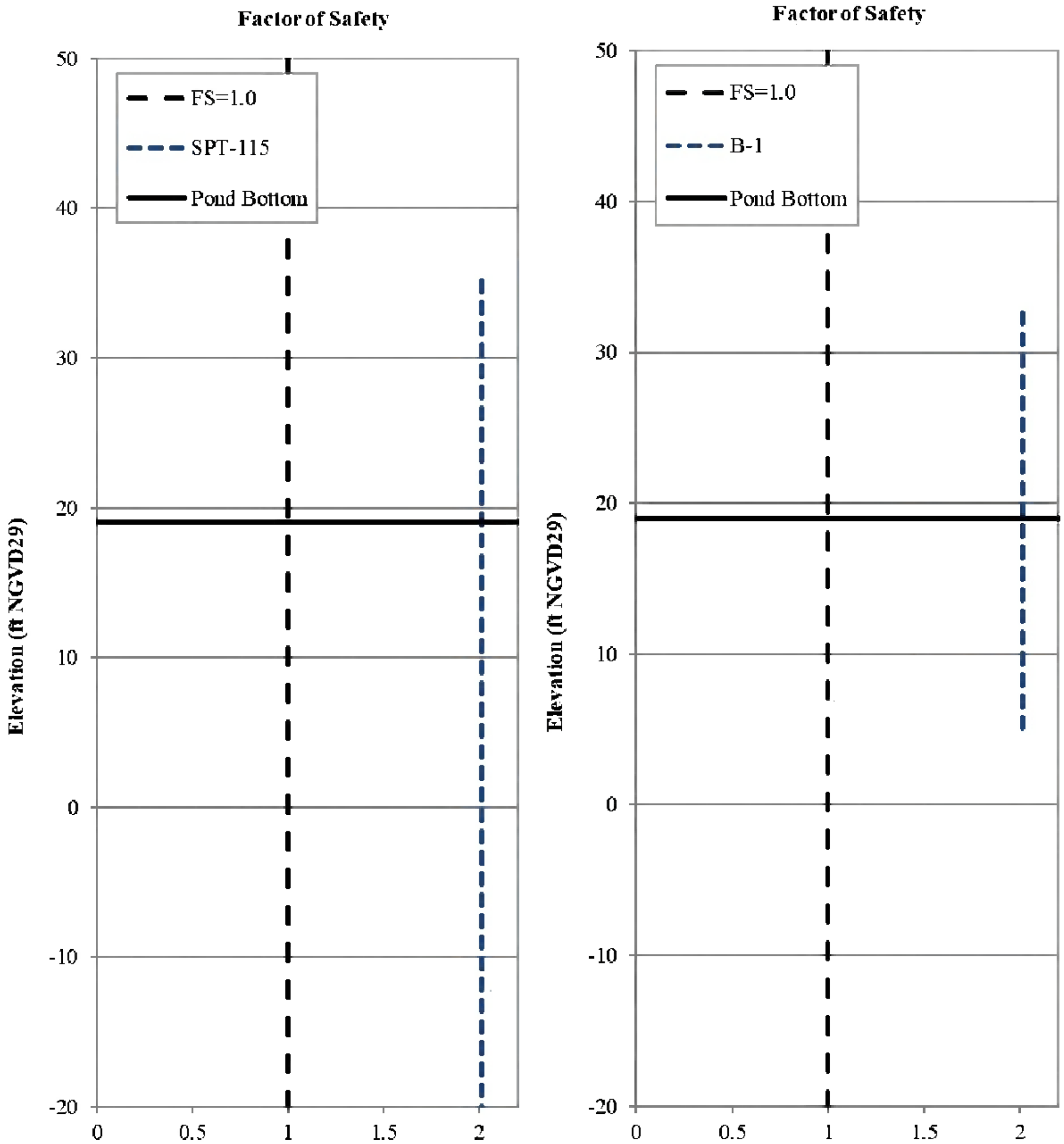

Figure 6. Liquefaction Results for Dike and Foundation Soils for SPT-115 and B-1

Notes:

1. Foundation soils were assumed to begin at the dike bottom which was selected based on the surface elevation of the Cooling Pond.
2. Soil boring B-1 (PCRA, 1993) was not advanced to refusal at the top of the Chicora stratum.

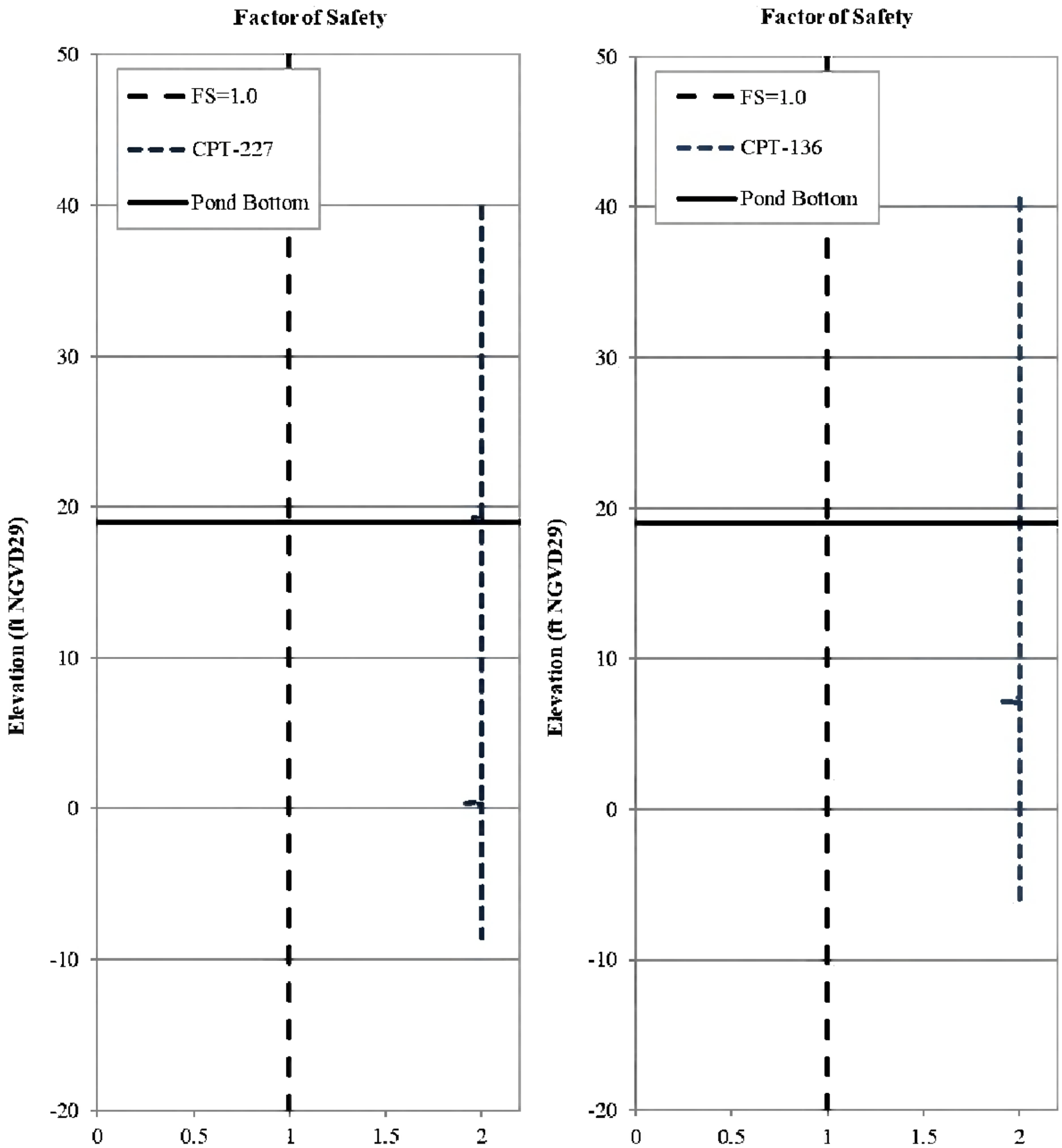

Figure 7. Liquefaction Results for Dike and Foundation Soils for CPT-227 and CPT-136

Note:

1. Foundation soils were assumed to begin at the dike bottom which was selected based on the surface elevation of the Cooling Pond.

Appendix 1

MathCAD® Example Calculation

SPT - Based Liquefaction Analysis

$BoringID := \text{"SPT-114"}$ $\qquad tsf := \frac{tonf}{ft^2}$ $\qquad kPa := \frac{1}{95.760518} \cdot tsf$

Site Parameters:

Age Correction Factor of Pleistocene Soils: $K_{dr} := 1.2$

Earthquake Magnitude: $M := 7.3$

Site Response Profile: $Prof := \text{"Profile2"}$

$$CyclicStress := \left\| \begin{array}{l} \text{if } Prof = \text{"Profile2"} \\ \quad \left\| \text{READEXCEL}(\text{"APB\_Profile\_2.xlsx"}) \right. \end{array} \right.$$

SPT-Specific Data:

Import the SPT-Specific Data in the form of Depth, Blow Count, Visual Classification ("Sand-Like"/"Clay-Like"), fines content, and USCS Classification. Upper two rows contain the headers and units for each field:

$Full := \text{READEXCEL}(\text{concat}(BoringID, \text{".xlsx"}))$

$Data := \text{submatrix}(Full, 2, \text{rows}(Full) - 1, 0, \text{cols}(Full) - 1)$

$depth := Data^{\langle 0 \rangle} \cdot ft$ $\qquad N_{blows} := Data^{\langle 1 \rangle}$ $\qquad Class := Data^{\langle 2 \rangle}$

$Fines := Data^{\langle 3 \rangle}$ $\qquad USCS := Data^{\langle 4 \rangle}$

Investigation Information:

Ground Surface Elevation: $Elevation := 41.48 \cdot ft$ NGVD29

Groundwater Depth at Time of Boring (TOB): $GWT_b := 19.1 \cdot ft$ bgs

Groundwater Depth at Time of Analysis (TOA): $GWT := 19.1 \cdot ft$ bgs

Boring Diameter: $Diameter := 4$ *inches*

Bottom of Holocene Elevation / Bottom of Dike Fill Soils: $Elev_h := 19.0 \cdot ft$ NGVD29

Energy Calibration: $ER := 88$ % (SCI, 2014)

Sampling Method: $C_S := 1.0$

$RodDepth := depth + 5 \cdot ft$ (Assume 5 ft of rod stick up during SPT test)

Compute Calibration Factors:

$$C_E := \frac{ER}{60}$$

$$C_B := \begin{array}{|l} \text{if } Diameter \le 4.0 \\ \quad 1.0 \\ \text{also if } 4.0 < Diameter < 6.0 \\ \quad 1.05 \\ \text{else} \\ \quad 1.15 \end{array}$$

$$C_R := \begin{array}{|l} \text{for } i \in 0 .. \text{rows}(depth) - 1 \\ \quad \text{if } RodDepth_i \le 13 \cdot ft \\ \quad\quad rod_i \leftarrow 0.75 \\ \quad \text{also if } 13 \cdot ft < RodDepth_i \le 20 \cdot ft \\ \quad\quad rod_i \leftarrow 0.85 \\ \quad \text{also if } 20 \cdot ft < RodDepth_i \le 33 \cdot ft \\ \quad\quad rod_i \leftarrow 0.95 \\ \quad \text{else} \\ \quad\quad rod_i \leftarrow 1 \\ rod \end{array}$$

Compute N60:

$$N_{60} := \begin{array}{|l} \text{for } i \in 0 .. \text{rows}(depth) - 1 \\ \quad x_i \leftarrow C_B \cdot C_E \cdot C_S \cdot N_{blows_i} \cdot C_{R_i} \\ x \end{array}$$

Compute CN:

Develop Representative Unit Weight Profile:

Unit weight values to be assigned based on density and material class:

<u>*Adjust according to specific site conditions*</u>

1. Coal Combustion Residuals $\gamma_1 := 100 \cdot pcf$
2. Loose Sands (Nblows <10) $\gamma_2 := 105 \cdot pcf$

3. Medium Dense Sands (10<Nblows <30) $\gamma_3 := 115 \cdot pcf$

4. Dense Sands $\gamma_4 := 120 \cdot pcf$

5. Soft Clays $\gamma_5 := 100 \cdot pcf$

6. Chicora Member $\gamma_6 := 130 \cdot pcf$

7. Williamsburg Formation Clay $\gamma_7 := 105 \cdot pcf$

Relate Depth to Elevation to Screen for Williamsburg Formation Clay

$Elev := (Elevation - depth)$ $WMElev := -8 \cdot ft$ (Approx. Top of Williamsburg Formation Clay)

$$
\begin{aligned}
Class_2 := \; & \text{for } i \in 0..\text{rows}(depth) - 1 \\
& \quad y_i \leftarrow 7 \\
& \quad \text{if } Class_i = \text{"SILT"} \\
& \quad\quad y_i \leftarrow 1 \\
& \quad \text{if } Class_i = \text{"SAND"} \wedge N_{blows_i} \le 10 \\
& \quad\quad y_i \leftarrow 2 \\
& \quad \text{if } Class_i = \text{"SAND"} \wedge 10 < N_{blows_i} \le 30 \\
& \quad\quad y_i \leftarrow 3 \\
& \quad \text{if } Class_i = \text{"SAND"} \wedge 30 < N_{blows_i} \\
& \quad\quad y_i \leftarrow 4 \\
& \quad \text{if } Class_i = \text{"CLAY"} \wedge Elev_i > WMElev \\
& \quad\quad y_i \leftarrow 5 \\
& \quad \text{if } Class_i = \text{"CHICORA"} \\
& \quad\quad y_i \leftarrow 6 \\
& y
\end{aligned}
$$

Unit Weight Based on Soil Classification:

$$\gamma_{fin} := \left\| \begin{array}{l} \text{for } i \in 0..\text{rows}(depth) - 1 \\ \quad \left\| \begin{array}{l} \text{for } m \in 1..7 \\ \quad \left\| \begin{array}{l} \text{if } Class_{2_i} = m \\ \quad \left\| \gamma2_i \leftarrow \gamma_m \right. \end{array} \right. \end{array} \right. \\ \gamma2 \end{array} \right.$$

$\gamma := \gamma_{fin}$ $\gamma_{water} := 62.4 \cdot pcf$

$i := 0..\text{rows}(depth) - 1$

Final Static Pore Pressure Calculation at Time of Boring:

$$u_{0b_i} := \left\| \begin{array}{l} \text{if } depth_i > GWT_b \\ \quad \left\| \left(depth_i - GWT_b\right) \cdot \gamma_{water} \right. \\ \text{else} \\ \quad \left\| 0 \right. \end{array} \right.$$

Final Total and Effective Overburden Pressure:

$\sigma_{v0b_0} := depth_0 \cdot \gamma_0$

$$\sigma_{v0b_i} := \left\| \begin{array}{l} \text{if } i > 0 \\ \quad \left\| \left(depth_i - depth_{i-1}\right) \cdot \left(\dfrac{\gamma_i + \gamma_{i-1}}{2}\right) + \sigma_{v0b_{i-1}} \right. \\ \text{else} \\ \quad \left\| depth_0 \cdot \gamma_0 \right. \end{array} \right.$$

$\sigma_{v0beff} := \sigma_{v0b} - u_{0b}$

Calculation of CNL (for Liquefaction)

$$
\begin{aligned}
C_{NLit} := \ & c \leftarrow 0 \\
& \text{"initial CN"} \\
& \text{for } i \in 0 .. \text{rows}(depth) - 1 \\
& \quad C_{N_i} \leftarrow 1.7 \\
& \text{for } i \in 0 .. \text{rows}(depth) - 1 \\
& \quad \text{while } c < 600 \\
& \quad\quad N_{160L_i} \leftarrow C_{N_i} \cdot N_{60_i} \\
& \quad\quad C_{N_i} \leftarrow min\left(1.7, \left(\frac{1 \cdot atm}{\sigma_{v0beff_i}}\right)^{\left(0.784 - 0.0768 \cdot \sqrt{min\left(46, N_{160L_i}\right)}\right)}\right) \\
& \quad\quad c \leftarrow c + 1 \\
& \quad c \leftarrow 0 \\
& \left[C_N \ \ N_{160L}\right]
\end{aligned}
$$

$$C_{NL} := \left(C_{NLit}{}^{\langle 0 \rangle}\right)_0$$

Compute (N1)60:

$$N_{160_i} := C_{NL_i} \cdot N_{60_i}$$

Compute Clean Sand-Corrected (N1)60-L (For Liquefaction) [SCDOT 2019, Eq. 13-15]:

$$
\begin{aligned}
\Delta N_{160L} := \ & \text{for } i \in 0 .. \text{rows}(depth) - 1 \\
& \quad x_i \leftarrow min\left(5.5, \exp\left(1.63 + \left(\frac{9.7}{\left(Fines_i + 0.01\right)}\right) - \left(\frac{15.7}{\left(Fines_i + 0.01\right)}\right)^2\right)\right) \\
& x
\end{aligned}
$$

$$N_{160cs_i} := N_{160_i} + \Delta N_{160L_i}$$

Compute the CRR (Mw=7.5, 1 atm) based on the SPT Values [SCDOT 2019, Eq. 13-16]:

Cyclic Resistance Ratio (CRR):

$$CRR1_i := \exp\left(\left(\frac{N_{160cs_i}}{14.1}\right) + \left(\frac{N_{160cs_i}}{126}\right)^2 - \left(\frac{N_{160cs_i}}{23.6}\right)^3 + \left(\frac{N_{160cs_i}}{25.4}\right)^4 - 2.8\right)$$

Overburden Correction Factor (Kσ):

$$C_{\sigma_i} := min\left(\frac{1}{18.9 - 2.55 \cdot \left(min\left(N_{160cs_i}, 37\right)\right)^{0.50}}, 0.3\right)$$

$$K_{\sigma_i} := min\left(1 - C_{\sigma_i} \cdot \ln\left(\frac{\sigma_{v0beff_i}}{2117 \cdot psf}\right), 1.1\right)$$

Corrected CRR: $CRR2_i := CRR1_i \cdot K_{\sigma_i}$

Magnitude Scaling Factor (MSF) [SCDOT 2019, Eq. 13-11]:

$$MSF_i := min\left(1.80, 6.9 \cdot \exp\left(-0.25 \cdot M\right) - 0.058\right)$$

Corrected CRR: $CRR3_i := CRR2_i \cdot MSF_i$

Age Correction Factor for Pleistocene Sands (Kdr) [SCDOT 2019, Section 13.9.5]:

Kdr is only applicbale for Sands that are of Pleistocene-Age or older (e.g., foundation soils)

$$CRR_{final_i} := \begin{array}{l} \text{if } Class\_{}_i = \text{"SAND"} \wedge Elev_i < Elev_h \\ \quad CRR3_i \cdot K_{dr} \\ \text{else} \\ \quad CRR3_i \end{array}$$

Compute the CSR for the Soil Profile:

Final Static Pore Pressure Calculation at Time of Analysis:

$$u_{0_i} := \begin{array}{l} \text{if } depth_i > GWT \\ \quad \left(depth_i - GWT\right) \cdot \gamma_{water} \\ \text{else} \\ \quad 0 \end{array}$$

Final Total and Effective Overburden Pressure at Time of Analysis:

$$\sigma_{v0_0} := depth_0 \cdot \gamma_0$$

$$\sigma_{v0_i} := \begin{array}{l} \text{if } i > 0 \\ \quad \left(depth_i - depth_{i-1}\right) \cdot \left(\frac{\gamma_i + \gamma_{i-1}}{2}\right) + \sigma_{v0_{i-1}} \\ \text{else} \\ \quad depth_0 \cdot \gamma_0 \end{array}$$

$$\sigma_{v0eff_i} := \sigma_{v0_i} - u_{0_i}$$

$$\tau_{cyc} := \text{submatrix}\left(CyclicStress, 1, \text{rows}\left(CyclicStress\right) - 1, 1, 1\right) \cdot psf$$

$$d_{cyc} := \text{submatrix}\left(CyclicStress, 1, \text{rows}\left(CyclicStress\right) - 1, 0, 0\right) \cdot ft$$

$\tau_{max} := \text{linterp}\left(d_{cyc}, \tau_{cyc}, depth\right)$

$$CSR_i := \frac{0.65 \cdot \tau_{max_i}}{\sigma_{v0eff_i}}$$

Compute Factor of Safety:

$$FS_i := \left\| \begin{array}{l} \text{if } Class_i = \text{“CHICORA”} \\ \quad \| 2.01 \\ \text{also if } Class_i = \text{“CLAY”} \\ \quad \| 2.01 \\ \text{also if } depth_i < GWT \\ \quad \| 2.01 \\ \text{else} \\ \quad \left\| min\left(\frac{CRR_{final_i}}{CSR_i}, 2.01\right) \right. \end{array} \right.$$

__Assume Chicora and Williamsburg Clay layers do NOT Liquefy__

Export Results:

$Headers := \text{augment}\left(\text{“Depth”}, \text{“Elevation”}, \text{“N160”}, \text{“Class”}, \text{“FScyclic”}\right)$

$Units := \text{augment}\left(\text{“ft”}, \text{“ft NGVD29”}, \text{“-”}, \text{“-”}, \text{“-”}\right)$

$$Export := \text{augment}\left(\frac{depth}{ft}, \frac{Elev}{ft}, N_{160}, Class, FS\right)$$

$Export2 := \text{stack}\left(Headers, Units, Export\right)$

$FileName := \text{concat}\left(BoringID, \text{“\_Results”}, \text{“.xlsx”}\right)$

$Export3 := \text{WRITEEXCEL}\left(FileName, Export2\right)$

CPT - Based Liquefaction Analysis

$BoringID := \text{"CPT\_135"}$ $tsf := 2116 \cdot psf$

Site Parameters:

Age Correction Factor of Pleistocene Soils: $K_{dr} := 1.2$

Earthquake Magnitude: $M := 7.3$

Site Response Profile: $Prof := \text{"Profile2"}$

$$CyclicStress := \left\| \begin{array}{l} \text{if } Prof = \text{"Profile2"} \\ \quad \left\| \text{READEXCEL}(\text{"APB\_Profile\_2.xlsx"}) \right. \end{array} \right\|$$

CPT-Specific Data:

Import the CPT-Specific Data in the form of depth (ft), tip resistance (tsf), sleeve friction (tsf), porepressure (tsf), and fines content profile (%) with headers and units:

$Full := \text{READEXCEL}(\text{concat}(BoringID, \text{".xlsx"}))$

$Data := \text{submatrix}(Full, 2, \text{rows}(Full) - 1, 0, \text{cols}(Full) - 1)$

$depth := Data^{\langle 0 \rangle} \cdot ft$ $qc := Data^{\langle 1 \rangle} \cdot tsf$ $f_s := Data^{\langle 2 \rangle} \cdot tsf$

$u_2 := Data^{\langle 3 \rangle} \cdot tsf$ $Fines := Data^{\langle 4 \rangle}$

Simple counter used in the Algorithm: $i := 0 .. \text{rows}(Data) - 1$

Tip net area ratio (correction applied when converting .cpt to .xls format): $a := 1$

Investigation Information:

Ground Surface Elevation: $Elevation := 40.47 \cdot ft$ NGVD 29

Groundwater Depth at Time of Boring (TOB): $GWT_b := 14.55 \cdot ft$ bgs

Groundwater Depth at Time of Analysis (TOA): $GWT := 14.55 \cdot ft$ bgs

Bottom of Holocene Elevation / Bottom of Dike Fill Soils: $Elev_h := 19.0 \cdot ft$ NGVD 29

Profile with Elevations: $Elev := Elevation - depth$

Initial Unit Weight Estimates to be Used with Robertson and Campanella (1983):

Adjust according to specific site conditions

1. Sand $\gamma_1 := 115 \cdot pcf$
2. Silty Sand $\gamma_2 := 105 \cdot pcf$
3. Sandy silt and silt $\gamma_3 := 100 \cdot pcf$
4. Silty clay/Clayey silt $\gamma_4 := 90 \cdot pcf$
5. Clay $\gamma_5 := 90 \cdot pcf$

Water $\gamma_{water} := 62.4 \cdot pcf$

Tip Resistance Back-Calculated from qt and Tip Net Area Ratio a Provided in the Original Data: $qt_i := qc_i - (1 - a) \cdot u_{2_i}$

Average Friction Ratio: $Rf_i := \left(\left(\frac{f_{s_i}}{qt_i}\right) \cdot 100\right)\%$

Robertson and Campanella 1983 Plot data:

Sand-Silty Sand $S01 := \text{submatrix}(\text{READPRN}(\text{"Robertson1983.txt"}), 0, 11, 0, 1)$

Silty Sand-Silts $S02 := \text{submatrix}(\text{READPRN}(\text{"Robertson1983.txt"}), 0, 12, 2, 3)$

Silts-Silty Clay $S03 := \text{submatrix}(\text{READPRN}(\text{"Robertson1983.txt"}), 0, 18, 4, 5)$

Clay $S04 := \text{submatrix}(\text{READPRN}(\text{"Robertson1983.txt"}), 0, 19, 6, 7)$

Linear interpolation used to evaluate Qt as a function of depth based on plot lines:

$s01(x) := \text{linterp}\left(S01^{\langle 0 \rangle}, S01^{\langle 1 \rangle}, x\right)$ $s02(x) := \text{linterp}\left(S02^{\langle 0 \rangle}, S02^{\langle 1 \rangle}, x\right)$

$s03(x) := \text{linterp}\left(S03^{\langle 0 \rangle}, S03^{\langle 1 \rangle}, x\right)$ $s04(x) := \text{linterp}\left(S04^{\langle 0 \rangle}, S04^{\langle 1 \rangle}, x\right)$

Initial Estimate of Unit Weight Based on Robertson 1983 Soil Classification:

$$class_{1983} := \left\| \begin{array}{l} \text{for } i \in 0..\text{rows}(qt)-1 \\ \quad \left\| \begin{array}{l} class_i \leftarrow 5 \\ \text{if } \dfrac{qt_i}{100 \cdot kPa} \geq s04\left(Rf_i\right) \\ \quad \| \ class_i \leftarrow 4 \\ \text{if } \dfrac{qt_i}{100 \cdot kPa} \geq s03\left(Rf_i\right) \\ \quad \| \ class_i \leftarrow 3 \\ \text{if } \dfrac{qt_i}{100 \cdot kPa} \geq s02\left(Rf_i\right) \\ \quad \| \ class_i \leftarrow 2 \\ \text{if } \dfrac{qt_i}{100 \cdot kPa} \geq s01\left(Rf_i\right) \\ \quad \| \ class_i \leftarrow 1 \end{array} \right. \\ class \end{array} \right.$$

$$\gamma 1 := \left\| \begin{array}{l} \text{for } i \in 0..\text{rows}(qt)-1 \\ \quad \left\| \begin{array}{l} \text{for } m \in 1..5 \\ \quad \left\| \begin{array}{l} \text{if } class_{1983_i} = m \\ \quad \| \ \gamma 1_i \leftarrow \gamma_m \end{array} \right. \end{array} \right. \\ \gamma 1 \end{array} \right.$$

Refined Soil Classification Using Robertson and Cabal 2010:

Static Pore Pressures at time of Sounding:

$$u_{0b_i} := \left\| \begin{array}{l} \text{if } depth_i > GWT_b \\ \quad \| \ \left(depth_i - GWT_b\right) \cdot \gamma_{water} \\ \text{else} \\ \quad \| \ 0 \end{array} \right.$$

Total and Effective Overburden Pressure:

$$\sigma_{v0b_0} := depth_0 \cdot \gamma 1_0$$

$$\sigma_{v0b_i} := \left\| \begin{array}{l} \text{if } i > 0 \\ \quad \left\| \ \left(depth_i - depth_{i-1}\right) \cdot \left(\dfrac{\gamma 1_i + \gamma 1_{i-1}}{2}\right) + \sigma_{v0b_{i-1}} \right. \\ \text{else} \\ \quad \| \ depth_i \cdot \gamma 1_0 \end{array} \right.$$

$$\sigma_{v0beff_i} := \sigma_{v0b_i} - u_{0b_i}$$

Normalized Parameters:

$$Q_{t_i} := \frac{qt_i - \sigma_{v0b_i}}{\sigma_{v0beff_i}} \qquad B_{q_i} := \frac{u_{2_i} - u_{0b_i}}{qt_i - \sigma_{v0b_i}} \qquad F_{r_i} := \frac{f_{s_i}}{qt_i - \sigma_{v0b_i}} \cdot 100$$

__Unit Weight Values to be Assigned to Robertson (1990) Classification:__

__Adjust according to specific site conditions__

1. Sensitive, fine grained $\gamma_1 := 85 \cdot pcf$
2. Organic Soils-peat to Clay $\gamma_2 := 100 \cdot pcf$
3. Clay mixtures $\gamma_3 := 100 \cdot pcf$
4. Silt mixtures $\gamma_4 := 100 \cdot pcf$
5. Sand mixtures $\gamma_5 := 110 \cdot pcf$
6. Sands $\gamma_6 := 120 \cdot pcf$
7. Gravelly sand to sand $\gamma_7 := 125 \cdot pcf$
8. Very stiff sand to clayey sand $\gamma_8 := 105 \cdot pcf$
9. Very stiff fine grained $\gamma_9 := 105 \cdot pcf$

Compute Soil Behavior Index (Ic) Corresponding to Initial Unit Weight Classification:

$$I_{c_i} := \left(\left(3.47 - \log\left(Q_{t_i}\right)\right)^2 + \left(\log\left(F_{r_i}\right) + 1.22\right)^2 \right)^{.5}$$

Soil Classification for Robertson (2010) (updated from Robertson, 1990):

$$class_{2010} := \left\| \begin{array}{l} \text{for } i \in 0..\text{rows}(Q_t) - 1 \\ \quad \left\| \begin{array}{l} class_i \leftarrow 2 \\ \text{if } 2.95 < I_{c_i} \le 3.6 \\ \quad \| \; class_i \leftarrow 3 \\ \text{if } 2.60 < I_{c_i} \le 2.95 \\ \quad \| \; class_i \leftarrow 4 \\ \text{if } 2.05 < I_{c_i} \le 2.60 \\ \quad \| \; class_i \leftarrow 5 \\ \text{if } 1.31 < I_{c_i} \le 2.05 \\ \quad \| \; class_i \leftarrow 6 \\ \text{if } I_{c_i} \le 1.31 \\ \quad \| \; class_i \leftarrow 7 \end{array} \right. \\ class \end{array} \right.$$

Unit Weight based on Soil Classification:

$$\gamma_{fin} := \left\| \begin{array}{l} \text{for } i \in 0..\text{rows}(Q_t) - 1 \\ \quad \left\| \begin{array}{l} \text{for } m \in 1..9 \\ \quad \left\| \begin{array}{l} \text{if } class_{2010_i} = m \\ \quad \| \; \gamma 2_i \leftarrow \gamma_m \end{array} \right. \end{array} \right. \\ \gamma 2 \end{array} \right.$$

$\gamma := \gamma_{fin}$ $class := class_{2010}$

Final Static Pore Pressure Calculation for CPT Interpretation:

$$u_{0b_i} := \left\| \begin{array}{l} \text{if } depth_i > GWT_b \\ \quad \| \; \left(depth_i - GWT_b\right) \cdot \gamma_{water} \\ \text{else} \\ \quad \| \; 0 \end{array} \right.$$

Final Total and Effective Overburden Pressure for CPT Interpretation:

$$\sigma_{v0b_i} := \begin{array}{|l} \text{if } i > 0 \\ \quad \left(depth_i - depth_{i-1}\right) \cdot \left(\frac{\gamma_i + \gamma_{i-1}}{2}\right) + \sigma_{v0b_{i-1}} \\ \text{else} \\ \quad depth_0 \cdot \gamma_0 \end{array}$$

$$\sigma_{v0beff_i} := \sigma_{v0b_i} - u_{0b_i}$$

Final Normalized Parameters:

$$Q_{t_i} := \frac{qt_i - \sigma_{v0b_i}}{\sigma_{v0beff_i}} \qquad Q_i := \frac{qt_i - \sigma_{v0b_i}}{\sigma_{v0beff_i}} \qquad B_{q_i} := \frac{u_{2_i} - u_{0b_i}}{qt_i - \sigma_{v0b_i}} \qquad F_{r_i} := \frac{f_{s_i}}{qt_i - \sigma_{v0b_i}} \cdot 100$$

Recompute Soil Behavior Index (Ic) corresponding to Final Unit Weight Classification:

$$I_{c_i} := \left(\left(3.47 - \log\left(Q_{t_i}\right)\right)^2 + \left(\log\left(F_{r_i}\right) + 1.22\right)^2\right)^{.5}$$

Corrected Normalized CPT Sounding:

Overburden Corrected Tip Resistance:

$$q_{c1\_it} := \begin{array}{|l} c \leftarrow 0 \\ \text{“initial CN”} \\ \text{for } i \in 0..\text{rows}(qt) - 1 \\ \quad C_{N_i} \leftarrow 1.7 \\ \text{for } i \in 0..\text{rows}(qt) - 1 \\ \quad \text{while } c < 500 \\ \quad\quad q_{c1_i} \leftarrow C_{N_i} \cdot qt_i \\ \quad\quad q_{c1N_i} \leftarrow \frac{q_{c1_i}}{1 \cdot atm} \\ \quad\quad C_{N_i} \leftarrow min\left(1.7, \left(\frac{1 \cdot atm}{\sigma_{v0beff_i}}\right)^{1.338 - 0.249 \cdot \left(\max\left(21, min\left(q_{c1N_i}, 254\right)\right)\right)^{0.264}}\right) \\ \quad\quad c \leftarrow c + 1 \\ \quad c \leftarrow 0 \\ \left[\frac{q_{c1}}{psf} \quad q_{c1N}\right] \end{array}$$

$$q_{c1} := \left(q_{c1\_it}{}^{\langle 0 \rangle}\right)_0 \cdot psf \qquad q_{c1N} := \left(q_{c1\_it}{}^{\langle 1 \rangle}\right)_0$$

Compute the CRR (Mw=7.5, 1 atm) based on the CPT Data:

Cyclic Resistance Ratio (CRR):

$i := 0 .. \text{rows}(qc) - 1$

Correction Factor for Soils with Fines:

$$\Delta q_{c1N_i} := \left(11.9 + \frac{q_{c1N_i}}{14.6}\right) \cdot \exp\left(1.63 - \frac{9.7}{Fines_i + 2} - \left(\frac{15.7}{Fines_i + 2}\right)^2\right)$$

Equivalent Clean Sand Corrected Tip Resistance: $q_{c1Ncs_i} := q_{c1N_i} + \Delta q_{c1N_i}$

$$CRR_i := \begin{cases} \exp\left(\frac{q_{c1Ncs_i}}{113} + \left(\frac{q_{c1Ncs_i}}{1000}\right)^2 - \left(\frac{q_{c1Ncs_i}}{140}\right)^3 + \left(\frac{q_{c1Ncs_i}}{137}\right)^4 - 2.8\right) & \text{if } I_{c_i} \le 2.60 \wedge q_{c1Ncs_i} < 211 \\ 2.0 & \text{also if } I_{c_i} \le 2.60 \wedge q_{c1Ncs_i} > 211 \\ 2.0 & \text{else} \end{cases}$$

Overburden Correction Factor (Kσ) for Sands [SCDOT 2019, Eq. 13-22, 13-25]:

$$C_{\sigma_i} := min\left(\frac{1}{37.3 - 8.27 \cdot \left(min\left(q_{c1Ncs_i}, 211\right)\right)^{0.264}}, 0.3\right)$$

$$K_{\sigma_i} := \begin{cases} min\left(1 - C_{\sigma_i} \cdot \ln\left(\frac{\sigma_{v0beff_i}}{1 \cdot tsf}\right), 1.1\right) & \text{if } I_{c_i} \le 2.60 \\ 1.0 & \text{else} \end{cases}$$

Corrected CRR: $CRR1_i := CRR_i \cdot K_{\sigma_i}$

***Magnitude Scaling Factor (MSF) [SCDOT 2019, Eq. 13-11]*:**

<u>MSF is dependent on material type and for cyclic softening calculations, two MSF correlations are applicable</u>

$MSF_i := min\left(1.80, 6.9 \cdot \exp(-0.25 \cdot M) - 0.058\right)$

Corrected CRR: $CRR2_i := CRR1_i \cdot MSF_i$

Age Correction Factor for Pleistocene Sands (Kdr) [SCDOT 2019, Section 13.9.5]:

Kdr is only applicbale for Sands that are of Pleistocene-Age or older (e.g., foundation soils)

$$CRR_{final_i} := \begin{array}{|l} \text{if } I_{c\_i} \le 2.60 \wedge Elev_i < Elev_h \\ \quad \| \; CRR2_i \cdot K_{dr} \\ \text{else} \\ \quad \| \; CRR2_i \end{array}$$

Compute the CSR for the Soil Profile:

Final Static Pore Pressure Calculation at Time of Analysis:

$$u_{0_i} := \begin{array}{|l} \text{if } depth_i > GWT \\ \quad \| \; (depth_i - GWT) \cdot \gamma_{water} \\ \text{else} \\ \quad \| \; 0 \end{array}$$

Final Total and Effective Overburden Pressure at Time of Analysis:

$$\sigma_{v0_0} := depth_0 \cdot \gamma_0$$

$$\sigma_{v0_i} := \begin{array}{|l} \text{if } i > 0 \\ \quad \| \; (depth_i - depth_{i-1}) \cdot \left(\dfrac{\gamma_i + \gamma_{i-1}}{2}\right) + \sigma_{v0_{i-1}} \\ \text{else} \\ \quad \| \; depth_0 \cdot \gamma_0 \end{array}$$

$$\sigma_{v0eff_i} := \sigma_{v0_i} - u_{0_i}$$

$$\tau_{cyc} := \text{submatrix}(CyclicStress, 1, \text{rows}(CyclicStress) - 1, 1, 1) \cdot psf$$

$$d_{cyc} := \text{submatrix}(CyclicStress, 1, \text{rows}(CyclicStress) - 1, 0, 0) \cdot ft$$

$$\tau_{max} := \text{linterp}(d_{cyc}, \tau_{cyc}, depth)$$

$$CSR_i := \frac{0.65 \cdot \tau_{max_i}}{\sigma_{v0eff_i}}$$

Compute Factor of Safety:

$$FS_i := \begin{cases} \text{if } depth_i < GWT_b \\ \quad 2.00 \\ \text{else} \\ \quad min\left(\dfrac{CRR_{final_i}}{CSR_i}, 2.00\right) \end{cases}$$

Export Results:

$Headers :=$ augment (“Depth” , “Elevation” , “qc1N” , “SBT Index” , “FScyclic”)

$Units :=$ augment (“ft” , “ft NGVD29” , “-” , “-” , “-”)

$$Export := \text{augment}\left(\frac{depth}{ft}, \frac{Elev}{ft}, q_{c1N}, I_c, FS\right)$$

$Export2 :=$ stack $(Headers, Units, Export)$

$FileName :=$ concat ($BoringID$, “_Results” , “.xlsx”)

$Export3 :=$ WRITEEXCEL $(FileName, Export2)$

ATTACHMENT 5
SAFETY FACTOR ASSESSMENT

Written by:	Z. Li	Date:	10/14/2021	Reviewed by:	C. Carlson/B. Gin	Date:	10/14/2021
Client:	Santee Cooper	Project:	Winyah Generating Station	Project/ Proposal No.:	GC8100	Task No.:	03

SAFETY FACTOR ASSESSMENT: ASH POND B

INTRODUCTION

This calculation package was prepared as Attachment 5 to the *2021 Periodic Safety Factor Assessment: Ash Pond B* (2021 Safety Factor Assessment Report) and presents the slope stability analyses for the critical portion of the Ash Pond B perimeter dikes at Winyah Generating Station (WGS), Georgetown County, South Carolina. On 17 April 2015, the United States Environmental Protection Agency (USEPA) published the CCR Rule (40 Code of Federal Regulations [CFR] Parts 257 and 261). Under the CCR Rule, Ash Pond B is classified as an "existing surface impoundment" and must meet specific requirements with respect to periodic safety factor assessments. This calculation package presents the slope stability analysis performed as part of the periodic safety factor assessment required by §257.73(e)(1) of the CCR Rule for existing CCR surface impoundments. The remainder of this calculation package presents: (i) safety factor criteria; (ii) methodology; (iii) cross section geometry; (iv) engineering parameters; (v) results; and (vi) conclusions.

SAFETY FACTOR CRITERIA

Slope stability analyses were conducted to assess whether the critical portion of the Ash Pond B perimeter dikes satisfies the factor of safety (FS) criteria described within §257.73(e)(1) of the CCR Rule. Specifically, §257.73(e)(1) requires that:

> *"(i) The calculated static factor of safety under the long-term, maximum storage pool loading condition must equal or exceed 1.50.*
> *(ii) The calculated static factor of safety under the maximum surcharge pool loading condition must equal or exceed 1.40.*
> *(iii) The calculated seismic factor of safety must equal or exceed 1.00.*
> *(iv) For embankments constructed of soils that have susceptibility to liquefaction, the calculated liquefaction factor of safety must equal or exceed 1.20."*

It is noted that the liquefaction potential analysis results presented in Attachment 4: *Liquefaction Potential Analysis: Ash Pond B* (Liquefaction Package) of the 2021 Safety Factor Assessment Report did not indicate that the Ash Pond B dike fill or foundation soils immediately beneath the perimeter dikes are expected to undergo triggering of liquefaction under the design earthquake. Therefore, the liquefaction FS for the Ash Pond B perimeter dikes utilizing post-liquefaction residual shear strengths was not evaluated as part of this safety factor assessment.

METHODOLOGY

Static Slope Stability

Global slope stability analyses were performed using Spencer's method (Spencer, 1973), as implemented in the computer program SLIDE®, version 6.039 (Rocscience, 2016). Spencer's method, which satisfies vertical and horizontal force equilibrium as well as moment equilibrium, is considered to be more rigorous than other methods, such as the simplified Janbu method (Janbu, 1973) and the simplified Bishop method (Bishop, 1955).

Both the rotational mode and the non-rotational mode were considered for the stability analyses presented in this calculation package. SLIDE® generates potential slip surfaces, calculates the FS for each of these surfaces, and identifies the critical slip surface with the lowest calculated FS. The critical slip surfaces are reported in the results of this calculation package. Information required for these analyses include the slope geometry, subsurface soil stratigraphy, phreatic surface elevation, external loading conditions, and engineering properties of subsurface materials.

Seismic Slope Stability

Pseudo-static slope stability analyses were performed to evaluate the seismic performance of the perimeter dike structures using a procedure consistent with Hynes-Griffin and Franklin (1984). The procedure is described as follows:

1. Estimate the maximum horizontal equivalent acceleration (MHEA) for the potential critical slip surfaces of the perimeter dike system based on results from the site response analyses presented in Attachment 3: *Seismic Hazard Evaluation and Site Response Analysis: Ash Pond B* (Site Response Package) of the 2021 Safety Factor Assessment Report.

2. Compute the seismic horizontal force coefficient (k_h) using the ratio of the critical acceleration (N) to the peak value of earthquake acceleration (A) based on an allowable deformation (u) for which the perimeter dikes are considered stable (from Figure 7 of Hynes-Griffin and Franklin [1984]). The critical acceleration, N, was selected as the k_h for the purposes of this analysis, and the MHEA at the depth of the critical slip surface was selected as the peak earthquake acceleration, A.

3. Perform slope stability analysis applying the seismic horizontal force coefficient to compute a horizontal force ($F = k_h \times W$) on each slice based on slice weight (W) and evaluate the resulting FS. If the calculated FS meets or exceeds the target FS (i.e., FS $\geq$ 1.0), the slope is

expected to experience less deformation than the selected allowable displacement and meet the requirements of the CCR Rule.

It is noted that during pseudo-static slope stability analyses, undrained shear strengths were conservatively reduced by 20 percent to account for potential strength degradation during cyclic loading in accordance with a suggestion in Hynes-Griffin and Franklin (1984).

CROSS SECTION GEOMETRY

The following section describes the development for the (i) external geometry; (ii) subsurface stratigraphy; and (iii) water levels and phreatic surface for the cross section evaluated as part of this safety factor assessment.

External Geometry

The current height of the Ash Pond B perimeter dikes ranges from approximately 15 feet (ft) adjacent to the Discharge Canal to 21 ft adjacent to the Cooling Pond. The upstream and downstream side slopes range from 2 horizontal to 1 vertical (2H:1V) to 3H:1V, while the dike crest is typically 12 to 15 ft wide (Thomas and Hutton, 2012). The perimeter dikes of Ash Pond B were raised by approximately 7 ft to their current crest elevation of 41.0 ft NGVD29 in 1999. Design cross sections provided by Paul C. Rizzo & Associates (PCRA, 1993) were utilized in conjunction with topographic survey data to develop the geometry of each cross section in this safety factor assessment.

Four cross sections were developed and evaluated as part of the 2016 Safety Factor Assessment Report (Geosyntec, 2016). These cross sections were selected based on the critical slope geometry, engineering parameters of subsurface materials, and phreatic conditions. The external geometry of each cross section was based on a topographic survey prepared by Thomas and Hutton (2012). The locations of the four cross sections analyzed in the 2016 Safety Factor Assessment are shown in Figure 1.

For the 2021 Safety Factor Assessment Report, only the critical cross section identified in the 2016 Safety Factor Assessment was analyzed. In the 2016 Safety Factor Assessment for Ash Pond B, Cross Section C had the lowest calculated FS for the static slope stability analyses (both maximum normal storage pool and maximum surcharge pool loading conditions) and the seismic slope stability analyses. Therefore, updated slope stability analyses were performed only for Cross Section C as part of the 2021 Safety Factor Assessment Report. Updated topographic survey data from August 2021 (McKim & Creed, 2021) were also incorporated into this cross section.

Subsurface Stratigraphy

The subsurface stratigraphy for each cross section was developed based on soil borings and cone penetration tests (CPTs) conducted as part of Geosyntec's 2013 and 2016 subsurface investigations. Santee Cooper personnel indicated that no additional geotechnical investigations were conducted in the area of Ash Pond B since 2016 ; therefore, the subsurface stratigraphy developed in the 2016 Safety Factor Assessment remains valid. Generally, the subsurface in the depth of interest for slope stability analyses consists of the following strata (from top to bottom): Dike Fill, Foundation Soils, Chicora Member, and Williamsburg Formation Clay. Further discussion on the development of subsurface conditions can be found in the 2016 Safety Factor Assessment Report (Geosyntec, 2016).

Water Levels

The CCR Rule requires the evaluation of safety factors considering static and seismic slope stability analyses under long-term "Maximum Normal Storage Pool" conditions and static slope stability analyses under short-term "Maximum Surcharge Pool" conditions. Water levels in the retained ash and perimeter dike, and downstream toe were determined as described below.

Maximum Normal Storage Pool Condition: As described within the 2016 Safety Factor Assessment Report (Geosyntec, 2016), the surface water level in Ash Pond B was maintained at an elevation of 34.9 ft NGVD29 by 4-ft by 4-ft concrete riser structure. The average operating elevation provided by Santee Cooper from February 2011 through September 2021 is 34.1 ft NGVD 29. Ash Pond B receives stormwater from the pond area and stormwater from Ash Pond A through a series of rim ditches and culverts to Ash Pond B. Santee Cooper provided available water level measurements from wells in the area of Ash Pond B. The recorded water levels in these wells have generally been steady over the last five years. Based on the review of the available water level measurements, the water level within the perimeter dike and beyond the downstream toe of the perimeter dike is similar to the water level used for the 2016 Safety Factor Assessment Report. Based on the information described above, an operating level of 34.9 ft NGVD29 in Ash Pond B was used as the "Maximum Normal Storage Pool" for Ash Pond B in the static and seismic slope stability analyses herein.

Maximum Surcharge Pool Condition: Because Ash Pond B has been classified as a "Low Hazard Potential" surface impoundment (Geosyntec, 2021), the 100-yr rainfall event with a rainfall duration of 72 hours was selected as the Inflow Design Flood (IDF), as required by §257.73(d)(1)(v)(B). The "maximum surcharge pool" elevation within Ash Pond B was established based on the maximum surface water elevation within Ash Pond B computed from the hydrologic and hydraulic (H&H) analysis with the IDF and selected as a more conservative water level (37.2 ft NGVD29) than the maximum surface water level (36.1 ft NGVD 29) from the H&H analyses. Details of the H&H analyses are provided in a document titled "*Inflow Design Flood Control System Plan: Ash Pond B*" and the H&H analysis results are included as Attachment 2 to the 2021 Safety Factor Assessment Report.

Final Cross Section Geometry

The final geometric models implemented within SLIDE® for Cross Section C are provided in Figures 2 and 3 for the maximum normal and surcharge storage pool conditions, respectively.

ENGINEERING PARAMETERS

The following sections describe the engineering parameters selected for the analyses presented herein.

Material Parameters

Material parameters for dike fill, foundation soils, and underlying strata were evaluated in the 2016 Safety Factor Assessment Report (Geosyntec, 2016) using in-situ and laboratory data collected in the vicinity of Ash Pond B. Table 1 provides a summary of the material properties selected for the evaluated cross section as part of the 2021 Safety Factor Assessment. The interpretation and selection of properties for Cross Section C are shown in Figure 4. Drained shear strength parameters for cross section-specific dike fill and sandy foundation soil were predominantly developed from in-situ measurements (i.e., SPT N-values, etc.).

It was assumed that seismic waves generated during the design seismic event may load clayey foundation soils rapidly enough to develop elevated pore pressures and induce an undrained loading condition. In accordance with a recommendation made by Hynes-Griffin and Franklin (1984), the selected undrained shear strength value for the clayey foundation soils was conservatively reduced by 20 percent for the seismic slope stability analyses to account for potential cyclic degradation during an earthquake at the Site.

Seismic Loading and Allowable Displacement

The seismic hazard evaluation for WGS and the site response analysis for the Ash Pond B perimeter dikes are presented in the Site Response Package of the 2021 Safety Factor Assessment Report. Within that package, maximum shear stress profiles for the six ground motions were computed for the critical soil column of Ash Pond B. The maximum shear stress profiles were used to compute the MHEA profile in general accordance with Bray et al. (1995). Preliminary seismic slope stability analyses of the Ash Pond B perimeter dikes indicated that a typical depth of the critical slip surface is located approximately 20 ft below the dike crest. The MHEA at the anticipated critical slip surface was selected based on the preliminary seismic slope stability analyses. The largest MHEA from the six ground motions at the critical slip surface depth was selected to compute the horizontal seismic coefficients for the seismic slope stability analyses. The MHEA profile to an approximate depth of 100 ft below ground surface (bgs) is provided in Table 2. An MHEA value of 0.064g was selected for Cross Section C.

As described in the Methodology section, the horizontal seismic coefficient (k_h) must be computed assuming an allowable deformation (u). An allowable deformation of 12 inches (in.) (30.5 centimeters [cm]) was selected for the Ash Pond B perimeter dike structures. This is a conservative allowable deformation typically used for seismic analyses of large waste disposal structures (e.g., landfills) (Kavazanjian, 1999). Using the Hynes-Griffin and Franklin (1984) chart and assuming the "Upper Bound" displacement, the ratio of N/A (or k_h/MHEA) was conservatively selected as 0.5, as shown in Figure 5. Thus, k_h value of 0.032 was used as seismic loading for Cross Section C.

RESULTS

The safety factor evaluation for Cross Section C was performed according to the methodology and parameters discussed above, and the results are summarized within Table 3. Computed FS were found to exceed the minimum safety factors required by §257.73(e)(1) of the CCR Rule. Figures 6 through 8 depict the calculated safety factors for Cross Section C. While the rotational and non-rotational slip surfaces were considered in the analyses, rotational slip surfaces were consistently more critical failure modes of concern and are the critical slip surfaces as presented in Figures 6 through 8.

CONCLUSIONS

Based on the assumptions, analyses, and results presented herein, Ash Pond B at WGS satisfies the safety factor requirements described in §257.73(e)(1) of the CCR Rule.

REFERENCES

Bishop, A. (1955), "The Use of the Slip Circle in the Stability Analysis of Slopes," *Géotechnique*, Vol. 5, No. 1, Jan 1955, pp. 7-17.

Bray, J.D., Augello, A.J., Leonards, G.A., Repetto, P.C., & Byrne, R.J. (1995), "Seismic Stability Procedures for Solid-Waste Landfills," *Journal of Geotechnical Engineering*, Vol. 121, No. 2, pp. 139-151.

Geosyntec Consultants, Inc. (2016), "2016 Surface Impoundment Periodic Safety Factor Assessment Report: Ash Pond B, Winyah Generating Station, Georgetown, South Carolina", submitted to Santee Cooper.

Geosyntec Consultants, Inc. (2021), "Periodic Hazard Potential Classification Assessment: Ash Pond B", Project No. GC8100.

Hynes-Griffin, M. and Franklin, A. (1984), "Rationalizing the Seismic Coefficient Method", Department of the Army, Waterways Experiment Station, Corps of Engineers, Vicksburg, Mississippi, Miscellaneous Paper GL-84-14, Jul.

Janbu, N., (1973), "Slope Stability Computations in Embankment-Dam Engineering", R.C. Hirschfeld and S.J. Poulos, Eds. New York: Wiley, pp. 47-86.

Kavazanjian, E., (1999), "Seismic Design of Solid Waste Containment Facilities", Proceedings of the 8th Canadian Conference on Earthquake Engineering, Vancouver, BC, June, pp. 51-89.

McKim & Creed (2021), "Topographic Survey for Winyah Generating Station."

Rocscience (2016), "SLIDE® – 2-D Limit Equilibrium Slope Stability for Soil and Rock Slopes," User's Guide, Rocscience Software, Inc., Toronto, Ontario, Canada.

Spencer, E. (1973), "The Thrust Line Criterion in Embankment Stability Analysis," *Géotechnique*, Vol. 23, No. 1, pp. 85-100, Mar.

Thomas and Hutton (2012), "Topographic Survey of a Portion of Santee Cooper Winyah Generating Station", prepared for Santee Cooper, 14 Jan.

Tables

Table 1. Selected Material Parameters for Analysis

Material	Total Unit Weight (pcf)	Drained Parameters		Undrained Parameters[1]	
		ϕ' (°)	c' (psf)	S_u/σ'_{vo}	$S_{u,min}$ (psf)
Dike Fill	125[2]	38[3]	0	-	-
Foundation Soils (Clayey)	100[2]	18	250	0.36[4]	100
Upper Sandy Foundation Soils	115[2]	38[3]	0	-	-
Lower Sandy Foundation Soils	115[2]	31[3]	0	-	-
Chicora	130[2]	50[2]			
Williamsburg Formation Clay	105[2]	50[2]	0	-	-
Fly Ash	100[2]	34[2]	0	-	-
Riprap Buttress	150	45	0	-	-

Notes:

1. Undrained strength parameters for clayey foundation soils were applied for the seismic slope stability case only.
2. The selection of shear strength parameters for Chicora, Williamsburg Formation Clay, and Fly Ash, as well as total unit weights for all materials, is explained in the 2016 Safety Factor Assessment Report (Geosyntec, 2016).
3. These drained shear strengths (ϕ') vary by location. Interpretation of in-situ results applied in the selection is provided in Figure 4.
4. The selected undrained strength ratio (S_u/σ'_{vo}) varies between locations. Interpretation of in-situ results applied in the selection is provided in Figure 4. A more detailed explanation of the undrained strength ratio for clayey foundation soils is provided in the 2016 Safety Factor Assessment Report (Geosyntec, 2016).

Table 2. Maximum Equivalent Horizontal Acceleration (MHEA) from Site Response Analysis for Ash Pond B Perimeter Dikes

Profile 2	
Depth (ft)	MHEA
1.5	0.107
5	0.096
7	0.078
9	0.080
13	0.069
17	0.065
20.5	0.063
22	0.065
24.5	0.062
29.5	0.057
34.5	0.051
39.5	0.047
44.5	0.044
49.5	0.049
57	0.056
67	0.059
77	0.063
87	0.068
97	0.072
107	0.078

Note:

1. Cross Section C, located adjacent to the Cooling Pond, was found to have depths to the critical slip surface of 20 ft. An MHEA of 0.064g was selected for Cross Section C.

Table 3. Summary of Calculated Factors of Safety (FS)

Safety Factor Case	Target FS	Cross Section C
Static - Maximum Normal Storage Pool	1.50	*1.54*
Static - Maximum Surcharge Pool	1.40	*1.51*
Seismic - Maximum Normal Storage Pool	1.00	*1.06*
Liquefaction Slope Stability[1]	1.20	Not Applicable

Notes:

1. The liquefaction safety factor was not evaluated since dike fill soils and foundation soils beneath the dike fill were not found to be liquefiable (Liquefaction Package).
2. Only critical failure surfaces passing through the perimeter dikes were considered.

Figures

LEGEND

W-SW-APB	EXISTING STAFF GAUGE
CPT-144	GEOSYNTEC CONE PENETRATION TEST
PPZ-5	PIEZOMETER
SPT-111	GEOSYNTEC SOIL BORING
B-1	HISTORICAL BORING
WAP-9	GROUNDWATER MONITORING WELL
	POND BOUNDARY
	PROPERTY BOUNDARY
	EXISTING GAS LINE
	EXISTING RAILROAD

N

NOTES:
1. Aerial imagery was obtaied from ESRI online database.
2. The position of underground utilities shown should be considered approximate.

600 300 0 600 Feet

ASH POND B
WINYAH GENERATING STATION

GEORGETOWN, SOUTH CAROLINA

Geosyntec consultants

Charlotte, NC | October 2021

Figure 1

Y:\S\Santee Cooper\Santee Cooper - Winyah\2021 - 5 Yr CCR Rule Requirements\7 - Safety Factor Assessment\GIS\MXD\September 2021\FigureX_Ash Pond B.mxd; Abby.Wesley; 10/12/2021

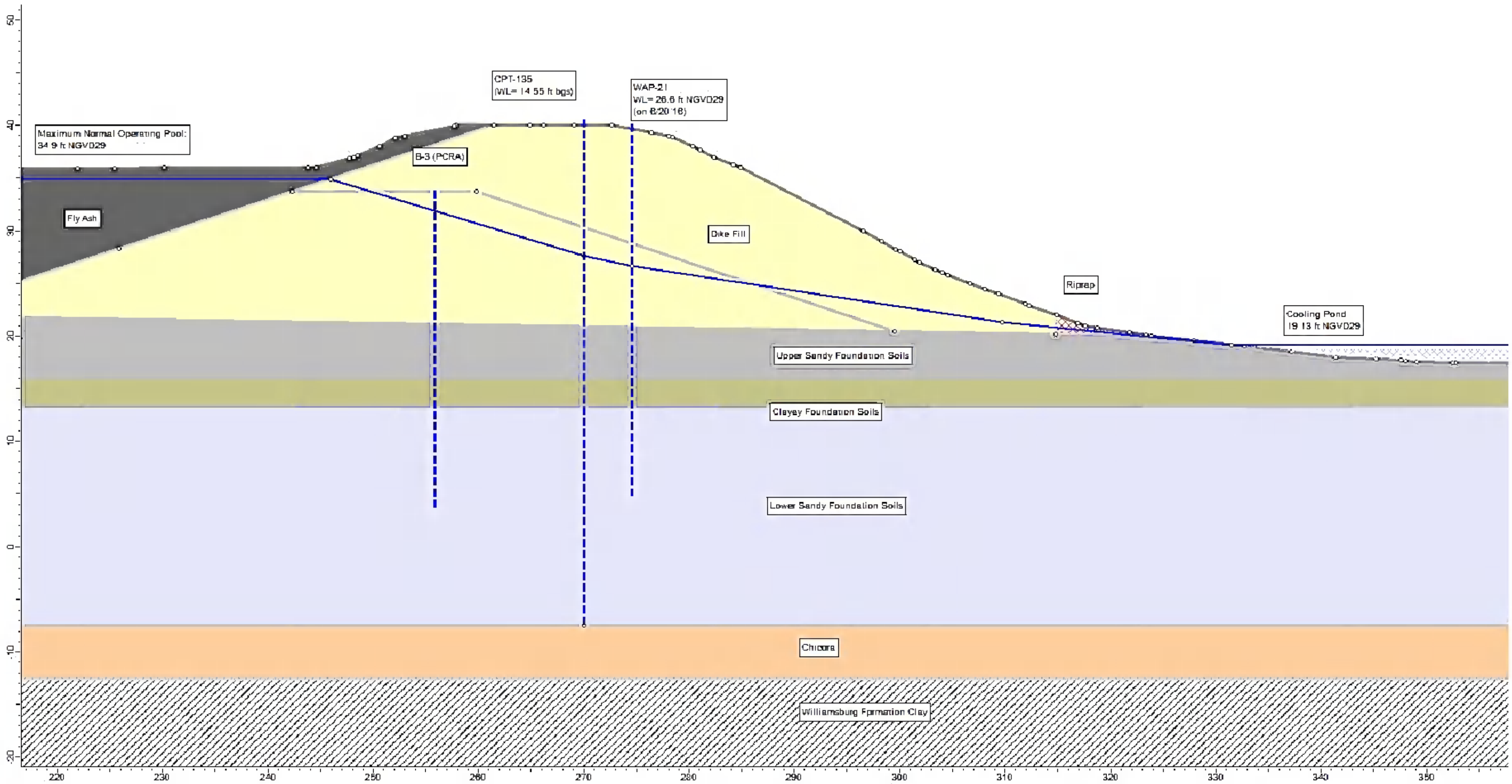

Figure 2. Cross Section C Geometry for Maximum Normal Storage Pool Conditions

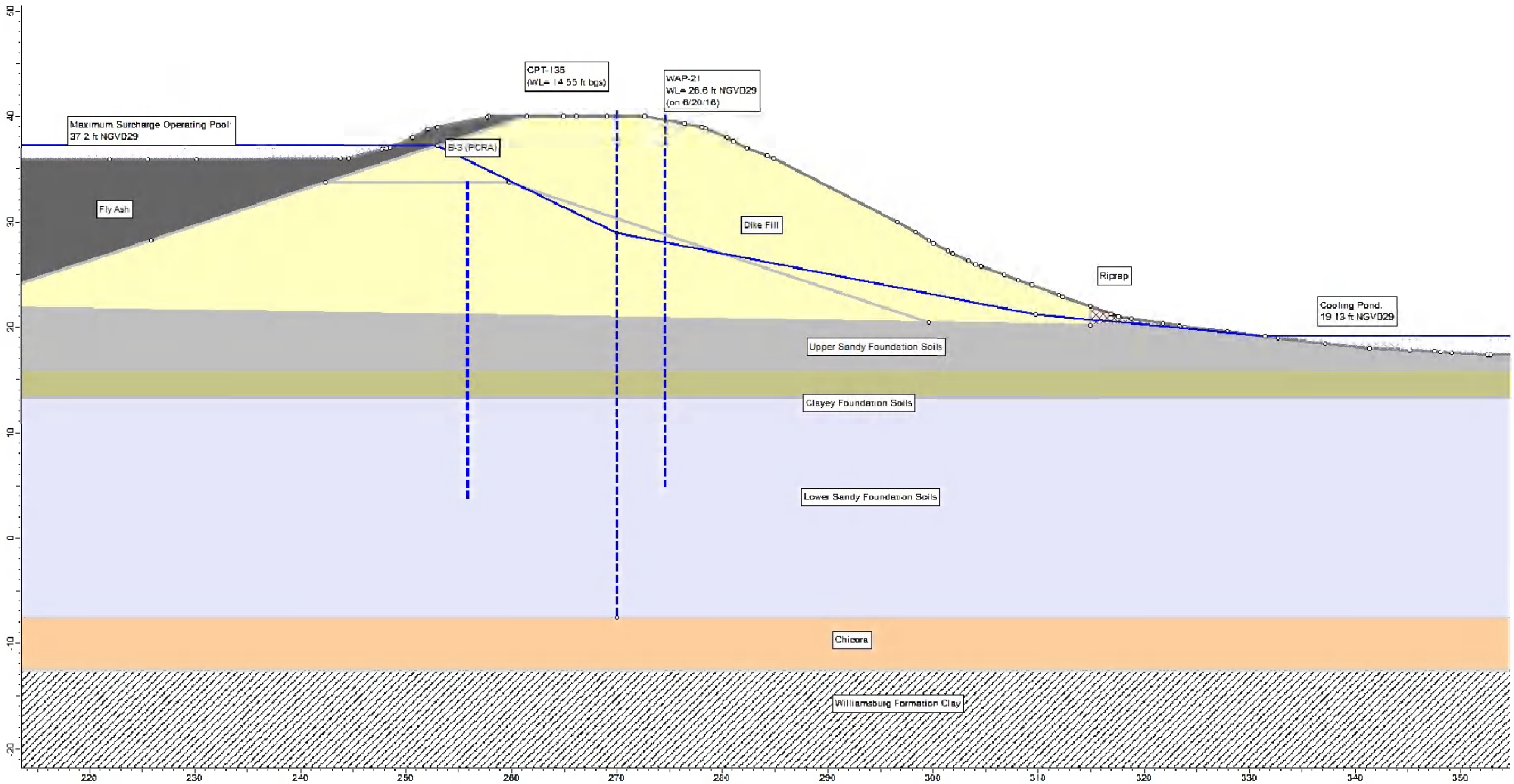

Figure 3. Cross Section C Geometry for Maximum Surcharge Storage Pool Conditions

Note:

1. "Maximum Surcharge Pool" was conservatively selected at 37.2 ft NGVD29 within Ash Pond B.

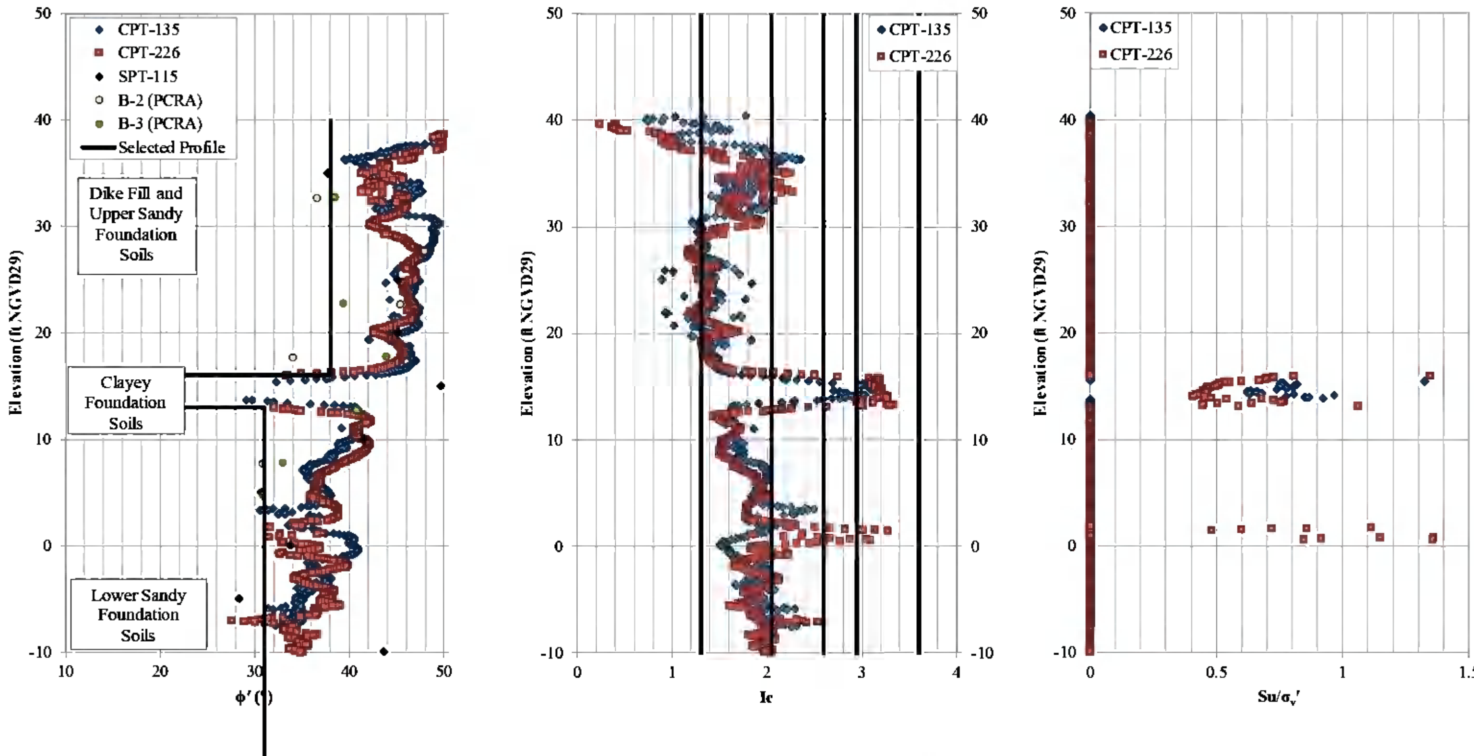

Figure 4. Subsurface Stratigraphy and Shear Strength Model for Cross Section C

Notes:

1. Clayey foundation soils were modeled with a ϕ'=18° and a c′=250 psf during static slope stability and with 80% of the S_u/σ'_v = 0.45 (i.e., S_u/σ'_v = 0.36) and a $S_{u,min}$ =100 psf during pseudo-static stability analysis (i.e., seismic safety factor analysis).
2. A soil behavior index (I_c) >2.60 was considered a "clay-like" soil during this evaluation. I_c < 2.60 were plotted as zero within the plot of S_u/σ'_v vs. elevation above.

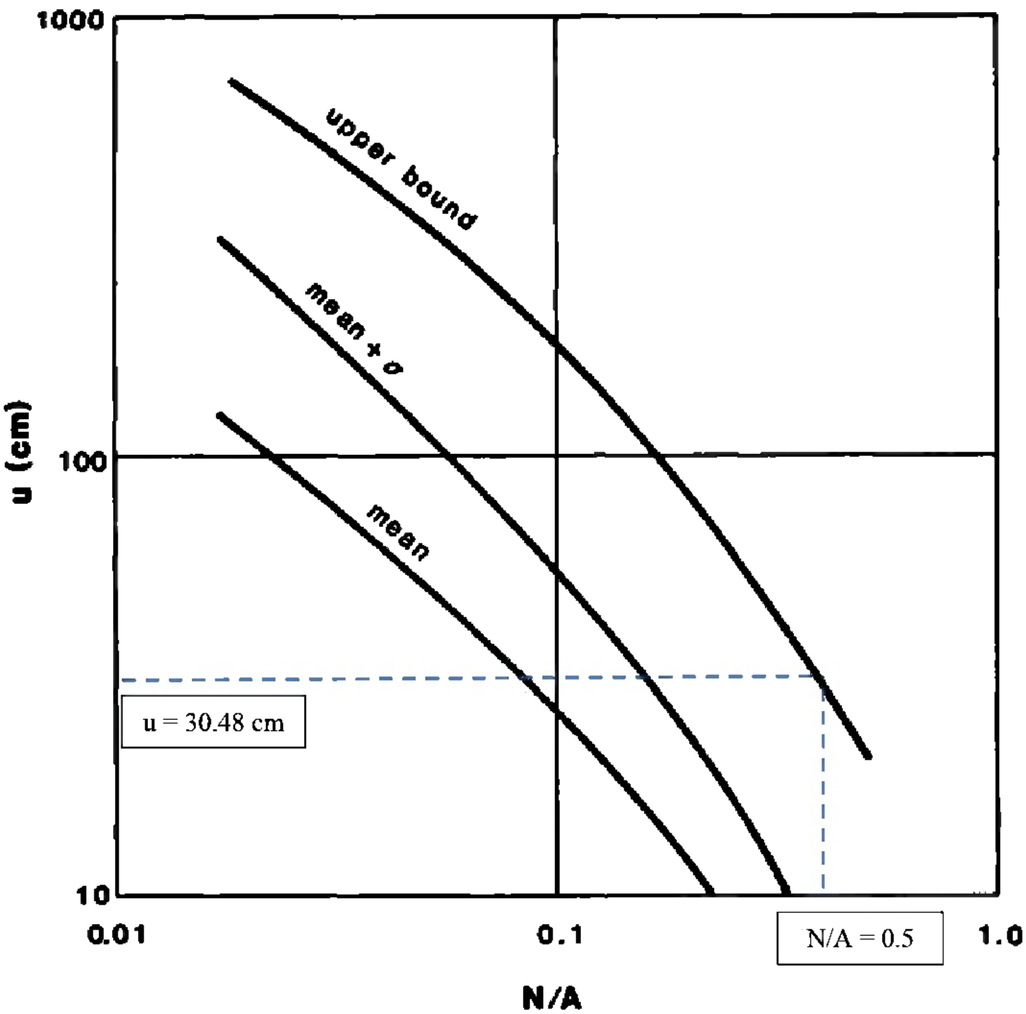

Figure 5. Allowable Deformation (u) vs. N/A
(from Figure 7 of Hynes-Griffin and Franklin, 1984)

Notes:

1. An allowable deformation (u) of 12 in. (30.48 cm) and the "Upper Bound" curve were selected for the 2021 Safety Factor Assessment.
2. A ratio of N/A of 0.50 was selected assuming 12 in. of allowable deformation.

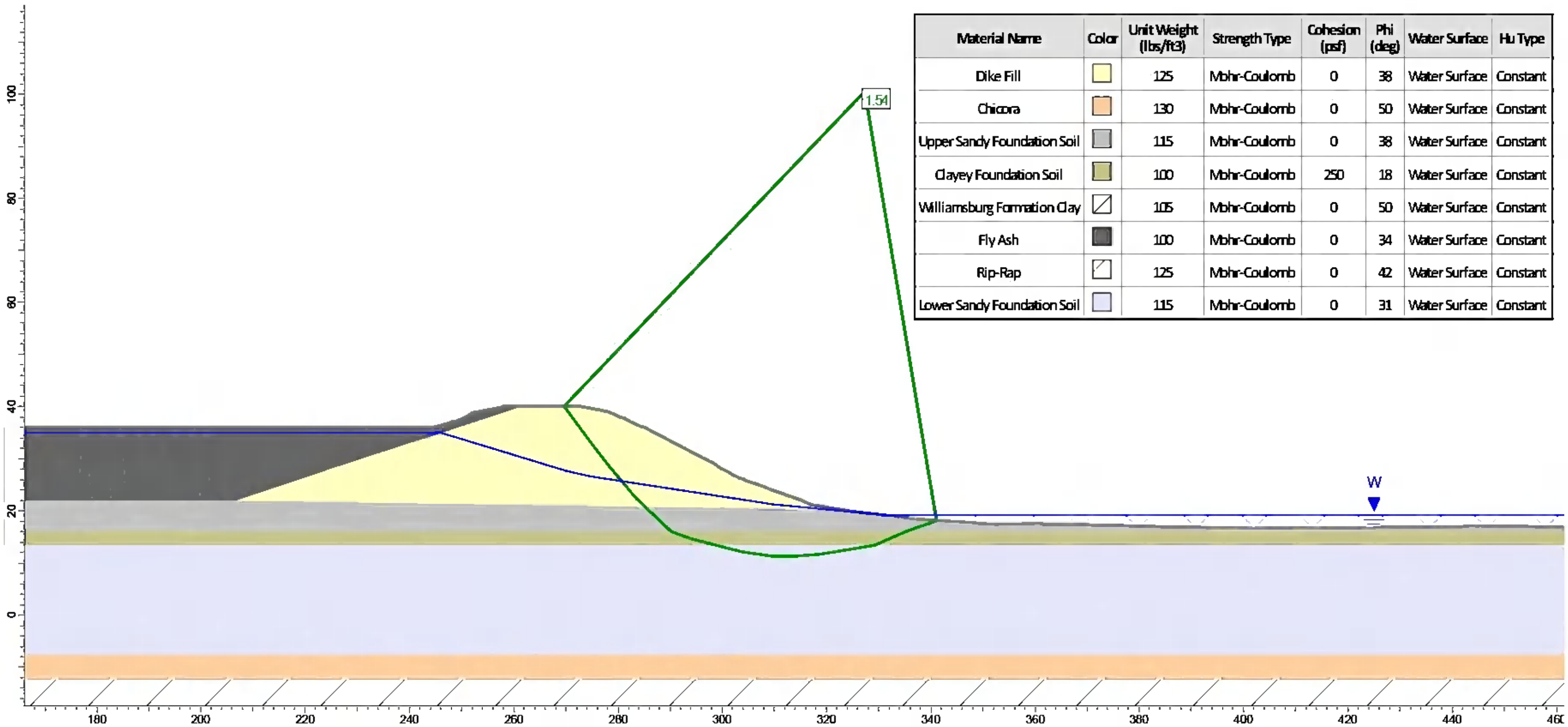

Figure 6. Calculated Factor of Safety for Cross Section C: Static Factor of Safety – Maximum Normal Storage Pool

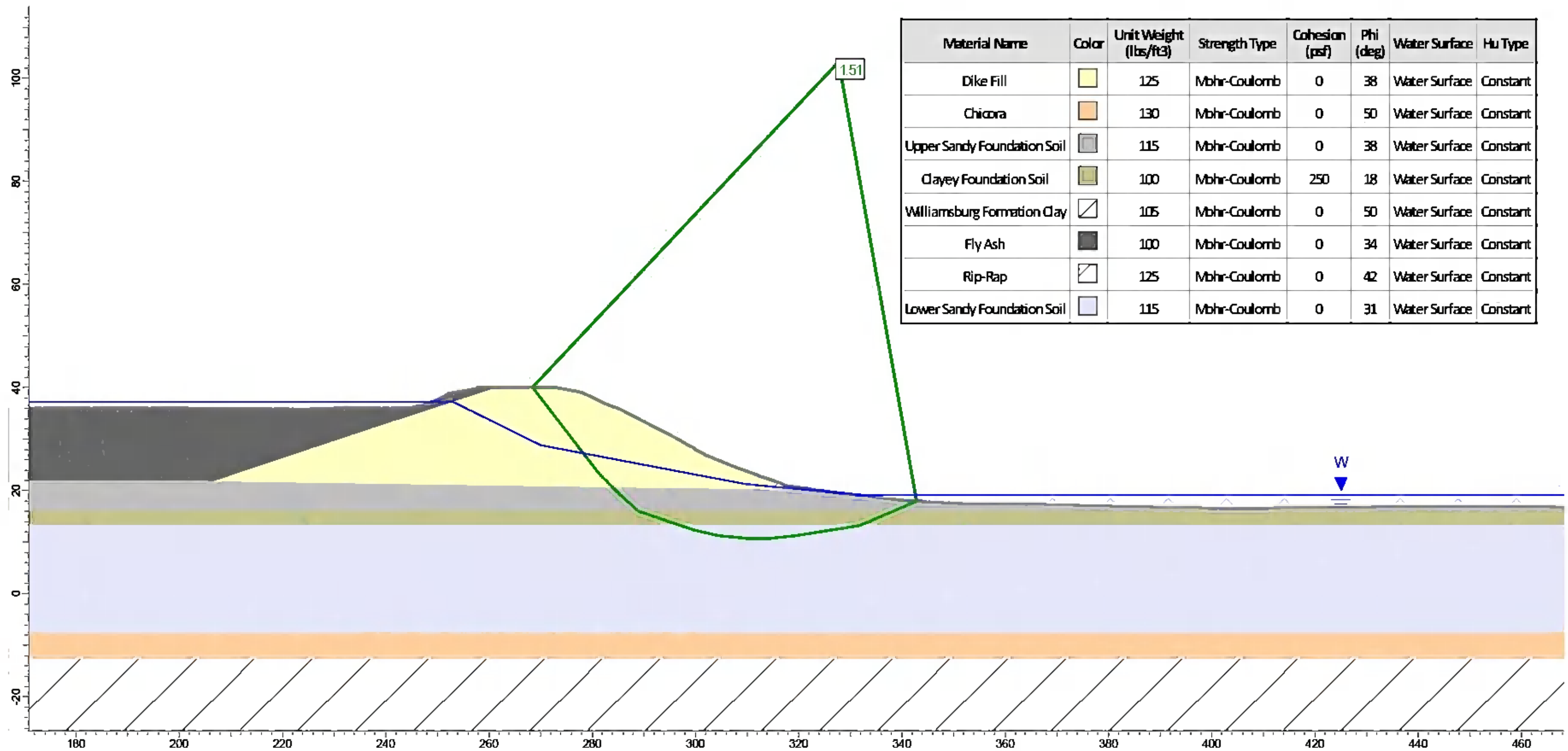

Figure 7. Calculated Factor of Safety for Cross Section C: Static Factor of Safety - Maximum Surcharge Pool

Note:

[1] “Maximum Surcharge Pool” was conservatively selected at 37.2 ft NGVD29 within Ash Pond B.

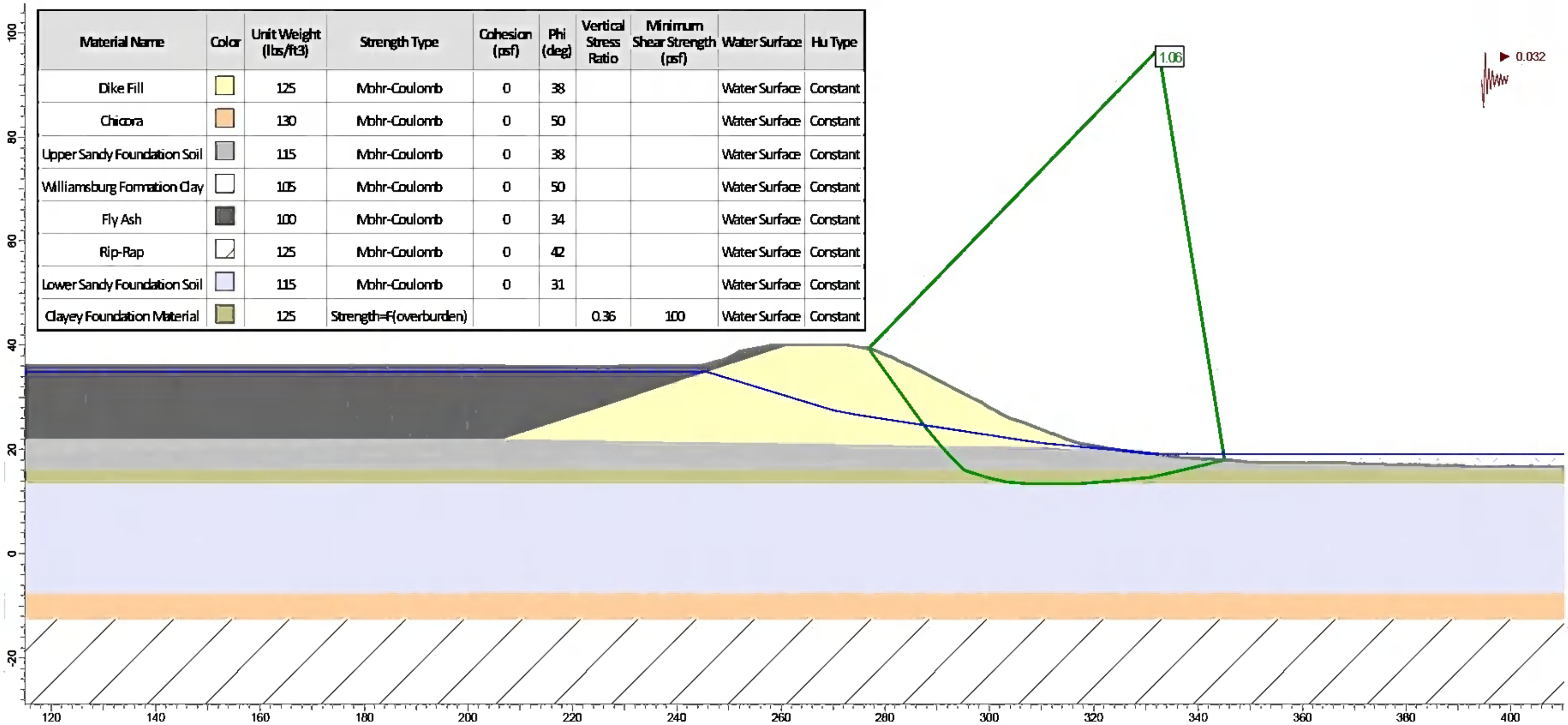

Material Name	Color	Unit Weight (lbs/ft3)	Strength Type	Cohesion (psf)	Phi (deg)	Vertical Stress Ratio	Minimum Shear Strength (psf)	Water Surface	Hu Type
Dike Fill		125	Mohr-Coulomb	0	38			Water Surface	Constant
Chicora		130	Mohr-Coulomb	0	50			Water Surface	Constant
Upper Sandy Foundation Soil		115	Mohr-Coulomb	0	38			Water Surface	Constant
Williamsburg Formation Clay		105	Mohr-Coulomb	0	50			Water Surface	Constant
Fly Ash		100	Mohr-Coulomb	0	34			Water Surface	Constant
Rip-Rap		125	Mohr-Coulomb	0	42			Water Surface	Constant
Lower Sandy Foundation Soil		115	Mohr-Coulomb	0	31			Water Surface	Constant
Clayey Foundation Material		125	Strength=F(overburden)			0.36	100	Water Surface	Constant

Figure 8. Calculated Factor of Safety for Cross Section C: Seismic Factor of Safety – Maximum Normal Storage Pool

Note:

[1] A horizontal seismic coefficient of 0.032g was used for the seismic factor of safety analysis.